Geographic patterns of genetic diversity under climate change: linking genes and ecosystems

A Dissertation Presented for the
Doctor of Philosophy
Degree
The University of Tennessee, Knoxville

Shannon Lee Jo-Ann Bayliss
December 2021

DEDICATION

I dedicate this dissertation to my father, whose ‘on-and-on’ gene I feel lucky to have inherited. Thank you for showing me how to be curious, generous, and grateful.

ACKNOWLEDGEMENTS

I need to first thank Joe Bailey and Jen Schweitzer: Your mentorship and friendship is invaluable, and your support and encouragement has helped me realize what my goals are, and to begin realizing them. Thank you for always encouraging us to be ourselves. Thanks also to Stephanie Kivlin, Mona Papes, Jon Hathaway, Mark Littmann, Julie Andsager, and Caroline Weinhold for all the conversations and guidance – all of you have been a huge part of my experience at the University of Tennessee. Thanks to Liam Mueller, Ian Ware, Rachel Wooliver, Alix Pfennigwerth, and Michael Van Nuland who made moving to Tennessee an easy decision. Liam, Ian, Rachel, Alex, Michael plus Kendall Beals, Megan Patel, Sophia Turner, Sarah Love, and Alex Neild: thank you for being wonderful lab mates, for all your scientific input, and most importantly for your friendship. Finally, thank you to my family for your constant love and support.

ABSTRACT

Climate change is having profound effects on species distributions. However, much less is understood about how climate change may alter the distribution of genetic variation within species across landscapes. Maintaining genetic diversity within populations is essential for the survival of species in the face of rapid climatic changes, but importantly, losses of genetic variation will also have significant consequences on entire ecosystems. The objective of this dissertation is to understand how genetic variation in a riparian cottonwood species, *Populus angustifolia*, affects mass and energy exchange between the land and atmosphere across ~1700 km of latitude of the western United States, and how genetic variation may respond to climate change. Specifically, I examine: (1) the potential for large-scale land-atmosphere feedbacks in hydrologic processes driven by geographic differences in plant population traits; (2) the extent to which including genetic population structure into species distribution models alters predictions of suitable conditions and geographic distributions; and (3) the extent to which genetic trait variation in bud break phenology is predicted to change in response to novel climatic conditions. The findings of this dissertation suggest that populations from landscapes with different hydrologic histories will differ in their ability to maintain favorable water balance with changing atmospheric demands for water; that species-range distribution models that do not include genetic information provide overly-broad projections of suitable conditions on the landscape compared to models that include population genetic structure; and, that a net loss of trait variation in future climates is predicted across all populations of *P. angustifolia*, with the trailing-edge population is predicted to lose the most. These ideas have broad implications for predicting population-level ecological and evolutionary responses to climate change as decreases to genetic variation reduce a species' ability to adapt to novel conditions and can have profound effects on ecosystem processes like resource cycling (e.g., water, carbon, nitrogen) and on species interactions within ecological communities.

TABLE OF CONTENTS

LIST OF TABLES

LIST OF FIGURES

INTRODUCTION

The hydrologic cycle is undergoing extreme changes due to shifts in atmospheric temperature and carbon dioxide concentrations. The frequency and magnitude of extreme precipitation, flood, and drought events are changing, as well as land water-storage, sea-level, and surface flow rates (Milly et al. 2005, Dragoni & Sukhija 2008, Famiglietti 2014, Reager et al. 2016). The unprecedented rate that these alterations are occurring (Georgakakos et al. 2014) will have far-reaching and unpredictable consequences for the ecology and evolution of entire ecosystems, all of which are inherently dependent on, and limited by, water (Bates et al. 2008, Catford et al. 2012, Perry et al. 2012).

Plants are central to Earth's water cycle, operating as hydraulic conduits from the soil to the atmosphere (Taiz & Zeiger 1991). As plant roots take up water for physiological processes (e.g., photosynthesis), leaves recycle water to the atmosphere through transpiration. On average, transpiration has been estimated to make up 80-90% of total terrestrial *evapo*transpiration (ET; evaporation + transpiration; Jasechko et al. 2013). This translates into approximately 68,000 cubic kilometers of water cycling through plants to the atmosphere each year – a volume roughly equivalent to emptying the Great Lakes of North America three times. As plants remove water from soil, they also affect other components of the water cycle including groundwater recharge and surface runoff (Scanlon et al. 2006, Ukkolo et al. 2016). Moreover, to do this, plants consume about one-half of all solar energy absorbed on land (Jasechko et al. 2013). Changes to the percent cover, the composition, and the diversity of plants on the landscape will have serious consequences for earth-atmosphere feedbacks, as they do for other ecosystem functions (Tilman et al. 1997, Whitham et al. 2003, 2006, Hooper et al. 2005, Baudeña et al. 2015).

Water vapor is the most important greenhouse gas and regulator of earth's climate such that changes to the amount of water in the atmosphere will have long-term feedback effects on climate. Atmospheric demand for water is described in potential evapotranspiration (PET), a measure that is governed primarily by temperature and the saturation vapor pressure of water. Saturation vapor pressure is the pressure of water vapor when it is in equilibrium with the liquid state of water – meaning water is not undergoing

a phase change. Importantly, it is highly sensitive to, and has a non-linear relationship with temperature (Allen & Ingram 2002). Indeed, in the United States, water stress on the landscape becomes more severe when considering both changes to the supply (precipitation) *and* the atmospheric demand (PET) for water (climate.gov). Unsurprisingly then, drought estimates in the western U.S. that are based on precipitation alone can hugely underestimate the chance of "megadroughts" – droughts that are equally severe as the worst droughts of the 20th century but that persist much longer (Ault et al. 2016). This underestimation of drought is a critical problem for ecologists who aim to understand population, community, and ecosystem responses to drought conditions. Additionally, precipitation changes are likely to be spatially heterogenous and not only include changes to the amount of water, but to the timing, variability, intensity, and type (e.g., rain, snow, fog) of water supplied to ecosystems (IPCC 2007, Beier et al. 2012).

The large body of literature documenting plant adaptations to water regimes (McDowell et al. 2008, Lytle & Poff 2004, Adams et al. 2017) and the centrality of plants to the water cycle (Jasechko et al. 2013) suggest the presence of a global scale eco-evolutionary feedback that has not been well explored (Ware et al. 2019). For example, changes to surface flow can be linked both to plant traits and to elevated levels of atmospheric carbon dioxide. With increased CO_2, plants reduce stomatal conductance (decreasing transpiration rates) thereby removing less water from the soil and increasing runoff (Milly et al. 2005, Ukkola et al. 2016). Genetic variation in plant physiological responses to drought include (non-exhaustively) variation in stomatal conductance, stomatal size and density, and water-use efficiency (Mitton et al. 1998, McDowell et al. 2008). These responses may help with tolerance or recovery but depend on the intensity and/or duration of the drought event (McDowell et al. 2008, Gilbert & Medina 2015). Mortality from drought is common and can largely be attributed to carbon starvation and the loss of xylem hydraulic conductivity (McDowell et al. 2008, Brodribb et al. 2009, Kursar et al. 2009, Urli et al. 2013, Rowland et al. 2015, Adams et al. 2017). Though water flow is a passive process responding to physical laws, plants have evolved mechanisms to control water flow through their hydraulic system. Plant populations will experience new

evolutionary selective pressures to manage their water resources as water changes in availability.

Whether or not plants will buffer or exacerbate changes to the water cycle will depend largely on their ability to acclimate or adapt to new conditions (Jump & Peñuelas 2005). To approach these questions, we need to understand how plant genetic and phenotypic variation is distributed across populations and across landscapes and conduct manipulative experiments testing the climatic tolerances of populations. These investigations should provide insight into the extent to which large-scale ecosystem processes like water cycling may be affected by past and contemporary evolutionary processes.

Populus angustifolia as a model system

Cottonwood riparian ecosystems in the western United States support upwards of 70% of the biodiversity in the region (Stettler et al. 1996). As a foundation species, the high levels of intraspecific variation have a strong effect on biodiversity, community structure, and ecosystem functions (Whitham et al. 2003, 2006). As a riparian species, *Populus angustifolia* is likely to be strongly influenced by (e.g., via natural selection) and influence various aspects of the water cycle. For instance, in another *Populus* species (*Populus fremontii*) gene flow is strongly related to the connectivity and size of the river network – smaller rivers with lower streamflow show less gene flow (Cushman et al. 2014). This model system is used for chapters 1-3.

The Budyko hydrological model

Eco-hydrologists consider how precipitation is distributed once it reaches the Earth's surface, acknowledging that not all water is available to plants as soil water. Ideas from hydrology can help ecologists address the spatial heterogeneity of water and temperature interactions on the landscape, and their effects on plant. The Budyko hydrologic model is a well-known model of supply and demand that gives an expectation of how water will cycle in various climates. The model also can provide indices that represent deviations

from those predictions describing how water cycles in different climates across landscapes (Budyko 1974). This model is detailed further in chapter 1.

Spatial modeling

Species distribution models aim to describe and predict suitable habitat for species using correlative methods connecting species occurrence data to environmental conditions (Phillips et al. 2006). These models traditionally assume that a species is a single unit not varying across its range (i.e., disregarding phenotypic and genotypic variation). Recently genetically informed spatial models support the need to incorporate information on population genetic structure into model predictions of species distributions in future climates (May et al. 2011, Gotelli & Stanton-Geddes 2015, Marcer et al. 2016, Ikeda et al. 2017, Peterson et al. 2019). This methodology is applied in chapters 2-3 and discussed in further detail therein.

REFERENCES

Adams HD, et al. (2017) A multi-species synthesis of physiological mechanisms in drought-induced tree mortality. *Nature Ecology and Evolution.* 1: 1285-1291.

Allen MR, and Ingram WJ. (2002) Constraints on future changes in climate and the hydrologic cycle. *Nature*, 419: 224-232.

Ault TR, Mankin JS, Cook BI, Smerdon JE. (2016) Relative impacts of mitigation, temperature, and precipitation on 21st century megadrought risk in the American Southwest. *Science Advances* 2(10)

Bates BC, et al. (2008) Climate Change and Water. Technical Paper of the Intergovernmental Panel on Climate Change, IPCC Secretariat, Geneva.

Baudeña M, Dekker SC, van Bodegom PM, Cuesta B, Higgins SI, et al. (2015) Forests, savannas, and grasslands: bridging the knowledge gap between ecology and Dynamic Global Vegetation Models. *Biogeosciences*, 12: 1833-1848.

Beier, C. *et al*. (2012) Precipitation manipulation experiments–challenges and recommendations for the future. *Ecology Letters* 15: 899–911.

Brodribb TJ, Cochard H. (2009) Hydraulic failure defines the recovery and point of death in water- stressed conifers. *Plant Physiology.*, 149: 575-584.

Budyko MI. Climate and Life; Academic Press: New York, NY, USA (1974).

Catford JA, Naiman RJ, Chambers LE, Roberts J, Douglas M, and Davies P. (2012) Predicting Novel Riparian Ecosystems in a Changing Climate. *Ecosystems.*

Cushman SA, Max T, Meneses N, Evans LM, Ferrier S, Honchak B, Whitham TG, Allan GJ. (2014) Landscape genetic connectivity in a riparian foundation tree is jointly driven by climatic gradients and river networks. *Ecological Applications,* 24: 1000-1014.

Dragoni W, and Sukhija B. (2008) Climate change and groundwater: a short review. *Geological Society, London, Special Publications*, 288(1): 1-12.

Famiglietti JS. (2014) The global groundwater crisis. *Nature Climate Change* 4: 945–948.

Georgakakos A, Fleming P, Dettinger M, Peters-Lidard C, Richmond T, Reckhow K, White K, Yates D. (2014) Climate Change Impacts in the United States: The Third National Climate Assessment: 69-112. Published by U.S. Global Change Research Program.

Gilbert ME and Medina V. (2016) Drought Adaptation Mechanisms Should Guide Experimental Design. *Trends in Plant Science*, 21(8): 639-647.

Gotelli NJ, and Stanton-Geddes J. (2015) Climate change, genetic markers, and species distribution modelling. *Journal of Biogeography,* 42: 1577-1585.

Hooper DU, Chapin III F, Ewel J, Hector A, et al. (2005) Effects of biodiversity on ecosystem functioning: a consensus of current knowledge. *Ecological Monographs*, 75: 3-35.

Ikeda, D.H. et al. (2017) Genetically informed ecological niche models improve climate change predictions. *Global Change Biology,* 23: 164-176.

Jasechko S, Sharp ZD, Gibson JJ, Birks, SJ, Yi Y, Fawcett, PJ. (2013) Terrestrial water fluxes dominated by transpiration. *Nature,* 496: 347-351.

Jump AS, and Peñuelas J. (2005) Running to stand still: adaptation and the response of plants to rapid climate change. *Ecology Letters*, 8: 1010-1020.

Kursar TA, Engelbrecht BMJ, Burke A, Tyree MT, El Omari B, Giraldo JP. (2009) Tolerance to low leaf water status of tropical tree seedlings is related to drought performance and distribution. *Functional Ecology*, 23: 93-102.

Lytle DA, and Poff NL. (2004) Adaptation to natural flow regimes. *TRENDS in Ecology and Evolution,* 19: 94-100.

Marcer A, Mendez-Vigo B, Alonso-Blanco C, Pico FX. (2016) Tackling intraspecific genetic structure in distribution models better reflects species geographical range. *Ecology and Evolution,* 6: 2084-2097.

May SE, Medley KA, Johnson SA, and Hoffman EA. (2011) Combining genetic structure and ecological niche modeling to establish units of conservation: A case study of an imperiled salamander. *Biological Conservation,* 144: 1441-1450

McDowell N, et al. (2008) Mechanisms of plant survival and mortality during drought: why do some plants survive while others succumb to drought? *New Phytologist*, 178: 719-739.

Milly PCD, Dunne, KA, Vecchia AV. (2005) Global pattern of trends in streamflow and water availability in a changing climate. *Nature Letters*, 438: 347-350.

Mitton JB, Grant MC, and Yoshino AM. (1998) Variation in allozymes and stomatal size in pinyon (*Pinus edulis, Pinaceae),* associated with soil moisture. *American Journal of Botany*, 85(9): 1262-1265.

Perry LG, Andersen, DC, Reynolds LV, Nelson SM, Shafroth PB. (2012) Vulnerability of riparian ecosystems to elevated CO2 and climate change in arid and semiarid western North America. *Global Change Biology*, 18: 821-842.

Peterson ML, Doak DF, and Morris WF. (2019) Incorporating local adaptation into forecasts of species' distribution and abundance under climate change. *Global Change Biology*, 25: 775-793.

Phillips SJ, et al. (2006) Maximum entropy modeling of species geographic distributions. *Ecological Modeling*, 190: 231-259.

Reager JT, Gardner AS, Famiglietti JS, Wiese DN, Eicker A, and Lo M-H. (2016) A decade of sea level rise slowed by climate-driven hydrology. *Science,* 351(6274): 699-703.

Rowland L, et al. (2015) Death from drought in tropical forests is triggered by hydraulics not carbon starvation. *Nature*, 528: 119-122.

Scanlon BR, Keese KE, Flint AL, Flit LE, Gaye CB, Edmunds WM, and Simmers I. (2006) Global synthesis of groundwater recharge in semiarid and arid regions. *Hydrological Processes*, 20: 3335-3370.

Stettler RF, Bradshaw HD Jr, Heilman PE, and Hinckley TM. (1996) Biology of *Populus* and its implications for management and conservation. NRC Research Press, Ottawa, Ontario, Canada.

Taiz L, and Zeiger E (1991) Plant Physiology. The Benjamin/Cummings Publishing Company, Inc.

Tilman D, Lehman C, and Thomson K (1997) Plant diversity and ecosystem productivity: theoretical considerations. *PNAS USA*, 94: 1857-61.

Ukkola, AM, Prentice IC, Keenan TF, van Dijk AIJM, Viney NR, Myneni RB, and Bi J. (2016). Reduced streamflow in water-stressed climates consistent with CO2 effects on vegetation. *Nature Climate Change*, 6: 75-80.

Urli M, Porte AJ, Cochard H, Guengant Y, Burlett R, Delzon S. (2013) Xylem embolism threshold for catastrophic hydraulic failure in angiosperm trees. *Tree Physiology*, 33: 672-683.

Ware IM, Fitzpatrick CR, Senthilnathan A, Bayliss SLJ, Beals KK, Mueller LO, et al. (2019) Feedbacks link ecosystem ecology and evolution across spatial and temporal scales: Empirical evidence and future directions. *Functional Ecology*, 33: 31-42.

Whitham TG, Young WP, Martinsen GD, Gehring CA, Schweitzer JA, Shuster SM, Wimp GM, Fischer DG, Bailey JK, Lindroth RL, Woolbright S, Kuske CR. (2003) Community and Ecosystem Genetics: A Consequence of the Extended Phenotype. *Ecology*, 84: 559-573.

Whitham, TG et al. (2006) A framework for community and ecosystem genetics: from genes to ecosystems. *Nature Reviews Genetics*, 7: 510-523.

CHAPTER I
PLANT GENETIC VARIATION DRIVES GEOGRAPHIC DIFFERENCES IN ATMOSPHERE-PLANT-ECOSYSTEM FEEDBACKS

A version of this chapter was originally published by Shannon L. J. Bayliss, Liam O. Mueller, Ian M. Ware, Jennifer A. Schweitzer, and Joseph K. Bailey:

S.L.J. Bayliss et al. (2020). "Plant genetic variation drives geographic differences in atmosphere-plant-ecosystem feedbacks." *Plant-Environment Interactions*, 00:1-15. http://doi.org/10.1002/pei3.10031

SLJB and JKB conceived of the manuscript and ideas held within. SLJB collected data, analyzed data, and wrote the manuscript. LOM, IMW, JAS, and JKB all assisted with data collection and provided significant editorial and analytical advice.

Abstract

The objective of this study was to understand how genetic variation in a riparian species, *Populus angustifolia*, affects mass and energy exchange between the land and atmosphere across ~1700 km of latitude of the western United States. To examine the potential for large-scale land-atmosphere feedbacks in hydrologic processes driven by geographic differences in plant population traits, we use a physical hydrology model, paired field and greenhouse observations of plant traits, and stable isotope compositions of soil, stem, and leaf water of *P. angustifolia* populations. Populations show patterns of local adaptation in traits related to landscape hydrologic functioning – a 47% difference in stomatal density in greenhouse conditions and a 74% difference in stomatal ratio in the field. Trait and stable isotope differences reveal that populations use water differently which is related to historical landscape hydrologic functioning (evapotranspiration and streamflow). Overall, results suggest that populations from landscapes with different hydrologic histories will differ in their ability to maintain favorable water balance with changing atmospheric demands for water, with ecosystem consequences.

Introduction

Alterations to species distributions will accompany global climatic changes, consequently destabilizing the functions and services that diverse ecosystems provide (Parmesan 2006; Burrows *et al.* 2011; Naeem *et al.* 2012; Urban 2015). However, much of our understanding of distribution shifts are limited by the common assumption in models that all populations of a species will respond in a similar manner to environmental changes,

despite knowledge to the contrary (Gotelli & Stanton-Geddes 2015; Benito Garzón *et al.* 2019; Peterson *et al.* 2019). Further, research to date tends to over-simplify the relationship between temperature and precipitation on the landscape, rarely considering energy and water as a more dynamic relationship (Bates *et al.* 2008; Jones *et al.* 2012). This interaction affects the atmospheric supply and demand of water that drives population, community and ecosystem dynamics (Bates *et al.* 2008; Jones *et al.* 2012). Taken together, both water-energy interactions and intraspecific variation in plant climatic tolerance vary across small and large spatial scales needs to be considered in order to understand feedbacks between population structure and large-scale ecosystem processes (e.g., water fluxes; Bates *et al.* 2008; Hendry 2017; Jones *et al.* 2012; Thompson 2005).

The Budyko water-budget model is widespread in the field of hydrology. The model considers the mass-balance (amount of water) and energy-balance (phase change potential) of systems by reflecting actual evapotranspiration (AET) as a function of precipitation (P) and potential evapotranspiration (PET; Budyko 1974; Sposito 2017). The theoretical model is useful for predicting water cycling in various climates, though values based on data (actual values) deviate from the theoretical curve to represent interactions with ecological factors such as soil type, vegetation cover, and/or other biotic factors (Gentine *et al.* 2012; Troch *et al.* 2013). While distributions of terrestrial species are most often described and strongly driven by patterns in soils, precipitation, temperature, and distance to water (Bradie & Leung 2017), PET actually explains more variation in natural selection globally in terrestrial biomes than does temperature (Siepielski *et al.* 2017), and leaf economic traits are more strongly correlated with vapor pressure deficit and PET than it is with precipitation or temperature (Wright *et al.* 2004). Though PET is derived from temperature, it more accurately reflects the temperature during the period of time when plants are actively using energy and water (i.e., the growing season) (Siepielski *et al.* 2017; Eller *et al.* 2018).

As water and energy change in availability and variability on the landscape, plant population responses will likely vary due to differing amounts of intraspecific variation, genetic architecture or due to adaptations to differing historical abiotic conditions. For instance, the ability of plants to use water to produce biomass depends strongly on soil

water availability which varies significantly across the landscape and is also affected by temperature (Rodriguez-Iturbe & Porporato 2005; Beier *et al.* 2012). If atmospheric demand for water increases (i.e., high atmospheric vapor pressure deficit), which is predicted to occur globally, plants must prevent excessive water loss (Grossiord *et al.* 2020). Rapid responses to high vapor pressure deficits include adjusting stomatal aperture, while longer-term responses include altering the density, distribution, and size of stomatal pores (Cowan & Farquhar 1977; Oren *et al.* 1999; Hetherington & Woodward 2003; McAdam & Brodribb 2014; Bertolino *et al.* 2019). Genetically-based variation stomatal density or size (Mitton *et al.* 1998) result in variations of maximum stomatal conductance, affect a plant's ability to manage limited resources, and affect large-scale ecosystem processes (Novick *et al.* 2016). Transpiration directly supports primary productivity, biomass accumulation, and carbon assimilation, thus is directly related to carbon, water, and energy fluxes on the landscape (Hetherington & Woodward 2003; Kominoski *et al.* 2013, Sposito 2017). Here, we consider variation in historic water cycling on the landscape and examine local adaptation of plant populations to understand ecological and evolutionary linkages on a landscape scale.

Using the Budyko physical hydrology model, paired field and greenhouse observations of *P. angustifolia* traits, and stable isotope compositions of soil, stem, and leaf water, this study considers the potential for large-scale land-atmosphere feedbacks in hydologic processes driven by geographic differences in plant population traits. With the observation that the supply and atmospheric demand for water, as well as water use differ on the landscape across populations of *P. angustifolia*, we test the following specific hypotheses: (1) Populations of *P. angustifolia* show genetic divergence in stomatal density, stomatal distribution, stomatal size, and aboveground biomass, (2) consistent with patterns of genetic divergence and local adaptation, stomatal traits are related to hydrologic variables on the landscape, (3) populations draw water from different sources (e.g., stream water or precipitation), and (4) populations vary in water-use given atmospheric demands. Overall, results show that divergent plant populations have evolved in response to geographic variation in dryness.

Materials & Methods

Building site-level energy and water budgets

We built energy and water budgets using Budyko model parameters describing how precipitation (P) is recycled to the atmosphere via actual evapotranspiration (AET) or held on land as streamflow (Q) across a continuum of humid to arid systems (PET/P; Figure 1b; Budyko 1974; All tables and figures are in the Appendix 1 at the end of this chapter). The theoretical model (note, the modeled curve is not depicted in Figure 1b) provides expectations for the energy-balance and water-use based on physical processes (i.e., evapotranspiration consumes heat as latent energy flux during the phase change of liquid water to vapor) and the assumption that P = Q + AET (Budyko 1974; Trenberth *et al.* 2009; Wang & Dickinson 2012). Values derived from real data represent long-term patterns describing how water *actually* cycles on the landscape, taking into account more than physical processes – in other words, landscape variation in interactions between soil, vegetation, and atmospheric conditions. The dryness index (PET/P) on the x-axis of the model represents the aridity of the climate, with values greater than 1 indicating arid climates whereby plants are limited by water rather than by energy. The evaporative index (AET/P) on the y-axis describes how precipitation is distributed on land, or the percentage of P recycled back to the atmosphere through AET. An energy-limit exists where AET = PET (i.e., demand-limit; at which atmospheric demand for water is met), and a mass-limit exists where AET=P (also known as a water-limit, or supply-limit; i.e., 100% of P is partitioned back to the atmosphere) (Budyko 1974; Jones *et al.* 2012; Creed *et al.* 2014). In this paper, we are explicitly interested in unique long-term patterns of water cycling on the landscape which capture landscape heterogeneity, and not in the theoretical predictions (Figure 1b; Gentine *et al.* 2012; Troch *et al.* 2013). We extracted mean annual precipitation from WorldClim (Fick & Hijmans 2017) and mean annual PET and AET from the CGIAR-CSI GeoPortal (Trabucco & Zomer 2009) using geo-referenced locations of our collection sites.

Study species and sites

To understand plant-energy-water relationships we used a dominant riparian tree species: *Populus angustifolia* James (Rood *et al*. 2010), the narrowleaf cottonwood, that is widely distributed along the Rocky Mountains from northern Mexico to southern Canada (Evans *et al.* 2015) and span large precipitation, temperature, stream flow, and soil water gradients. Cottonwoods, *Populus ssp.*, are an ideal study system for examining these relationships as they show intraspecific variation in physiological and morphological responses to changes in the water cycle, including groundwater, precipitation, and streamflow (Rood *et al.* 2003). Further, *Populus ssp.* are foundation species in riparian ecosystems in the western U.S. contributing greatly to ecosystem transpiration, but have been generally labelled as "drought sensitive" species that are declining in recent years (Schaeffer *et al.* 2000; Kominoski *et al.* 2013). It is also clear that these riparian forests do not recieve enough precipitation during the growing season to support the levels of transpiration to meet atmospheric demand (Scott *et al.* 2000; Flanagan *et al.* 2017; Yang *et al.* 2019). Populations under such environmental constraints are ideal for identifying genetic divergence in response to varying hydrologic dynamics.

We have established field sites along 17 rivers in the western United States that span significant environmental gradients and nearly 1,700 kilometers of latitude (Figure 1a). In 2012, over 525 genotypes of *P. angustifolia* were collected and geo-located from multiple (minimum three, maximum five) sites along each river, including at the highest and lowest elevations. The collected trees have been established in a greenhouse at the University of Tennessee and all tree replicates were tagged with a number and randomized in the common environment to minimize microspatial variation in light or temperature (details in Ware *et al.* 2019). This is a conservative experimental approach to examining genetic variation at multiple genetic hierarchies, including provenance, population, site, and genotype, that reduces observer sample bias. No plants were water limited in the greenhouse, and temperature conditions were maintained between 65-75 degrees Fahrenheit. Testing for variation in trait measurements in the common environment and relating these traits to environmental parameters allows us to infer patterns of local adaptation (Kawecki & Ebert 2004; Leimu & Fischer 2008). We refer to populations as

groupings of all genotypes from sites along each river, resulting in 17 river populations. These 17 populations vary locally and regionally, grouping into three genetically-distinct provenances which have been geographically isolated by large landscape features including the Great Basin, the Rocky Mountains, and the Mogollon Rim (Figure 1a; Evans *et al.* 2015).

Plant functional and performance traits

Field biomass measurements were made in the summer of 2012, and greenhouse biomass measurements were later made from established clonal cuttings of the same genotypes in 2016. In June 2017, we re-visited a subsample of the genotypes visited in 2012 to obtain field stomatal measurements. At this time, we also collected cuttings and established clones in the greenhouse. We measured the same suite of stomatal traits on these trees between October 27-31, 2017. Details of trait measurements are described below. Because development and leaf age can affect stomatal traits (e.g., Pearce *et al.* 2005; Hamanishi *et al.* 2012), we checked for ontogenetic differences in traits between older clones from which biomass was derived and their respective younger clones (from the same "source" tree in the field). Seven of the same genotypes were measured for stomatal traits in the "older" (2012) trees in October 2017. A two-tailed unpaired t-test on stomatal density and stomatal distribution showed no difference between the two age groups ($p=0.56$, $p=0.39$ respectively).

Aboveground biomass. In the field, aboveground biomass estimates of *P. angustifolia* genotypes were made in 2012 by measuring tree circumference (m) which was used to calculate DBH (cm): DBH=100*circumference/3.14). We estimated biomass (kg) using an allometric equation for *Populus* from Chojnacky *et al.* (Chojnacky *et al.* 2014) who developed from a meta-analysis of ten existing allometric equations based on tree DBH: Aboveground biomass (kg) = -2.6863 +((2.4561)*ln(DBH)). In the greenhouse, aboveground biomass measurements were made in 2016, four years after cuttings were established in the common environment. To estimate biomass (grams of C) for saplings, we created an allometric equation using six *P. angustifolia* genotypes grown in the greenhouse environment and measurements collected across 3 years (June 2012, 2013, and

2014; described and used in Van Nuland *et al.* (Van Nuland *et al.* 2017) and Ware *et al.* (Ware *et al.* 2019b)). The following allometric equation was used: Aboveground biomass (g) = (stem volume (mm^3) * 0.41899) – 2.40137.

Stomatal traits. We measured three traits related to stomatal function: density, distribution, and size. Stomata control the movement of gases in and out of the leaf (e.g., carbon dioxide for photosynthesis, water via transpiration). Variation in the size and the density of stomata as well as the location on leaf surfaces (i.e., adaxial (top), abaxial (bottom)) reflect ways that plants can control water loss, and thus are important to plant function (Aasamaa *et al.* 2002; Cornelissen *et al.* 2003; Hetherington & Woodward 2003; Sack *et al.* 2006; Bertolino *et al.* 2019). Prior studies on *Populus* reveal positive relationships between stomatal density and ratio with conductance and carbon assimilation rates (Pearce *et al.* 2005; Guy & Gornall 2007; Soolanayakanahally *et al.* 2009) and changes in water-use efficiency with drought (Hamanishi *et al.* 2012).

Leaves were collected in the field in June 2017 from two genotypes along (3 sites) six rivers distributed across the three genetic provenances (Provenance 1: Blue River, NM and Oak Creek, AZ; Provenance 2: San Miguel River, CO and Indian Creek, UT; Provenance 3: Weber River, UT and Snake River, WY). These collections resulted in 6 genotypes per river, or 12 genotypes per genetic provenance, and were the same genotypes that were visited in 2012 collection described above. We chose three leaves from the terminal shoots of lower exterior branches of each tree to minimize intra-canopy and age variation in stomatal density (Sack *et al.* 2006). Impressions of the leaf epidermis were made on the adaxial and abaxial side of each leaf using clear nail varnish and tape, then individually arranged on glass slides. Counts were made in the software ImageJ (Schneider *et al.* 2012) from light microscopy photographs with a 10X objective. We calculated the total number of stomata per area by adding the number of stomata on both leaf surfaces (henceforth "stomatal density"), and we calculated the relative placement of stomata by calculating the ratio of adaxial density to abaxial density (henceforth "stomatal ratio"). These methods resulted in 6 impressions per genotype, or 216 total impressions. Finally, we made 20 measurements of stomatal pore length on each photograph in ImageJ

(Schneider et al. 2012). As stomatal density on photographs was often higher than 20, we overlayed a grid in ImageJ and randomly selected a row across which to begin measurements. If density was too low to obtain 20 measurements, more often on the adaxial impressions, we measured the pore length of every present stoma. These methods resulted in 120 pore length measurements per genotype. We repeated the same measures from leaves collected from the same genotypes of trees growing in the common environment, described above, though we lost 3 genotypes from the San Miguel and the Weber Rivers and 1 genotype from both the Blue River and the Snake River. Greenhouse measurements therefore consisted of a leaf collected from 3 clonal replicates of 28 genotypes.

Water stable isotope measurements. We analyzed river water, stem, leaf, and soil samples for stable isotope measurements ($\delta^{18}O$ and $\delta^{2}H$) to determine plant water source. In June 2017, at the mid-elevation site along each of the six rivers, we collected stem and leaf samples for stable isotope analysis from two unique genotypes of *P. angustifolia*. Soil samples were collected from underneath each genotype at a depth of approximately 10 cm. River water samples were collected below the surface of the water in each of the six rivers. All samples were kept on dry ice until delivered to the Colorado Plateau Stable Isotope Laboratory (CPSIL; www.isotope.nau.edu) at Northern Arizona University in Flagstaff, AZ. The samples were stored in a freezer until extraction and analysis. Water was extracted from woody stem samples via cryogenic vacuum extraction. Samples were extracted in September 2017 and analyzed for the stable oxygen ($^{18}O/^{16}O$) and hydrogen ($^{2}H/^{1}H$) ratios (expressed per mille). All the extractions were made via LGR DLT-100 laser spectroscopy.

Statistical analyses

All analyses were performed using the statistical software R (version 3.6.1; R Development Core Team, 2016). To confirm our observations that water availability and the atmospheric demand for water vary across the range of *P. angustifolia*, we built linear models predicting variation in the two axes of the Budyko water budget (dryness index and evaporative index) with population. Separate models were built for the 17 populations examined for biomass, the six-population subset used for stomatal measurements, and the three genetic provenances (with population as a random effect; R package lme4 (Bates *et al.* 2015)).

Hypothesis testing for each linear model was done by marginal sums of squares ANOVA in the R package car (Fox *et al.* 2018) and the null hypothesis was rejected at an α=0.05.

To test the hypothesis that stomatal and growth traits from *P. angustifolia* genetic provenances reveal patterns of local adaptation, we ran linear mixed effects models with biomass, stomatal density, and stomatal ratio as response variables, provenance as a fixed effect, and population (river) as a random effect in the lme4 R package (Bates *et al.* 2015). For stomatal density and ratio, genotype was also included as a random effect. Models were compared to null models with random effects only using likelihood ratio tests and by comparing AIC values. Post-hoc pairwise differences comparisons were made of provenance-level means with Tukey contrasts using the ghlt function in R package "multcomp" (Hothorn *et al.* 2008) with the null hypothesis rejected at an α=0.05.

To test the hypothesis that water-regulation and functional traits are related to hydrologic variables on the landscape, we used restricted estimated maximum likelihood (REML) linear mixed models (R package lme4 (Bates *et al.* 2015)). We included water budget parameters as fixed effects and we included genetic provenance in models as a random effect to remove "blocked" variation that can be attributed to genetic grouping. Response variables included *P. angustifolia* greenhouse biomass, stomatal density, stomatal ratio, and stomatal pore length measurements. Hypothesis testing for each linear model was done by marginal sums of squares ANOVA in the car R package (Fox *et al.* 2018) and the null hypothesis was rejected at an α=0.05.

To test the hypothesis that populations draw water from different sources, we used stable isotope values to calculate deuterium excess values (d-excess) as d-excess = $\delta^2H - 8 * \delta^{18}O$ (Dansgaard, 1964). This metric represents deviations from the average global relationship between δ2H and δ18O in precipitation, the global meteoric water line (GMWL; Craig 1961). Because the global relationship varies across latitudes and continents (for example; (Sprenger *et al.* 2016), we also calculated local meteoric water lines (LMWL) that are regionally specific. We used precipitation isotopic signatures for the month of June (when samples were collected) obtained from the OIPC (The Online Isotopes in Precipitation Calculator; Welker 2000; Bowen *et al.* 2005; Bowen 2019) by inputting the latitudes, longitudes, and elevations for sampling locations. From this, we

derived line-conditioned excess values (lc-excess; Landwehr *et al.* 2014; Sprenger *et al.* 2016), calculated as: lc-excess = δ^2H - a *$\delta^{18}O$ – b, where a and b are the slope and intercept of the LMWL (Table 1.2, R^2=0.988). Negative values of both d-excess and lc-excess represent water isotope ratios that have been evaporatively enriched.

Results

Water supply, atmospheric demand for water, and water use differ across the range of P. angustifolia

Populus angustifolia riparian forests across the western U.S. (Figure 1a) are water limited; all field sites fall to the right of 1 on the dryness index (where PET=P; Figure 1b), indicating that on average, all sites and populations are limited by the supply of water. Along this axis, however, sites span a large range of dryness (min=1.00, max=5.89; Figure 1b) and differ by genetic provenances (inset boxplots, Figure 1b). Additionally, all sites fall below 1 on the evaporative index (where AET=P; blue line, Figure 1b) indicating that no more water is recycled to the atmosphere than falls as precipitation. This is expected for annual averages, which are constrained by the amount of water available in a system. Site-level values on this axis span from about 63% to 94% of water recycling to the atmosphere through AET annually (min=0.63, max=0.94) and differ across genetic provenances (inset boxplots, Figure 1b). Landscape differentiation in average dryness and evaporative indices across provenances is important, as is the situation of points within a single river on the plot, as this represents variation in water cycling regimes. For example, a river may span a wide range of climatic conditions (dryness index) but function similarly along points of the river (no variation in evaporative index, e.g., 80% of P goes to AET everywhere along the river), while another river may span a narrow range of climatic conditions (dryness index) but cycle water quite differently along the river (large range in evaporative index). In this way, the model parameters also capture effects of elevation. A comprehensive representation of sites from all 17 rivers can be found on the Budyko curve in the supplementary information (Figure 9 in Appendix 4).

Populations of P. angustifolia show patterns of genetic divergence in traits related to the water cycle

Biomass: In the field, we find that biomass is lowest in Provenance 1 compared to Provenances 2 and 3 which do not show significant differences (Figure 2a, Table 1). Conversely, in the common environment we find that Provenance 1 had the highest biomass (μ_{p1} = 294.8 g), while Provenance 3 had the lowest average aboveground biomass (μ_{p3} = 89.7 g). Overall, this represents a 69% genetically based difference in biomass across the three provenances. These results demonstrate a pattern of genetic divergence at the provenance level (Figure 2b, Table 1) and environmental constraints on biomass production in the field within the range of provenance 1, likely related to limitations in the supply of water and plant strategies to mitigate water-limitation. A post-hoc Tukey test reveals significant differences between Provenance 1 and 2, and Provenances 1 and 3 (Table 1). Provenances 2 and 3 show marginally significant differences in biomass (p=0.09; Table 1) though these provenances have the lowest sample size (N_{p2} = 213 and N_{p3} = 75 respectively). To check if these differences could be explained by growth duration (e.g., Evans et al. 2016), we also ran models including growing season length in the greenhouse (recorded as the number of days between first bud break in the spring and plant senescence in the fall), and latitude as a proxy for growing season length in the field. Our findings did not change with consideration of these variables.

Stomatal Traits: While the average stomatal density does not differ between provenances in the field (Figure 2c; Table 1), Provenance 1 shows 47.3% difference in stomatal density in the common environment compared to Provenance 3 (μ_{p1} = 118.1; μ_{p3} = 80.2; p<0.001), and a 23.7% increase relative to Provenance 2 (μ_{p2}= 95.5; p=0.062) (Figure 2d; Table 1). Overall, this represents nearly a doubling of the total number of stomata on leaf surfaces across the provenances. Additionally, we find that provenances differ in the field in stomatal ratio (Figure 2e; Table 1): Provenance 1 has a significantly lower stomatal ratio (μ_{p1}=0.103) compared to provenances 2 and 3 (which do not significantly differ from each other; μ_{p2}=0.40 and μ_{p3}=0.37 respectively). These data confirm those found previously, showing a species average of stomatal ratio to be about 0.32 (Pearce et al. 2005). In field conditions, Provenance 1 has more stomates on the abaxial leaf surface, and though the

greenhouse trend reflects this field trends, the only emergent significant difference is between Provenances 1 and 2 (Figure 2f; Table 1). Finally, we found no significant differences between the three provenances in *adaxial* stomatal pore length. However, while *abaxial* stomatal pore length did not differ between provenances in the field (Figure 2g; Table 1), with an average length of 32.4µm, we did find differences in the greenhouse. Like the patterns of stomatal distribution in the greenhouse, abaxial stomatal pore length in the greenhouse of Provenance 1 (μ_{p1}=29.0 µm) was significantly smaller than Provenance 2 (μ_{p2}=33.8 µm; p=0.009), and marginally different from provenance 3 (μ_{p3}=32.8 µm; p=0.0596) (Figure 2h; Table 1). Conforming to trends commonly found in the literature (e.g., Brodribb *et al.* 2013), our data show significant negative logarithmic relationships between stomatal density and stomatal pore length in the field and in the greenhouse, though this relationship depends on leaf surface.

Genetic divergence in water-regulatory traits is related to hydrological processes on the landscape

In the common environment, we show that plant biomass is positively related to the dryness index (PET/P) with plants originating from more arid sites showing ~21.3g more biomass for each unit on the dryness index (Figure 3a; N=381, p=0.00025). In the common environment, the stomatal density (stomates/area) of P. angustifolia leaves increases as the atmospheric demand for water (PET) increases at plant site of origin (Figure 3b), though leaves in the field show no significant difference in stomatal density across this gradient (grey line; Figure 3b). Further, higher biomass plants generally have higher water demands that may be reflected in stomatal density. We show that stomatal density is positively correlated to biomass (g) in greenhouse plants, accounting for 80% of the variation (Figure 3c; R^2=0.80, p=0.016). In the field, stomatal ratio appears to be positively related to biomass (kg) of field plants (R^2=0.55, p=0.089).

Water stable isotope compositions

Fitting expectations, our stream water samples overlap the local meteoric water line (LMWL; Figure 4a; Table 2), and the stable isotope compositions from nonsaturated soil

zones plot below the LMWL (Sprenger *et al*. 2016; Figure 4a). Negative lc-excess values for soil samples indicate that the water in the nonsaturated soil zone was exposed to evaporative enrichment, and even more so in Provenance 1 and 2 (Figure 4b; Landwehr & Coplen 2014; Sprenger *et al.* 2016). Also adhering to expectations, we find that lc-excess in the soil is significantly correlated with streamflow in the month prior to collection (May, R^2=0.38, p=0.033) and marginally correlated with mean annual streamflow (R^2=0.297, p=0.066). Though we do not have deep groundwater samples for our sampling locations, groundwater is known to consistently plot along the LMWL (Sprenger *et al.* 2016). We acknowledge that throughfall water may already be enriched when it reaches the nonsaturated soil zone and that tree cover may decrease fractionation processes in soil (Sprenger *et al.* 2016). These stable isotope ratios (Figure 4) combined with mean annual values on the Budyko Curve (Figure 1b) which show higher atmospheric demand for water than the supply of it (PET/P > 1) confirm previous observations that riparian cottonwood forests do not get enough precipitation during the growing season to support the levels of transpiration to meet atmospheric demand (Flanagan *et al.* 2017, Yang *et al*. 2019).

P. angustifolia stem and leaf oxygen and hydrogen isotope compositions are shown in relation to the LMWL (precipitation), stream, and nonsaturated soil in Figure 4a. A linear regression between the stem water isotopes of hydrogen and oxygen has a lower slope than the LMWL suggesting that the water had been evaporatively enriched upon plant use (Figure 4a, Table 2). Though this regression is significant and shows good fit (Table 2; R^2=0.77), regressions of stem isotope compositions split by provenance each show a stronger fit (respectively by provenance, R^2= 0.90, 0.95, 0.96), and different slopes (respectively by provenance, 3.5, 10.4, 3.9; Figure 10 in Appendix 4). Despite this, lc-excess values of stem water do not significantly differ between provenances (Figure 4c). As expected, the slope for leaf isotopic composition is lower than all others, as leaves experience substantial isotopic enrichment during evapotranspiration (Figure 4a, Table 2). Values of lc-excess in leaves are significantly higher in Provenance 3 samples (Figure 4d), supporting local adaptation patterns found in leaf traits (Figure 2) as well as the relationship between AET and stomatal ratio (Figure 5a). Stomatal ratio in the field is significantly

correlated with leaf lc-excess (R^2=0.53, p=0.0076). Deuterium-excess (d-excess) values showed the same patterns as line conditioned excess values (lc-excess).

Our results suggest that *P. angustifolia* populations may draw water from different water sources (stream, soil, or precipitation) and/or may have locally adapted rooting structures as lower lc-excess values often correlate with shallower soil-water use (Sprenger *et al.* 2016). Previous research on *Populus* in Arizona shows that some trees can opportunistically use precipitation water when it is available but rely on groundwater or stream water during dry periods (Snyder & Williams 2000). We acknowledge that drawing comparative inferences from soil and plant stable isotope data across space is cautioned (Goldsmith *et al.* 2019), as is assuming plant accession to specific water sources based on matching isotope compositions (Zhao *et al.* 2016).

Populations' role in the water cycle varies on the landscape

The evaporative index (AET/P) represents the percentage of precipitation water recycled to the atmosphere through plants. Stomatal ratio, in field and greenhouse plants, is related to the evaporative index (AET/P) such that stomatal ratios are lower (more stomates on the bottom of leaves) when a higher percentage of available water is cycled back to the atmosphere in a given location (Figure 5a). Though this relationship holds in both the field and the greenhouse, the relationship is ~11.5% stronger in the field possibly indicating a level of trait plasticity (solid black line; Figure 5a). Despite a greater percentage of precipitation water being used by plants in provenance 1 (EI; Figure 1b), the relationship between AET:PET (Figure 5c) shows that Provenance 1 is furthest from meeting atmospheric demand for water. Further, with the Budyko model assumption that all water falling as precipitation is divided into AET or Q (streamflow), we predicted the fraction of water that should be available as streamflow across the landscapes where the three populations exist and compared that to actual streamflow data derived from the National Hydrology Dataset (NHDPlusV2; McKay *et al.* 2012). Predicted Q/P minus Actual Q/P (Figure 1.5d) shows that Provenance 1, and 2 (on average), hold less water in Q than actually predicted to be in that pool (positive values), whereas Provenance 3 has more water held in Q than predicted (negative values). Positive values indicate that water is "lost" or

held in another pool that is not captured by this model (e.g., in plant biomass) while negative values indicate that water is supplied to the system by means other than precipitation (e.g., snowmelt).

Discussion

Interacting global change gradients

Atmospheric hydrologic model parameters that capture variation in water-energy interactions across landscapes do a 30% better job of explaining patterns of plant biomass than temperature and precipitation in statistical models (Figure 11 in Appendix 4), consistent with predictions that, though derived from temperature, PET should select more strongly than temperature on water-use traits and plant biomass (Wright *et al.* 2004; Siepielski *et al.* 2017). While impossible to simultaneously consider all interacting gradients across a landscape, these hydrologic variables do capture nuances in climatic interactions that independent gradients of temperature and precipitation do not: For example, physical water-energy interactions on the landscape vary across factors such as soil type, vegetation type and cover, and other biotic factors that the metrics in this study inherently capture (Zhang *et al.* 2001; Brown *et al.* 2004; Troch *et al.* 2013; Ambrose & Sterling 2014). Temperature and water on the landscape are fundamental regulators of plant growth, survival, and reproduction (Guisan & Zimmermann 2000) and thus are critical to the functioning and persistence of ecosystems. A 2016 review of plant distribution models revealed that temperature and water-related variables appear in 88.5% of models, but that water-related variables that *depend* on temperature (e.g., evapotranspiration, moisture deficit) appeared in less than 20% of the models (Mod *et al.* 2016). Our results and this identified gap in modeling distributions highlight the importance of including variables that more accurately represent the availability of water in ecosystems and demands for water from the atmosphere. Understanding complex interactions of global change gradients is a significant challenge for modeling the evolutionary (e.g., plant adaptation) and ecosystem consequences (e.g., plant function) of climate change.

Evolution

Variation in water-use traits will determine plant response to changing water availability on the landscape. We show that stomatal traits and plant biomass have evolved among genetic groups of *P. angustifolia* across a landscape gradient of dryness (PET/P). Plants derived from more arid regions (higher dryness index values) produced more biomass in the greenhouse and biomass was positively related to stomatal density (Figure 3c). These results conform to those found previously in *P. trichocarpa, P. balsamifera, and P. angustifolia* (Guy & Gornall 2007; Soolanayakanahally *et al.* 2009). Interestingly, Kaluthota *et al.* 2015 found that differences in density between provenances were not related to aridity (Kaluthota *et al.* 2015) confusing the relationship we found that supports predictions that plants with high stomatal conductance in dry conditions may demonstrate rapid opportunistic biomass production (rate of photosynthesis) during infrequent or short periods of water availability (Snyder & Williams, 2000; Hetherington & Woodward 2003). Conversely, populations derived from regions with historically high water supply may be less able to control water use and be at higher risk to drought-induced mortality (Dudley 2006), though experiments are necessary to confirm these predictions (e.g., Barton *et al.* 2020). Numerous other physiological studies on *Populus* species show that water-stress through reductions in precipitation, groundwater, or streamflow, can lower leaf gas exchange, water potentials, xylem cavitation, stomatal conductance, and net photosynthetic rates (Tyree *et al.* 1994; Horton *et al.* 2001; Rood *et al.* 2003), resulting in morphological changes such as lower biomass production, increased branch sacrifice and crown reduction, leaf size, or stomatal size and number (Rood *et al.* 2000, 2003; Dunlap & Stettler 2001). On the other hand, inundation with water, as would occur with flooding, has been shown to lower net photosynthetic rate, stomatal conductance, transpiration, and growth in *Populus* (Amlin & Rood 2001; Rood *et al.* 2010). Varying responses to these two extremes of water stress, drought, and flooding, emphasize the need to consider population-level responses to multiple aspects of the water cycle.

Global variation in plant growth is predominantly attributed to temperature and water (Babst *et al.* 2019; Bates *et al.* 2008; Jones *et al.* 2012; Lytle & Poff 2004; Milly *et al.* 2005; Poff & Zimmerman 2010). As temperature increases, trees are becoming

increasingly limited by water as the atmospheric demand for water (PET) increases (Novick *et al.* 2016; Babst *et al.* 2019). In relation to landscape water supply and demand, we show biomass and stomatal traits differ between field and greenhouse trees, suggesting that plasticity in these correlated traits may also vary on the landscape. Though, whether there are genetically-based differences in phenotypic plasticity requires further study (e.g., Barton *et al.* 2020) of population tolerance to environmental conditions as well as their capacity to display a range of phenotypes (Nicotra *et al.* 2010). If plastic, variation in these traits could affect population responses to a changing climate – either buffering against rapid environmental change or assisting in adaptation (Lande 2009; Chevin *et al.* 2010; Nicotra *et al.* 2010); could modify the strength and direction of plant-atmosphere feedbacks.

Feedback

Much variation in ecosystem function depends on the metabolic – often adaptive – characteristics of individual organisms, which are governed by laws of mass and energy balance (Brown *et al.* 2004). Above, we discussed how large-scale mass-energy relationships of the water cycle drive the evolution of plant populations to control water use (Figure 3a; 3b). These trait differences surely manifest in the observed landscape patterns seen in 1) actual evapotranspiration (AET) on the landscape (Figure 5a); 2) the relationship between AET and PET on the landscape (Figure 5c); and 3) predictions of Q on the landscape (Figure 5d). Transpiration totals, on average, 80% - 90% of evapotranspiration on the landscape (Jasechko *et al.* 2013), such that these genetically-based trait divergences across plant populations (Figure 2) should cause populations to respond, and feedback, differently to water and energy availability. Because the water cycle is influenced significantly by genetically based plant traits, we demonstrate how among-population level evolutionary processes can result in variation in plant-atmosphere feedbacks on a geographic scale. All other work at this scale has been in the context of plant-soil relationships (Van Nuland *et al.* 2016, 2017, 2019; Senior *et al.* 2018; Ware *et al.* 2019a). In drought conditions, the ability of plants to control water can alter feedbacks to the atmosphere (AET), while the ability of plants to opportunistically obtain water from

different sources (e.g., Snyder & Williams 2000) may alter stream flow (Q) and entire stream ecosystems.

Scaling ecosystem feedbacks to global processes is a difficult challenge for ecosystem ecologists yet is crucial for understanding how populations are spatially distributed and the selective forces that act on the populations. Functional traits of organisms generally vary across large environmental gradients making it likely that similar feedbacks are common due to the interaction between environmental gradients and legacy effects of trait-based species interactions (Van Nuland *et al.* 2019; Ware *et al.* 2019; Fitzpatrick *et al.* 2019). A separate exploration of the Budyko model revealed plant adaptations to be simultaneously a cause and consequence of the water cycle, showing how rooting structure and transpiration efficiency have adapted to the dryness index (Gentine *et al.* 2012) – plant adaptations can profoundly control the annual water cycle, revealing mechanisms for eco-evolutionary feedbacks (Eagleson 1978; Eagleson & Tellers 1982; Gentine *et al.* 2012). Similarly, soil moisture in zones of hybrid *Populus* (cross between parent species *P. angustifolia* and *P. fremontii*) was found to be lower than in adjacent zones dominated by the parent species (Schweitzer *et al.* 2002), reinforcing that genetically-based differences in transpiration rates (Fischer *et al.* 2004) and water-use traits (shown here) can be the basis for discovering feedbacks between population genetic variation and long-term variation in ecosystem fluxes of energy and water across large landscapes.

Implications

Increased drought conditions are predicted to become more widespread and more severe in many geographic locations (Famiglietti 2014; Georgakakos *et al.* 2014; Milly *et al.* 2005). The western U.S. is currently experiencing a 1000-year drought threatening the most diverse ecosystems in the desert (riparian ecosystems) with widespread mortality (Gitlin *et al.* 2006; Kominoski *et al.* 2013). Occurring at the terrestrial-freshwater interface (Naiman & Décamps 1997), riparian ecosystems are likely to be affected by changes to many aspects of the water cycle, such as streamflow or the atmospheric demand for water, as well as precipitation (Lytle & Poff 2004; Milly *et al.* 2005; Perry *et al.* 2012; Poff & Zimmerman

2010; Rood *et al.* 2003). Though threatened, these systems may be "hotspots" for adaptation to climate change as they historically have been highly exposed to extremes of these various climatic stimuli (Capon *et al.* 2013). We demonstrated that biomass and stomatal traits, estimates of carbon acquisition, primary productivity, and water-use efficiency (Cornelissen *et al.* 2003), differ across populations of an foundational riparian tree. These adaptations are important for the plant and the entire ecosystem to deal with drought (Aasamaa *et al.* 2002; Cornelissen *et al.* 2003; Hetherington & Woodward 2003; Sack *et al.* 2006). In drought conditions, the ability of plants to control water may alter feedbacks to the atmosphere (AET; Figure 5a-c), while the ability of plants to obtain water from different sources may alter stream flow (Q; Figure 5b; 5d) and the greater stream ecosystem.

Chapter conclusions

Integrating ecohydrology and landscape-level genetic variation using the theoretical Budyko Curve allowed us to consider fluxes of energy and matter, interacting climatic gradients, and population genetic structure together to understand linkages between large-scale hydrologic processes and evolutionary processes. The model accounts for interactions between temperature and water which enact long-term selection pressures on plant traits and captures the key role plants play in the ecosystem through recycling water to the atmosphere. Combined, results indicate a landscape-scale feedback, and provide information about where populations and watersheds may be at risk and where ecosystem processes may be stable.

REFERENCES

Aasamaa K, Sõber A, Rahi M. 2001. Leaf anatomical characteristics associated with shoot hydraulic conductance, stomatal conductance and stomatal sensitivity to changes of leaf water status in temperate deciduous trees. *Aust. J. Plant Physiol.* 28: 765-774.

Ambrose SM, Sterling SM. 2014. Global patterns of annual actual evapotranspiration with land-cover type: knowledge gained from a new observation-based database. *Hydrol. Earth Syst. Sci. Discuss.* 11: 12103-12135.

Amlin NA, Rood SB. 2001. Inundation Tolerances of Riparian Willows and Cottonwoods. *JAWRA* 37(6): 1709-1720.

Babst F, Bouriaud O, Poulter B, Trouet V, Girardin MP, Frank DC. 2019. Twentieth century redistribution in climatic drivers of global tree growth. *Sci. Adv.* 5: eaat4313.

Barton KE, Jones C, Edwards KF, Shiels AB, Knight T. 2020. Local Adaptation constrains drought tolerance in a tropical foundation tree. *Ecology* 00:1-13.

Bates BC, Kundzewicz ZW, Wu S, Palutikof JP. 2008. Climate Change and Water. Technical Paper of the Intergovernmental Panel on Climate Change, IPCC Secretariat, Geneva, 210.

Bates D, Maechler M, Bolker B, Walker S, Maechler Martin, Walker S. 2015. Package 'lme4': Linear Mixed-Effects Models using 'Eigen' and S4. J. *Stat. Softw.* 67.

Beier C, Beierkuhnlein C, Wohlgemuth T, Penuelas J, Emmett B, Körner C, de Boeck H, Christensen JH, Leuzinger S, Janssens IA, et al. 2012. Precipitation manipulation experiments - challenges and recommendations for the future. *Ecol. Lett.* 15: 899-911.

Benito Garzón M, Robson TM, Hampe A. 2019. ΔTraitSDMs: species distribution models that account for local adaptation and phenotypic plasticity. *New Phytol.* doi: 10.1111/nph.15716

Bertolino LT, Caine RS, Gray JE. 2019. Impact of Stomatal Density and Morphology on Water-Use Efficiency in a Changing World. *Front. Plant Sci.* 10:225.

Bowen GJ, Wassenaar LI, Hobson KA. 2005. Global application of stable hydrogen and oxygen isotopes to wildlife forensics. *Oecologia* 143: 337-348.

Bowen, GJ. 2019. The Online Isotopes in Precipitation Calculator, version 3.1. http://www.waterisotopes.org.

Bradie J, Leung B. 2017. A quantitative synthesis of the importance of variables used in MaxEnt species distribution models. *J. Biogeogr.* 44: 1344-1361.

Brodribb TJ, Jordan GJ, Carpenter RJ. 2013. Unified changes in cell size permit coordinated leaf evolution. *New Phytol.* 199: 559-570.

Brown JH, Gillooly JF, Allen AP, Savage VM, West GB. 2004. Toward a metabolic theory of ecology. *Ecology* 85(7): 1771-1789.

Budyko M. 1974. Climate and Life. New York, NY: Academic Press.

Burrows MT, Schoeman DS, Buckley LB, Moore P, Poloczanska ES, Brander KM, Brown C, Bruno JF, Duarte CM, Halpern BS, et al. 2011. The Pace of Shifting Climate in Marine and Terrestrial Ecosystems. *Science* 334: 652-655.

Capon SJ, Chambers LE, Mac Nally R, Naiman RJ, Davies P, Marshall N, Pittock J, Reid M, Capon T, Douglas M, et al. 2013. Riparian Ecosystems in the 21st Century: Hotspots for Climate Change Adaptation? *Ecosystems* 16: 359-381.

Chevin L-M, Lande R, Mace GM. 2010. Adaptation, plasticity, and extinction in a changing environment: Towards a predictive theory. *PLOS Biol.* 8(4): e1000357.

Chojnacky DC, Heath LS, Jenkins JC. 2014. Updated generalized biomass equations for North American tree species. *Forestry* 87: 129-151.

Cornelissen JHC, Lavorel S, Garnier E, Díaz S, Buchmann N, Gurvich DE, Reich PB, Steege H ter, Morgan HD, Heijden MGA van der, et al. 2003. A handbook of protocols for standardised and easy measurement of plant functional traits worldwide. *Aust. J. Bot.* 51(4): 335-380.

Cowan IR, Farquhar GD. 1977. Stomatal function in relation to leaf metabolism and environment. *Symposia of the Society for Experimental Biology* 31: 471-505.

Craig H. 1961. Isotopic Variations in Meteoric Waters. *Science* 133: 1702-1703.

Creed IF, Spargo AT, Jones JA, Buttle JM, Adams MB, Beall FD, Booth EG, Campbell JL, Clow D, Elder K, *et al*. 2014. Changing forest water yields in response to climate warming: results from long-term experimental watershed sites across North America. *Glob. Change Biol*. 20: 3191–3208.

Dansgaard W. 1964. Stable isotopes in precipitation. *Tellus* 16(4): 436-468.

Dudley SA. 1996. Differing Selection on Plant Physiological Traits in Response to Environmental Water Availability: A Test of Adaptive Hypotheses. *Evolution* 50(1): 92-102.

Dunlap JM, Stettler RF. 2001. Variation in leaf epidermal and stomatal traits of *Populus trichocarpa* from two transects across the Washington Cascades. *Can. J. Bot.* 79: 528–536.

Eagleson PS. 1978. Climate, soil, and vegetation: 1. Introduction to water balance dynamics. *Water Resour. Res.* 14(5): 705-712.

Eagleson PS, Tellers TE. 1982. Ecological Optimality in Water-Limited Natural Soil-Vegetation Systems: 2. Tests and Applications. *Water Resour. Res.* 18(2): 341-354.

Eller CB, Rowland L, Oliveira RS, Bittencourt PRL, Barros F V, da Costa ACL, Meir P, Friend AD, Mencuccini M, Sitch S, Cox P. 2018. Modelling tropical forest responses to drought and El Niño with a stomatal optimization model based on xylem hydraulics. *Phil. Trans. R. Soc. B.* 373: 20170315.

Evans LM, Allan GJ, Difazio SP, Slavov GT, Wilder JA, Floate KD, Rood SB, Whitham TG. 2015. Geographical barriers and climate influence demographic history in narrowleaf cottonwoods. *Heredity* 114: 387-396.

Evans LM, Kaluthota S, Pearce DW, Allan GJ, Floate K, Rood SB, Whitham TG. 2016. Bud phenology and growth are subject to divergent selection across latitudinal gradient in *Populus angustifolia* and impact adaptation across the distributional range and associated arthropods. *Ecol. Evol.* 6(13): 4565-4581.

Famiglietti JS. 2014. The global groundwater crisis. Nature Climate Change 4: 945-948.

Fick SE, Hijmans RJ, 2017. Worldclim 2: new 1-km spatial resolution climate surfaces for global land areas. *Int. J. Climatol.* 37: 4302-4315.

Fischer DG, Hart SC, Whitham TG, Martinsen GD, Keim P. 2004. Ecosystem implications of genetic variation in water-use of a dominant riparian tree. *Oecologia* 139(2): 288-297.

Fox J, Weisberg S, Adler D, Bates D, Baud-Bovy G, Ellison S, Firth D, Friendly M, Gorjanc G, Graves S, et al. 2018. car: Companion to Applied Regression. In: R Package Version 2.0-21.

Gentine P, D'Odorico P, Lintner BR, Sivandran G, Salvucci G. 2012. Interdependence of climate, soil, and vegetation as constrained by the Budyko curve. *Geophys. Res. Lett.* 39(19): L19404.

Georgakakos A, Fleming P, Dettinger M, Peters-Lidard C, Richmond T, Reckhow K, White K, Yates D. 2014. Ch. 3: Water Resources. Climate Change Impacts in the United States: The Third National Climate Assessment. JM Melillo, Terese (TC) Richmond, GW Yohe, Eds., U.S. Global Change Research Program, 69-112.

Gitlin AR, Sthultz CM, Bowker MA, Stumpf S, Paxton KL, Kennedy K, Muñoz A, Bailey JK, Whitham TG. 2006. Mortality Gradients within and among Dominant Plant Populations as Barometers of Ecosystem Change During Extreme Drought. *Conserv. Biol.* 20(5):1477-1486.

Goldsmith GR, Allen ST, Braun S, Engbersen N, González-Quijano CR, Kirchner JW, Siegwolf RTW. 2019. Spatial variation in throughfall, soil, and plant water isotopes in a temperate forest. *Ecohydrol.* 12:e2059.

Gotelli NJ, Stanton-Geddes J. 2015. Climate change, genetic markers and species distribution modelling. *J. Biogeogr.* 42: 1577-1585.

Grossiord C, Buckley TN, Cernusaka LA, Novick KA, Poulter B, Siegwolf RTW, Sperry JS, McDowell NG. 2020. Plant responses to rising vapor pressure deficit. *New Phytol.* 226: 1150-1566.

Guisan A, Zimmermann NE. 2000. Predictive habitat distribution models in ecology. *Ecol. Model.* 135(2-3): 147-186.

Guy RD, Gornall JL. 2007. Geographic variation in ecophysiological traits of black cottonwood (*Populus trichocarpa). Canadian Journal of Botany* 85: 1202-1213

Hamanishi ET, Thomas BR, Campbell MM. 2012. Drought induces alterations in the stomatal development program in *Populus*. J. Exp. Bot. 63(13): 4959-4971.

Hendry AP. 2017. Eco-evolutionary Dynamics. Princeton (New Jersey): Princeton University Press. ISBN: 978-0-691-14543-3. 2017.

Hetherington AM, Woodward FI. 2003. The role of stomata in sensing and driving environmental change. *Nature* 424: 901-908.

Hothorn T, Bretz F, Westfall P. 2008. Simultaneous Inference in General Parametric Models. *Biometrical J.* 50: 346-363.

Horton JL, Kolb TE, Hart SC. 2001. Physiological Response to Groundwater Depth Varies among Species and with River Flow Regulation. *Ecol. Appl.* 11(4): 1046–1059.

Jasechko S, Sharp ZD, Gibson JJ, Birks SJ, Yi Y, Fawcett PJ. 2013. Terrestrial water fluxes dominated by transpiration. *Nature* 496: 347–351.

Jones JA, Creed IF, Hatcher KL, Warren RJ, Adams MB, Benson MH, Boose E, Brown WA, Campbell JL, Covich A, et al. 2012. Ecosystem Processes and Human Influences Regulate Streamflow Response to Climate Change at Long-Term Ecological Research Sites. *BioScience* 62(4): 390-404.

Kaluthota S, Pearce DW, Evans LM, Letts MG, Whitham TG, Rood SB. 2015. Higher photosynthetic capacity from higher latitude: foliar characteristics and gas exchange of southern, central and northern populations of *Populus angustifolia*. *Tree Physiol.* 35: 936-948.

Kawecki TJ, Ebert D. 2004. Conceptual issues in local adaptation. *Ecol. Lett.* 7:1225-1241

Kominoski JS, Shah JJF, Canhoto C, Fischer DG, Giling DP, González E, Griffiths NA, Larrañaga A, Leroy CJ, Mineau MM, et al. 2013. Forecasting functional implications of global changes in riparian plant communities. *Front. Ecol. Environ.* 11(8): 423-432.

Lande R. 2009. Adaptation to an extraordinary environment by evolution of phenotypic plasticity and genetic assimilation. *J. Evol. Biol.* 22: 1435-1446.

Landwehr JM, Coplen TB. 2014. Spatial, seasonal, and source variability in the stable oxygen and hydrogen isotopic composition of tap waters throughout the USA. *Hydrol. Process.* 28(21): 5382-5422.

Leimu R, Fischer M. 2008. A meta-analysis of local adaptation in plants. *PLoS One* 3: e4010.

Lytle DA, Poff NL. 2004. Adaptation to natural flow regimes. *Trends Ecol. Evol.* 19(2): 94-100.

McAdam SAM, Brodribb TJ. 2014. Separating Active and Passive Influences on Stomatal Control of Transpiration. *Plant Physiol.* 164: 1578-1586.

McKay L, Bondelid T, and Dewald T. 2012. NHDPlus Version 2: User Guide. U.S. EPA and USGS.

Milly PCD, Dunne KA, Vecchia AV. 2005. Global pattern of trends in streamflow and water availability in a changing climate. *Nature Letters* 438: 347-350.

Mitton JB, Grant MC, Yoshino AM. 1998. Variation in allozymes and stomatal size in pinyon (Pinus edulis, Pinaceae), associated with soil moisture. *Am. J. Bot.* 85(9): 1262–1265.

Mod HK, Scherrer D, Luoto M, Guisan A. 2016. What we use is not what we know: environmental predictors in plant distribution models. *J. Veg. Sci*. 27: 1308-1322.

Naeem S, Duffy JE, Zavaleta E. 2012. The Functions of Biological Diversity in an Age of Extinction. *Science* 336: 1401-1406.

Naiman and RJ, Décamps H. 1997. The Ecology of Interfaces: Riparian Zones. *Annu. Rev. Ecol. Evol. Syst.* 28: 621-658.

Nicotra AB, Atkin OK, Bonser SP, Davidson AM, Finnegan EJ, Mathesius U, Poot P, Purugganan MD, Richards CL, Valladares F, et al. 2010. Plant phenotypic plasticity in a changing climate. *Trends Plant Sci.* 15(12): 684-692.

Novick KA, Ficklin DL, Stoy PC, Williams CA, Bohrer G, Oishi AC, Papuga SA, Blanken PD, Noormets A, Sulman BN, et al. 2016. The increasing importance of atmospheric demand for ecosystem water and carbon fluxes. *Nat. Clim. Change* 6: 1023-1027.

Oren R, Sperry JS, Katul GG, Pataki DE, Ewers BE, Phillips N, Schäfer KVR. 1999. Survey and synthesis of intra- and interspecific variation in stomatal sensitivity to vapour pressure deficit. *Plant Cell Environ.* 22: 1515-1526.

Parmesan C. 2006. Ecological and Evolutionary Responses to Recent Climate Change. *Annu. Rev. Ecol. Evol. Syst.* 37:637-669.

Pearce DW, Millard S, Bray DF, Rood SB. 2005. Stomatal characteristics of riparian poplar species in a semi-arid environment. *Tree Physiol.* 26: 211-218.

Perry LG, Andersen DC, Reynolds LV, Nelson SM, Shafroth PB. 2012. Vulnerability of riparian ecosystems to elevated CO2 and climate change in arid and semiarid western North America. *Glob. Change Biol.* 18: 821–842.

Peterson ML, Doak DF, Morris WF. 2019. Incorporating local adaptation into forecasts of species' distribution and abundance under climate change. *Glob. Change Biol.* 25(3): 775-793.

Poff NL, Zimmerman JKH. 2010. Ecological responses to altered flow regimes: a literature review to inform the science and management of environmental flows. *Freshw. Biol.* 55: 194–205.

R Development Core Team. 2016. R: A language and environment for statistical computing. R Foundation for Statistical Computing.

Rodriguez-Iturbe I, Porporato A. 2005. Ecohydrology of water-controlled ecosystems: Soil moisture and plant dynamics. Cambridge University Press.

Rood SB, Patiño S, Coombs K, Tyree MT. 2000. Branch sacrifice: Cavitation-associated drought adaptation of riparian cottonwoods. *Trees* 14: 248–257.

Rood SB, Braatne JH, Hughes FMR. 2003. Ecophysiology of riparian cottonwoods: Stream flow dependency, water relations and restoration. *Tree Physiol.* 23: 1113–1124.

Rood SB, Nielsen JL, Shenton L, Gill KM, Letts MG. 2010. Effects of flooding on leaf development, transpiration, and photosynthesis in narrowleaf cottonwood, a willow-like poplar. *Photosynth. Res.* 104: 31-39.

Sack L, Melcher PJ, Liu WH, Middleton E, Pardee T. 2006. How strong is intracanopy leaf plasticity in temperate deciduous trees? *Am. J. Bot.* 93(6): 829-839.

Schaeffer SM, Williams DG, Goodrich DC. 2000. Transpiration of cottonwood/willow forest estimated from sap flux. *Agric. For. Meteorol.* 105: 257-270.

Schneider, C.A., Rasband, W.S., Eliceiri, K.W. 2012. NIH Image to ImageJ: 25 years of image analysis. *Nat. Methods* 9: 671-675.

Schweitzer JA, Martinsen GD, Whitham TG. 2002. Cottonwood hybrids gain fitness traits of both parents: A mechanism for their long-term persistence? *Am. J. Bot.* 89(6): 981-990.

Senior JK, Potts BM, O'Reilly-Wapstra JM, Bissett A, Wooliver RC, Bailey JK, Glen M, Schweitzer JA. 2018. Phylogenetic trait conservatism predicts patterns of plant-soil feedback. *Ecosphere* 9(10): e02409.

Siepielski AM, Morrissey MB, Buoro M, Carlson SM, Caruso CM, Clegg SM, Coulson T, Dibattista J, Gotanda KM, Francis CD, et al. 2017. Precipitation drives global variation in natural selection. *Science* 355: 959–962.

Snyder KA, Williams DG. 2000. Water sources used by riparian trees varies among stream types on the San Pedro River, Arizona. Agric. For. Meteorol. 105: 227-240.

Soolanayakanahally RY, Guy RD, Silim SN, Drewes EC, Schroeder WR. 2009. Enhanced assimilation rate and water use efficiency with latitude through increased photosynthetic capacity and internal conductance in balsam poplar *(Populus balsamifera L.). Plant Cell Environ*. 32: 1821-1832.

Sposito G. 2017. Understanding the Budyko Equation. *Water* 9: 236.

Sprenger M, Leistert H, Gimbel K, Weiler M. 2016. Illuminating hydrological processes at the soil-vegetation-atmosphere interface with water stable isotopes. *Rev. Geophys*. 54: 674–704.

Thompson JN. 2005. Coevolution: The geographic mosaic of coevolutionary arms races. Current Biology.

Trabucco A, Zomer RJ. 2009. Global Aridity Index (Global-Aridity) and Global Potential Evapo-Transpiration (Global-PET) Geospatial Database. CGIAR Consortium for Spatial Information. Published online, available from CGIAR-CSI GeoPortal at: http://www.csi.cgiar.org.

Trenberth KE, Fasullo JT, Kiehl J. 2009. Earth's global energy budget. *Bull. Amer. Meteor. Soc.* 90(3): 311-324.

Troch PA, Carrillo G, Sivapalan M, Wagener T, Sawicz K. 2013. Climate-vegetation-soil interactions and long-term hydrologic partitioning: Signatures of catchment co-evolution. *Hydrol. Earth Syst. Sci.* 17(6): 2209-2013.

Tyree MT, Kolb KJ, Rood SB, Patino S. 1994. Vulnerability to drought-induced cavitation of riparian cottonwoods in Alberta: A possible factor in the decline of the ecosystem? *Tree Physiol.* 14(5): 455–466.

Urban MC. 2015. Accelerating extinction risk from climate change. *Science* 438(6234): 571-573.

Van Nuland ME, Bailey JK, Schweitzer JA. 2017. Divergent plant-soil feedbacks could alter future elevation ranges and ecosystem dynamics. *Nat. Ecol. Evol*. 1, 0150.

Van Nuland ME, Ware IM, Bailey JK, Schweitzer JA. 2019. Ecosystem feedbacks contribute to geographic variation in plant–soil eco-evolutionary dynamics across a fertility gradient. *Funct. Ecol.* 33(1): 95-106.

Van Nuland ME, Wooliver RC, Pfennigwerth AA, Read QD, Ware IM, Mueller L, Fordyce JA, Schweitzer JA, Bailey JK. 2016. Plant-soil feedbacks: connecting ecosystem ecology and evolution (C Fox, Ed.). *Funct. Ecol.* 30: 1032–1042.

Wang K, Dickinson RE. 2012. A review of global terrestrial evapotranspiration: Observation, modeling, climatology, and climatic variability. *Rev. Geophys.* 50(2).

Ware IM, Fitzpatrick CR, Senthilnathan A, Bayliss SLJ, Beals KK, Mueller LO, Summers JL, Wooliver RC, Van Nuland ME, Kinnison MT, et al. 2019a. Feedbacks link ecosystem ecology and evolution across spatial and temporal scales: Empirical evidence and future directions. *Funct. Ecol.* 33: 31-42.

Ware IM, Van Nuland ME, Schweitzer JA, Yang Z, Schadt CW, Sidak-Loftis LC, Stone NE, Busch JD, Wagner DM, Bailey JK. 2019b. Climate-driven reduction of genetic variation in plant phenology alters soil communities and nutrient pools. *Glob. Change Biol.* 25: 1514-1528.

Welker JM. 2000. Isotopic (δ18O) characteristics of weekly precipitation collected across the USA: An initial analysis with application to water source studies. *Hydrol. Process.* 14(8): 1449-1464.

Wright IJ, Reich PB, Westoby M, Ackerly DD, Baruch Z, Bongers F, Cavender-Bares J, et al. 2004. The worldwide leaf economics spectrum. *Nature* 428: 821-827.

Yang H, Rood SB, Flanagan LB. 2019. Controls on ecosystem water-use and water-use efficiency: insights from a comparison between grassland and riparian forest in the northern Great Plains. Agric. For. Meteorol. 271: 22-32.

Zhang L, Dawes WR, Walker GR. 2001. Response of mean annual evapotranspiration to vegetation changes at catchment scale. *Water Resour. Res.* 37: 701–708.

Zhao L, Wang L, Cernusak LA, Liu X, Xiao H, Zhou M, Zhang S. 2016. Significant Difference in Hydrogen Isotope Composition Between Xylem and Tissue Water in *Populus Euphratica*. *Plant Cell Environ.* 39: 1848-1857.

APPENDIX 1

Table 1. Summary of the linear mixed effects model rankings for determining importance of provenance for biomass, stomatal density, distribution (ratio), and size (abaxial pore length) in the field [F] and in the greenhouse [GH]. River is included as random effect for all models. Genotype is also included as a random effect for stomatal models.

Trait	Model Rank	Main Effects	AIC	Chisq, df	P (>Chisq)
[GH] Biomass	1 2	Provenance Null	4653.1 4667.1	17.99,2	**0.000124**
[GH] Stomatal Density	1 2	Provenance Null	785.9 791.94	10.04,2	**0.0066**
[GH] Stomatal Ratio	1 2	Provenance Null	-19.785 -19.233	4.563,2	0.102
[GH] Abaxial Pore Length	1 2	Provenance Null	168.14 168.9	4.755,2	0.093
[F] Biomass	1 2	Provenance Null	2140.8 2144.1	7.273,2	**0.0263**
[F] Stomatal Density	1 2	Provenance Null	874.97 872.62	1.646,2	0.439
[F Stomatal Ratio	1 2	Provenance Null	-138.44 -129.94	12.502,2	**0.00193**
[F] Abaxial Pore Length	1 2	Provenance Null	161.16 164.34	7.181,2	**0.0280**

Table 2: Summary of linear regression parameters for the relationship between oxygen (δ18O) and hydrogen isotopes (δ2H). Parameters are represented for precipitation (lmwl), stream, soil, stem, and leaf samples.

Sample	Slope	Intercept	R^2
lmwl	7.01	3.77	0.988
stream	7.39	2.30	0.983
soil	4.45	-53.6	0.824
stem	5.65	-38.1	0.771
leaf	3.22	-72.5	0.954

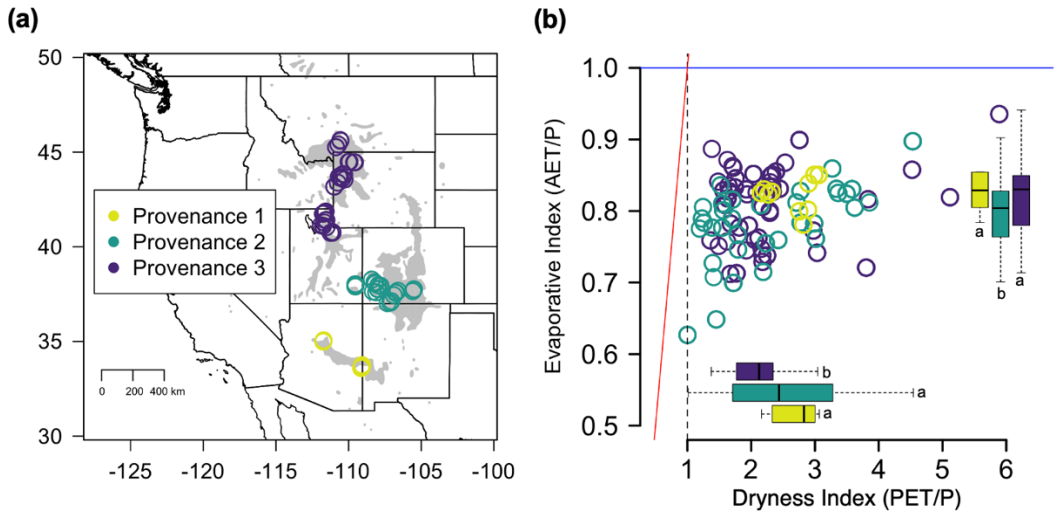

Figure 1. Map of field collection sites, genetic provenances, and geographic range of *Populus angustifolia* (a) and field collection sites within the 17 *Populus angustifolia* populations plotted with Budyko Model Parameters (b). Each point represents a unique sampling location: there are multiple collection sites within each of the 17 populations of the three genetic provenances (provenance represented by color). AET= Actual Evapotranspiration; P= Precipitation; PET= Potential Evapotranspiration. The blue line represents a water-limit (AET = P), at which 100% of water supplied to the landscape as precipitation (P) is cycled back to the atmosphere through evapotranspiration (AET). The red line represents an energy-limit (AET=PET), at which the amount of water recycled to the atmosphere through evapotranspiration (AET) meets the atmospheric demand for water (PET). Genetic provenance is represented by color as in panel A. Points are plotted using observed values of mean annual P, PET, and AET from georeferenced locations of field collection sites. Inset boxplots show provenance differences in the two Budyko parameters, with letters referring to statistically significant differences between provenances from post-hoc Tukey Contrasts.

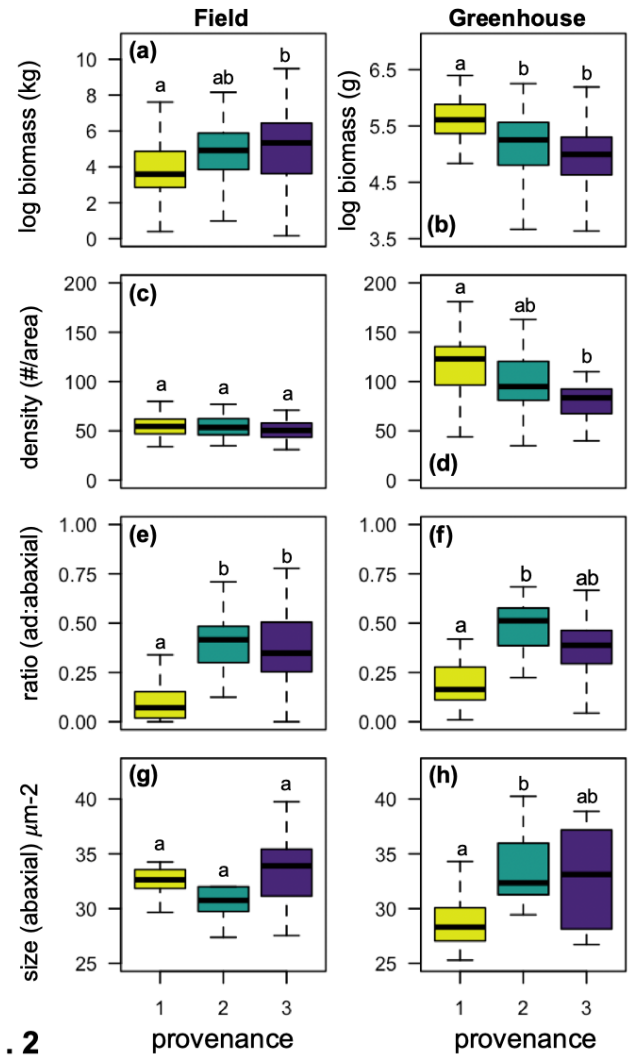

Figure 2. Genetic provenances of *Populus angustifolia* differ in traits relating to water-use and ecosystem function. Letters refer to statistically significant differences between provenances from post-hoc Tukey Contrasts. Note the difference in y-axis scale between field and greenhouse biomass. (a) Field Biomass (kg), log transformed ($Prov_{3-1}$ p=0.018); (b) Greenhouse Biomass (g), log transformed ($Prov_{2-1}$ p=0.001; $Prov_{3-1}$ p<0.001); (c) Field Stomatal Density (#/area); (d) Greenhouse Stomatal Density (#/area; $Prov_{3-1}$ p<0.001); (e) Field Stomatal Ratio (ad:abaxial; $Prov_{2-1}$ p<0.001; $Prov_{3-1}$ p<0.001); (f) Greenhouse Stomatal Ratio (ad:abaxial; $Prov_{2-1}$ p=0.068); (g) Field Abaxial Stomatal Pore Length (μm); (h) Greenhouse Abaxial Stomatal Pore Length (μm; $Prov_{2-1}$ p=0.009; $Prov_{3-1}$ p=0.059).

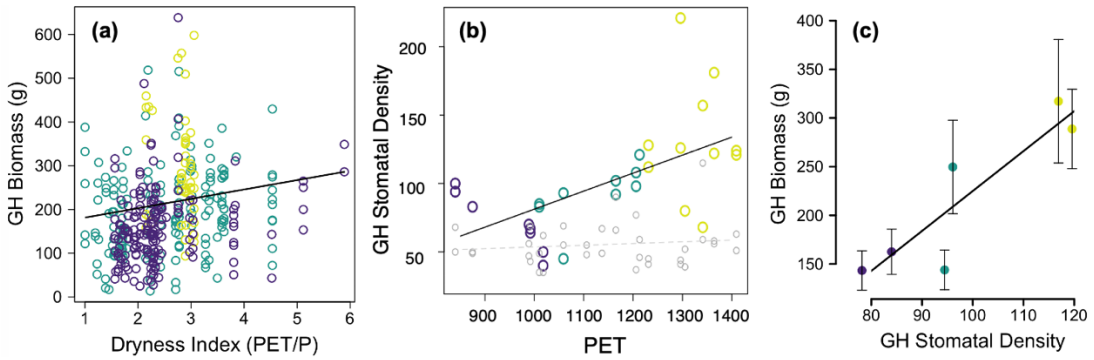

Figure 3. Water-regulatory traits related to hydrologic variables on the landscape. (a) Greenhouse biomass (g) of *Populus angustifolia* increases with Dryness Index (PET/P) (estimate=160.6, slope=21.3, N=381, p=0.00025); (b) Greenhouse stomatal density increases with atmospheric demand (PET); Field stomatal density does not (grey dotted line and points); (c) Genetic Trait Correlation. Population means and standard errors of greenhouse stomatal density and biomass (R^2=0.80, p=0.016). Provenance color follows Figure 1 for all panels.

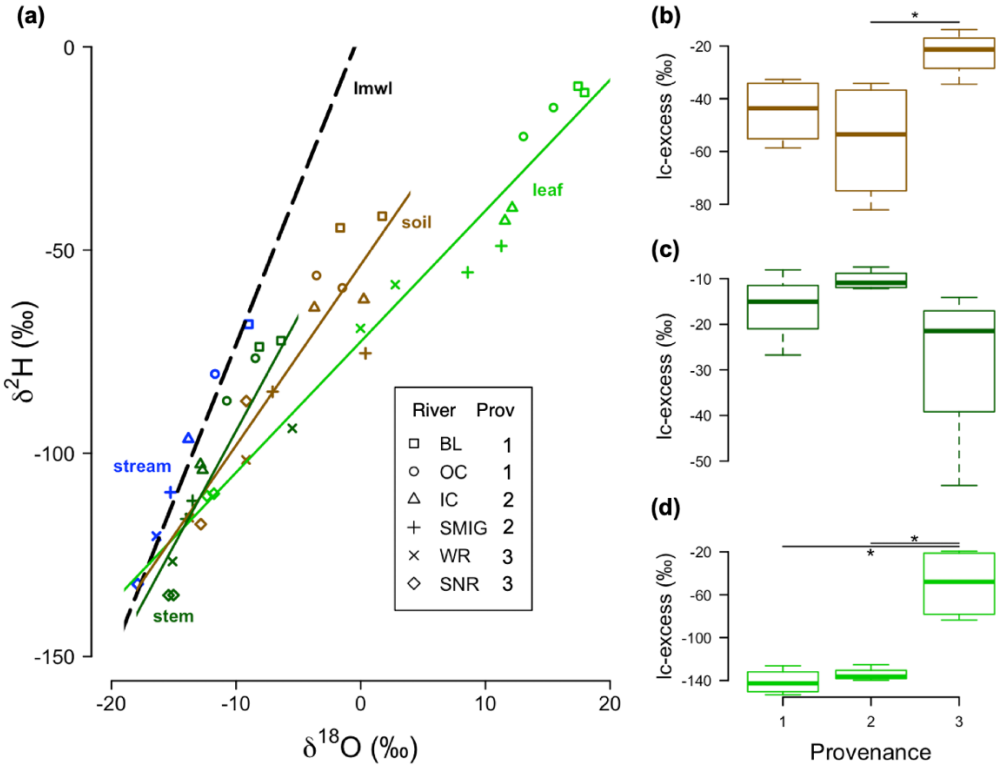

Figure 4. (a) Dual isotope plot comparing stable oxygen ($^{18}O/^{16}O$) and hydrogen ($^{2}H/^{1}H$) ratios (expressed per mille). The local meteoric water line (LMWL) representing isotopic composition of precipitation in June is represented by the dotted black line (y = 7.01x + 3.77, R^2 = 0.99). Blue points represent stream samples collected at the mid-elevation site along each of the six rivers. Soil (brown line; y = 4.45x – 53.6, R^2 = 0.82), *P. angustifolia* stem (dark green; y = 5.65x – 38.07, R^2 = 0.77) and leaf (light green; y = 3.22x -72.52, R^2 = 0.95) samples are also represented. Populations are represented by symbols. Line conditioned excess values for soil (b), stem (c), and leaf (d) samples by provenance. Asterisks refer to statistically significant differences between provenances.

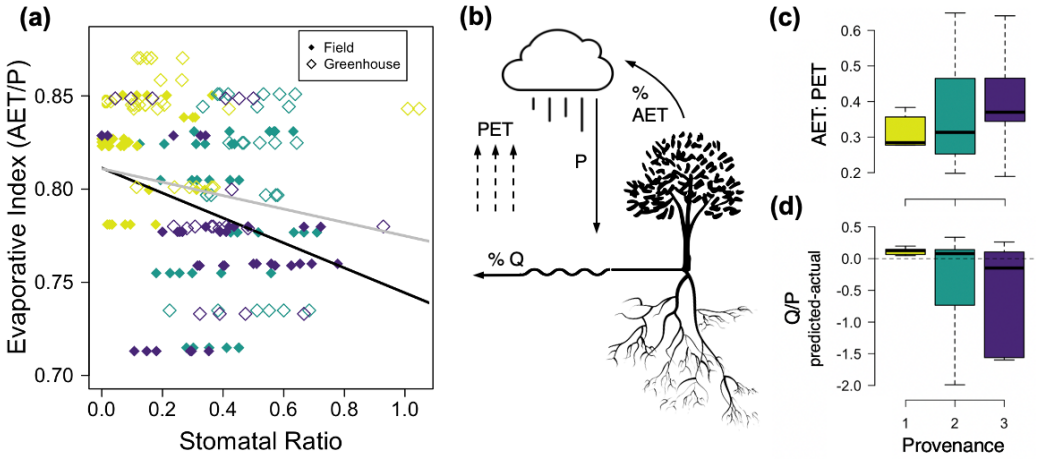

Figure 5. Landscape-Vegetation-Atmospheric Feedback. (a) The Evaporative Index (AET/P) is significantly related to stomatal ratio in the field (filled diamonds, black line; R^2= -0.35, df=106, p=0.00023) and in the greenhouse (open diamonds, grey line; R^2= -0.23, df=77, p=0.039); (b) Conceptual figure representing role of vegetation in the water cycle; (c) The ratio of actual evapotranspiration (AET) to potential evapotranspiration (PET) indicates the relationship between water-use on the landscape and atmospheric demand for water. The higher the ratio, the closer the landscape is to meeting the atmospheric demand for water; (d) Difference between predicted and actual streamflow, standardized by precipitation. Predicted streamflow standardized by precipitation was calculated as 1-[AET/P].

CHAPTER II
POPULATION-RANGE MODELS OUTPERFORM SPECIES-RANGE MODELS IN PREDICTING GEOGRAPHIC DISTRIBUTIONS

Abstract

Identifying and predicting how plant and animal species ranges will change in response to climate change is paramount for conservation and restoration. Ecological niche models (SDMs) are the most commonly used method to estimate potential distributions of species, but models traditionally omit knowledge that intraspecific variation can allow populations to respond uniquely to global change. Here, we test the extent to which population X environment relationships influence model predictions of suitable conditions and geographic distributions by manipulating the geographic training extent of models based on knowledge of genetic substructure. As hypothesized, the traditionally built species-range model provides broad projections of suitable conditions: when compared to models based on intraspecific genetic structure, the species-range models over-predicted extent of suitable conditions by as much as 62% and 87%, depending on the choice of environmental variables. SDMs are generally thought to increase in utility with the inclusion of genetic information, though it is rarely incorporated. This study also emphasizes the great extent to which these improvements depend on the type and selection of predictor variables, which has broad implications for predicting population-level ecological and evolutionary responses to climate change.

Introduction

Distribution models are a valuable tool for predicting species range dynamics in response to environmental changes, but an overwhelming number of species distribution models (SDMs) ignore intraspecific variation (reviewed in Benito Garzón et al. 2019; Peterson, Doak, & Morris 2019). This is highly problematic given the rate of climate change (Parmesan 2006, Burrows et al. 2011), advances in eco-evolutionary theory, and the frequency of distribution model use in the literature. Consequently, models disregard key genotype-by-environment (G x E) and biotic (G x G) interactions across landscapes (G x G x E; Bailey et al. 2014, Van Nuland et al. 2016, Ware et al. 2019). Researchers can incorporate intraspecific variation into distribution models with knowledge of phenotypic groups, taxonomic units, genetic groups, or biogeographic regions. Intraspecific models can then be compared to each other and to species-wide models for a better understanding

of lineage-level differences in climatic-drivers of distribution and potential consequences of climate change (Peterson, Doak, & Morris 2019). With information from these model comparisons, we can better identify where, and which, populations, communities, and ecosystems are most at risk to climate change.

One way to consider intraspecific variation in spatial models is to incorporate underlying genetic sub-structure when delineating the geographic areas to represent the range extent in the models. Species are *not* uniform entities across their geographic distributions, with common examples of locally adapted populations spread across geographic ranges and environmental gradients (Clausen, Keck, & Hiesey 1940, Leimu & Fisher 2008, Hereford 2009). Accommodating this information in models is critical, as locally adapted populations are likely to respond differently to environmental change, with implications for shifting species' distributions and range limits (Hargreaves et al. 2014). Evidence to date suggests that including this information can produce more accurate models (Pearman et al. 2010, Marcer et al. 2016, Ikeda et al. 2017) and broader predictions (e.g., Oney et al. 2013) of conserved distributions in future climate scenarios (Gotelli & Stanton-Geddes 2015, Ikeda et al. 2017, Benito-Garzón et al. 2019, Peterson, Doak, & Morris 2019). Further, incorporating genetic structure into spatial models can help address limitations of correlative models relating abiotic variables to species occurrences (Gotelli & Stanton-Geddes 2015, Phillips et al. 2006, Peterson et al. 2011). For instance, these methods perform well at predicting current distributions (Elith et al. 2010) but provide little insight into mechanisms underlying how and why species are distributed across environments (Warren et al. 2008, Dormann et al. 2012, Gotelli & Stanton-Geddes 2015).

The choice of relevant environmental predictors is important for the utility of models, especially as genetically distinct populations may be locally adapted or have varying tolerances to environmental stressors (Peterson, Doak, & Morris 2019). Assessments of environmental predictor choice in SDMs consistently show differences in model accuracy or transferability to future climatic conditions or different geographic regions. Predictor choice (e.g., bioclimatic variables vs. land-use variables) affects model performance and thereby confidence in future predictions (e.g., Synes & Osborne 2011). Model performance often improves with the inclusion of species-relevant predictors (e.g.,

Petitpierre et al. 2017), species ecological traits (e.g., McPherson & Jetz 2007), or ecosystem functioning variables ("EFAs"; Alcaraz-Segura et al. 2017, Arenas-Castro et al. 2018, Regos et al. 2019). Nevertheless, many models use substitute, or proximal, predictor variables rather than species-specific predictor variables, which limits the accuracy of predictions when models are transferred across space or time (Kühn & Dormann 2012; Regos et al. 2019). Assumptions about local adaptation to environmental conditions cannot be drawn without incorporating genetic structure into spatial models (Alvarado-Serrano & Knowles, 2014; Hällfors et al. 2016; Peterson, Doak, & Morris, 2019), and it is important to consider that different environmental variables may be relevant for genetically different populations or groups.

We used underlying genetic structure to delineate populations with which to build and compare spatial models and we recognize that this is just one way to include intraspecific variation in models (reviewed in Benito-Garzón et al. 2019 and Peterson, Doak, & Morris 2019). Consistent with pervasive G x E interactions known to exist on the landscape (Jump & Penuelas 2005, Ware et al. 2019), our study aims to test how differences in predictions can result from manipulating factors related to species' genetic variation and the environment in distribution models. Different predictor choices produce models with varying levels of transferability and accuracy – differences that are likely to compound with uncertainties inherent in future global change scenarios (McPherson & Jetz 2007, Synes & Osborne 2011, Petitpierre et al. 2017, Regos et al. 2019).

Using known occurrences of genetically differentiated *Populus angustifolia* provenances across the species distribution and Maxent modeling algorithms (Phillips et al. 2006), we compare predictions and model accuracy of multiple SDMs to assess the level of uncertainty that may arise from unique population X environment relationships on the landscape. To test the overarching hypothesis that species range-wide models will over-predict – make broader predictions of – the extent of suitability of genetic population ranges, we manipulated the *geographic training extent* of models using knowledge of *P. angustifolia* genetic substructure. If species models regularly over-predict suitable distributions, then SDMs may be less likely to predict at-risk populations or responses to global change factors.

Materials & Methods

Modeling approaches

We used Maxent to build our species distribution models. Maximum entropy (Maxent) is a high-performing modeling technique that approximates species niches using environmental parameters and presence-only occurrence data (Phillips et al. 2006, Elith et al. 2010). We ran 14 Maxent (Version 3.3.3k) experiments to address our hypothesis, manipulating training extent and variable selection of each model (Table 5; All tables and figures are in Appendix 2 at the end of this chapter).

Species occurrence data

The dominant riparian tree, *P. angustifolia* James, is a model system for incorporating intraspecific variation into SDMs: the species spans broad abiotic gradients and approximately 1700 km of latitude in the western United States, across which at least three genetic provenances exist (Evans et al. 2015). As *P. angustifolia* is a riparian tree, it is important to include non-climatic hydrological variables in models that are known to affect the evolution, ecology, and distribution of this and other riparian species (Mahoney & Rood 1998, Lytle & Poff 2004, Cushman et al. 2014, Bothwell et al. 2016). Further, this species has strong effects on community interactions and ecosystem functions across its geographic range (e.g., Whitham et al. 2006, Ware et al. 2019), making it important to understand the extent to which predictions differ with environment and genetic structure. The occurrence dataset (N=657) for *P. angustifolia* was collected May - June 2012. Latitude and longitude coordinates were collected for each sampled tree as decimal values using Oregon 500 Garmin GPS units with WGS 84 datum. Details of data collection have been published previously (Van Nuland et al. 2018). Occurrence data span the range of three genetic provenances around geographic features including the Great Basin, the Rocky Mountains, and the Mogollon Rim (Evans et al. 2015). The described sampling methods cover a range of broad environments as well as many locations near the edge of the species' geographical range. In contrast to random sampling across a species range, these methods are thought to provide more resolved predictions of range expansions and contractions expected with

climate change (Hampe & Petit 2005, Hargreaves et al. 2014, Woolbright et al. 2014, Gotelli & Stanton-Geddes 2015).

Model training extents

We created four training datasets based on different geographic extents (regions): one based on all occurrence points (SR, "species-range") and three based on occurrence points split into each of the three genetic provenances (P1, P2, and P3, summing to SR; Figure 6a). The exact extent of the training regions was based on assumptions about riparian dispersal within water basins, so we created geographic bounds by mapping HUC (hydrologic unit code) level 6 watersheds from the USGS Watershed Boundary Dataset (https://water.usgs.gov/GIS/huc.html) which allowed us to include all relevant occurrence data points with the lowest number of water basins. In this system riparian network connectivity is related to genetic connectivity of *P. angustifolia* (Cushman et al. 2014, Bothwell et al. 2016).

Environmental variables and variable selection

We used environmental variables from two sources, all modified in ArcMap (ESRI 2018) to be of the same extent (geographic bounds) and spatial resolution (1 km) and projected in the same coordinate system as the species occurrence data (WGS84). First, we extracted 23 bioclimatic variables and 4 seasonal variables from 1981-2010 from AdaptWest Project (AdaptWest Project, 2015; Hamaan et al. 2013). Second, we extracted hydrologic variables from the National Hydrology Dataset (NHDPlusV2; McKay et al. 2012), a companion to the Watershed Boundary Dataset that was used to delineate geographic training extents. This second dataset describes river and stream attributes of the riparian habitats of *P. angustifolia*. It is important to include these variables as stream properties affect the ecology and evolution, including dispersal ability, of riparian plants like *P. angustifolia* (Mahoney & Rood 1998; Lytle & Poff 2004; Bothwell et al. 2016). All included environmental variables are in Table 4. To test if environmental variables used in models differed across the three genetic provenances, we used redundancy analysis (RDA; R package vegan; Oksanen et al. 2017) with genetic provenance as a constrained axis.

Nine of the initial 27 bioclimatic variables were removed based on knowledge of the species natural history and/or high spatial correlation within the range-wide training extent, determined using SDMToolbox (Brown 2014). We first selected bioclimatic variables for the range-wide experiment by using the remaining 18 variables to train Maxent models with 5-fold cross-validation. The average test AUC (+/- standard error) for the 5 replicates was 0.865 +/- 0.022, and each replicate had test AUC values > 0.8, indicating good discriminatory ability of all replicates (Swets 1988). From these 18 variables, we then selected those which had cumulatively contributed between 90-95% to the gain in model fit of the five replicates, resulting in a final suite of seven bioclimatic variables: annual heat moisture index (ahm), Hargreave's climatic moisture index (cmd), Hargreave's reference evapotranspiration (eref), mean annual precipitation (map), winter (dec.-feb.) precipitation (ppt_wt), relative humidity (rh), and continentality (difference between mean temperature of the coldest and warmest months, td) (Table 4). Because many niche modeling studies rely solely on bioclimatic variables, we include in the supplement models that were built with only these seven bioclimatic variables to provide another dataset making comparisons between predictions and relative contributions of bioclimatic variables and ecosystem-relevant variables to models (supplemental information).

We also included distance to stream (near), mean annual streamflow (q_ma), stream order (strmord), stream velocity (v_ma) to the chosen seven bioclimatic variables. From these 11 variables, we selected final variables for the "range-wide" (see Table 3) model experiments in Maxent using 5-fold cross-validation, as described above. The average test AUC (+/- standard error) for the 5 replicates was 0.933 +/- 0.016, and the lowest replicate test AUC was 0.914, indicating very good model discriminatory ability. Again, we selected the top variables that cumulatively contributed between 90-95% to the gain in model fitting of each replicate, which included ahm, cmd, near, q_ma, strmord, td, and v_ma (Table 4). We refer to this group of variables as the "range-wide" (RW) variables throughout the manuscript as we also used these seven variables to build models at the provenance geographic extents (Table 3). Finally, we built *unique* provenance models by repeating the entire variable selection process described above *within* each provenance extent. We refer

to these three groups of uniquely-selected variables as P1, P2, or P3 variables throughout the manuscript (Table 3).

After variable selection for all experimental models, each was run a final time with 30% of the occurrence data as a subset for model testing. Each Maxent model was formatted to run with logistic output to best conceptualize the output as estimates of the probability of suitability between values of 0 (unlikely to be present) and 1 (likely to be present). We used the default Maxent options for background sample selection (10,000 points), number of iterations (500), and regularization multiplier (1). We applied a 10-percentile training presence threshold rule to obtain binary output to test our hypotheses. This threshold rule finds the suitability value at which 10% of the training presence points are predicted absent (i.e., omission error) and uses it to reclassify pixels with suitability values below that value as unsuitable (absent) and above as suitable (present). It should be noted that we have different sample sizes for each provenance, which does introduce variability in sizes of training and testing subsets, especially low for the P1- models (N train(test) = 9(3); Table 3).

Before comparing range-wide models to provenance models, we tested the effect of different types of environmental variables on model performance. Models trained with both bioclimatic and ecosystem-relevant hydrological variables more accurately predicted individual occurrences than models trained with only bioclimatic variables. SDMs generally had higher discriminatory ability with both variable types (i.e., higher AUC_{test} = lower type II error; Table 8 and Figure 16 in Appendix 4).

Comparing range-wide models to provenance models

To compare range-wide models to provenance models, we calculated the percent of the landscape that was predicted suitable by one, both, and neither binary model. This resulted in six comparisons. Our use of the term "over-prediction" is not meant to be synonymous with commission error – cases where a model predicts a species is present, but it is actually absent -- rather that one model predicts more suitable landscape than another model within the same geographic region. We also calculated Schoener's D, which provides a measure of niche overlap comparing density distributions (Warren et al., 2008). This metric

provides a value between 0-1, where values closer to zero represent little overlap between modeled niches and a value of 1 representing full overlap of modeled niches. Finally, we combined provenance model predictions to compare with range-wide predictions.

Results

Species range-wide models consistently over-predict provenance models in geographic space

Range-wide SDMs over-predicted environmental suitability within the ranges of the three known distinct genetic provenances of *P. angustifolia* for all model comparisons. After accounting for agreement in suitability between range-wide models and provenance models, we found that range-wide models predicted more suitable areas within the three provenance extents than did provenance models by 11.0 to 62.4 percent (Figure 7a). One hypothesis for the provenance differences in range-wide model over-prediction is that the environmental parameters that determine the suitability of *P. angustifolia* vary by provenance. Agreement of suitability between species models and provenance models ranged from 28.2 to 57.5 percent (Fig 7b). The highest degree of over-predictions in geographic space by the range-wide species model was made in provenance 3 – the northernmost provenance (Figures 6a and 7a). Accordingly, provenance 3 models show the lowest levels of niche overlap with the range-wide species model: Schoener's D between the species model and the provenance 3 model trained with range-wide variables (model P3-RW) was 0.118 and the provenance 3 model trained with provenance-selected variables (model P3-P3) was 0.169 (Table 5). In contrast, provenance 1 – the southernmost provenance (Figure 6a) – shows the highest degree of geographic spatial agreement with, and lowest over-predictions by the species model when built with the range-wide suite of variables – though this pattern switches when provenance 1 is built with variables selected within its extent (Figure 7). One explanation for this pattern is that the environmental conditions of provenance 1 are the most unique (Figure 6b), and thus contribute highly to the range-wide niche. Schoener's D values also support that niche overlap is the highest between the range-wide species model and the provenance 1 model built with range-wide selected variables (Figure 7c and Table 5). This similarity between the range-wide species

niche and the provenance 1 niche may explain the high values of spatial over-prediction made by the species model in provenance 3 (Figure 7a). These results indicate that a genetically based perspective is important for predicting the quantitative and qualitative projections of suitability.

The level of agreement in geographic space between species and provenance models depended on choices about which environmental predictor variables were used in models. For example, the degree of over-prediction was exaggerated in models that only used bioclimatic variables (range of 18.2 to 87.1 percent; Figure 18 in Appendix 4 (A4)). Interestingly, the geographic spatial agreement between range-wide species model and provenance 1 models decreased by as much as 43.7 percent (Table 8 in A4) while the geographic agreement between the range-wide species model and provenance 2 and provenance 3 models increased (Figure 18 in A4). Accordingly, over-predictions by the species models increased significantly for the southern-most provenance 1 (up to 87%) when only bioclimatic variables were included (Figure 18 in A4). These results further support the need to build genetically informed provenance-specific niches as range-wide species models are too broad to be usefully applied across genetic provenances.

Range-wide niche versus population-level niches

Significant environmental variation across species' ranges begs a more deliberate identification of bioclimatic and ecological niches through understanding how, why, and when to include different types of variables in models. We show that environmental variables vary on the landscape across the three genetic provenances of *P. angustifolia* with a redundancy analyses (RDA; R package vegan; Oksanen et al. 2017) that revealed 58.2 percent of the variance in all environmental response variables could be explained by the geographic extent of genetic provenance ($p<0.001$; Figure 6b). This significant environmental variation across the range of *P. angustifolia* provides an additional reason to examine environmental niches at the intraspecific level, and to carefully consider the types of environmental predictor variables included in models. The average percent contribution of ecosystem variables, those describing the riparian habitat of *P. angustifiolia*, was higher than the contribution of bioclimatic variables (17.9% and 11.3%,

respectively; Figure 18 in Appendix 4), though the difference was significant only at p=0.07. Repeating the RDA on each of these variable types (bioclimatic and ecosystem-related) reveals that genetic provenance explains 61.1 percent of the variation in ecosystem-related variables but just 11.2 percent of the bioclimatic variables ($p<0.001$ for both models; R package vegan; Oksanen et al. 2017).

Consistent with the hypothesis that range-wide species models are too broad, we did not find a single model could be applied to genetically distinct populations of *P. angustifolia.* Closer examination of important variables for the species range-wide model and provenance models reveals how the environmental niches differ between groups. The result of the range-wide species model indicates that the niche of *P. angustifolia* is driven largely by mean annual streamflow (35.7%) and stream order (19.6%; Table 4 and Figure 17 in Appendix 4 (A4)). Similarly, provenances 2 and 3 also show high contributions of mean annual streamflow (between 41.6 - 47.3%), while stream *order,* not flow, matters most for provenance 1 (Table 4 and Figure 17 in A4). This makes sense as stream flow can be intermittent across the extent of provenance 1 where water is less available at higher stream orders, and because *P. angustifolia* is an obligate riparian species. We predicted that uniquely selecting environmental variables within provenance extents would improve SDM accuracy compared to range-wide variable selection. We found that this method of variable selection did not consistently affect model discriminatory ability, though it did change predictions (Figure 6c and Table 3) – also supported by values of Schoener's D, showing the relative degree of niche overlap between the models (Table 5). With environmental variables tailored for each provenance, further differences in variable importance from the species model were noted, supporting the need to examine how population X environment relationships manifest within SDMs.

Though models were consistently improved with hydrological predictors across all four geographic extents (Figure 16 in Appendix 4 (A4)), their inclusion made predictions of markedly smaller suitable regions (Figure 8). Projecting provenance models showed that between 18.8 and 19.4 percent of the landscape was predicted suitable with range-wide and provenance-specific variables, respectively (Figure 8). Had we only used bioclimatic variables to model *P. angustifolia*, suitable distributions would have been predicted on as

high as 40.6 and 47.9 percent of the landscape, with greater uncertainty arising depending on variable selection method (Figure 8). This is a high level of potential error arising from models that ignore population X environment relationships within SDMs.

Discussion

Range-wide models consistently overpredict suitable distribution

Range-wide ecological niche models (SDMs) overpredicted suitable distribution within the geographic bounds delineated by genetic provenance, relative to each of the twelve SDMs built for provenances. We found that 18.2 and 11 percent were the *lowest* overpredictions, and 87 and 62 percent were the *highest* overpredictions. Overprediction was expected from range-wide models as a species' range spans broader environmental gradients and larger areas than intraspecific delineations (Gotelli & Stanton-Geddes 2015, Peterson, Doak, & Morris 2019). Whether the resulting overpredictions were affected by the inclusion of species-relevant ecosystem variables depended upon provenance (overprediction increased in provenances 2 and 3, decreased in the southernmost provenance 1). We are unable to assess whether including genetic provenance increases model accuracy because models were built in different geographic areas and with different numbers of occurrences – both range size and sample size affect model accuracy (Stockwell & Peterson 2002, McPherson, Jetz & Rogers 2004). However, overall, our study adds to accumulating evidence that building SDMs at the species-level can lead to overly broad and drastically misleading predictions for certain populations and genetic provenances.

There is no single species-level niche that can be applied to populations

Our results suggest that the use of bioclimatic variables does not suffice to define population-level niches (Figure 19 in A4). We consistently improved model discriminatory ability by incorporating predictor variables relevant to the ecology of *P. angustifolia* in addition to bioclimatic variables. Reassuringly, our models confirm much of what we already know about the habitat preferences of *P. angustifolia* – a riparian species influenced by hydrological processes (Cushman et al. 2014, Evans et al. 2016). Not only did model accuracy improve with the inclusion of hydrological variables, but hydrological

variables contributed more to models than bioclimatic variables did when both types were included (Tables 8-9 and Figures 16-17 in A4). Localized variables related to riparian systems (e.g., stream order) are not consistently correlated with coarser bioclimatic variables (e.g., precipitation), consequently resulting in misjudgments of occurrence-environment relationships if these variables are not included (McPherson & Jetz 2007). Though models were consistently improved with hydrological predictors across all four geographic extents, their inclusion made markedly smaller (by 75%) predictions of suitable geographic region for three of the four geographic extents (i.e., range-wide and all three genetic provenances), indicating population X environment interactions. Provenances 2 and 3 are less constrained by climate than provenance 1. Prediction differences may result from river attributes lessening stressful climatic conditions; for example, a lack of precipitation could be offset by subterranean stream flow, whereby riparian trees instead acquire water from rivers rather than soil storage (e.g., Snyder & Williams 2000).

Contrary to our expectations, genetic provenance SDMs trained on a tailored set of environmental variables (selected within each provenance's geographic bounds) did not consistently perform better than when SDMs were provided with variables selected within bounds of the species range. Higher average AUC_{test} values emerged for only four of the six comparisons. Though model performance did not necessarily *improve*, models did perform well overall ($AUC_{test} > 0.8$ for all but one model; Swets 1988), suggesting that it may instead be important to consider in which scenarios the different variable selection methods may be useful. For example, it may be more useful to select variables at the genetic provenance level when projecting models across space or time, given that the identity and contributions of variables selected differed considerably from the range-wide selection and across genetic groups (Table 9 and Figure 17 in A4). When combined into a single output, the three genetic provenance models predicted broader suitable distribution over the entire species' range than did range-wide models (Figure 8).

We compared predictions made by SDMs to test factors related to population X environment relationships. We manipulated geographic training extents based on the species' genetic constitution and the selection method of variables. Range-wide species SDMs always overpredicted suitable distribution regardless of variable type or selection

method. Though rarely incorporated, genetic information should increase the utility of SDMs. The lack of a "single niche" for the species that encompasses niches of provenance populations emphasizes the large extent to which improvements depend not only on the inclusion of genetic information but also on the type and selection of predictor variables that interact with that genetic information. These results have broad implications for predicting population-level ecological and evolutionary responses to climate change.

Climate change conclusions

Incorporating intraspecific variation into species distribution models (SDMs) has been hypothesized to increase model accuracy, change estimates of risk of species-level declines, and reveal differential responses of intraspecific groups to climate change depending on range-position (e.g., edge vs. central lineages) and/or performance-climate relationships (e.g., warm-adapted lineages; reviewed by Peterson, Doak, & Morris 2019). Here, we considered the disagreement among SDM predictions by manipulating factors related to population-environment relationships on the landscape to show that range-wide models provide over-predictions of suitable distribution. Overall, we emphasize the need to consider how and why environmental variables are selected for SDMs, *especially* when including genetic substructure within a species. More nuanced SDMs should allow for a more refined understanding of species and population-level risks in the face of climate change. Our findings advance current understanding of how distribution models should be interpreted and used. This may be critically important for conservation managers who need accurate predictions to better identify where, and which, populations, communities and ecosystems are most at risk due to climate change.

REFERENCES

AdaptWest Project. 2015. Gridded current and projected climate data for North America at 1km resolution, interpolated using the *ClimateNA v5.10* software (T. Wang et al., 2015). Available at adaptwest.databasin.org.

Alcaraz-Segura D, Lomba A, Sousa-Silva R, Nieto-Lugilde D, Alves P, Georges D, Vicente JR, Honrado JP. 2017. Potential of satellite-derived ecosystem functional attributes to anticipate species range shifts. *International Journal of Applied Earth Observation and Geoinformation* 57: 86-92.

Alvarado-Serrano DF, Knowles LL. 2014. Ecological niche models in phylogeographic studies: Applications, advances and precautions. *Molecular Ecology Resources* 14(2).

Arenas-Castro S, Gonçalves J, Alves P, Alcaraz-Segura D, Honrado JP. 2018. Assessing the multi-scale predictive ability of ecosystem functional attributes for species distribution modelling. *PLoS ONE* 13(6): e0199292.

Bailey JK, Genung MA, Ware IM, Gorman C, Van Nuland ME, Long H, Schweitzer JA. 2014. Indirect genetic effects: An evolutionary mechanism linking feedbacks, genotypic diversity and coadaptation in a climate change context. *Functional Ecology* 28(1).

Benito-Garzón M, Robson TM, Hampe A. 2019. ΔTraitSDMs: species distribution models that account for local adaptation and phenotypic plasticity. *New Phytologist* 222(4).

Bothwell HM, Cushman SA, Woolbright SA, Hersch-Green EI, Evans LM, Whitham TG, Allan GJ. 2017. Conserving threatened riparian ecosystems in the American West: Precipitation gradients and river networks drive genetic connectivity and diversity in a foundation riparian tree (*Populus angustifolia*). *Molecular Ecology* 26(19).

Brown JL. 2014. SDMtoolbox User Guide. *Methods in Ecology and Evolution.*

Burrows, MT, Schoeman DS, Buckley LB, Moore P, Poloczanska ES, Brander KM, Brown C, Bruno JF, Duarte CM, Halpern BS, Holding J, Kappel CV, Kiessling W, O'Connor MI, Pandolfi JM, Parmesan C, Schwing FB, Sydeman WJ, Richardson AJ. 2011. The pace of shifting climate in marine and terrestrial ecosystems. *Science* 334(6056): 652-655.

Chase JM, Leibold LM. 2003. *Ecological Niches: Linking Classical and Contemporary Approaches.* University of Chicago Press.

Clausen J, Keck DD, Hiesey WM. 1940. Experimental studies on the nature of species. I. Effect of varied environments on western North American plants. *Carnegie Inst Wash Publishing.*

Cushman SA, Max T, Meneses N, Evans LM, Ferrier S, Honchak B, Whitham TG, Allan GJ. 2014. Landscape genetic connectivity in a riparian foundation tree is jointly

driven by climatic gradients and river networks. *Ecological Applications* 24: 1000–1014.

Dormann CF, Schymanski SJ, Cabral J, Chuine I, Graham C, Hartig F, Kearney M, Morin X, Römermann C, Schröder B, Singer A. 2012. Correlation and process in species distribution models: Bridging a dichotomy. *Journal of Biogeography* 39(12): 2119–2131.

Elith J, Kearney M, Phillips S. 2010. The art of modelling range-shifting species. *Methods in Ecology and Evolution* 1(4).

Elton C. 1927. *Animal Ecology*. Sidgwick and Jackson, London.

Esri. 2018. ArcMap 10.6.1. In *ESRI*.

Evans LM, Allan GJ, Difazio SP, Slavov GT, Wilder JA, Floate KD, Rood SB, Whitham TG. 2015. Geographical barriers and climate influence demographic history in narrowleaf cottonwoods. *Heredity* 114: 387-396.

Evans LM, Kaluthota S, Pearce DW, Allan GJ, Floate K, Rood SB, Whitham TG. 2016. Bud phenology and growth are subject to divergent selection across latitudinal gradient in *Populus angustifolia* and impact adaptation across the distributional range and associated arthropods. *Ecol. Evol.* 6(13): 4565-4581.

Gotelli NJ, Stanton-Geddes J. 2015. Climate change, genetic markers and species distribution modelling. *Journal of Biogeography* 42(9).

Grinnell J. 1917. The Niche-Relationships of the California Thrasher. *The Auk 34*: 427–433.

Hällfors MH, Liao J, Dzurisin J, Grundel R, Hyvärinen M, Towle K, Wu GC, Hellmann JJ. 2016. Addressing potential local adaptation in species distribution models: Implications for conservation under climate change. *Ecological Applications* 26(4).

Hamann A, Wang T, Spittlehouse DL, Murdock TQ. 2013. A comprehensive, high-resolution database of historical and projected climate surfaces for western North America. *Bulletin of the American Meteorological Society* 94(9): 1307-1309.

Hampe A, Petit RJ. 2005. Conserving biodiversity under climate change: the rear edge matters. *Ecology Letters* 8(5): 461–467.

Hargreaves AL, Samis KE, Eckert CG. 2014. Are Species' Range Limits Simply Niche Limits Writ Large? A Review of Transplant Experiments beyond the Range. *The American Naturalist*, 183(2).

Hendry AP. 2017. *Eco-Evolutionary Dynamics*. Princeton University Press.

Hereford J. 2009. A quantitative survey of local adaptation and fitness trade-offs. *American Naturalist* 173(5).

Ikeda DH, Max TL, Allan GJ, Lau MK, Shuster SM, Whitham TG. 2017. Genetically informed ecological niche models improve climate change predictions. *Global Change Biology* 23(1).

Jump AS, Peñuelas J. 2005. Running to stand still: adaptation and the response of plants to rapid climate change. *Ecology Letters* 8(9): 1010–1020.

Kühn I, Dormann CF. 2012. Less than eight (and a half) misconceptions of spatial analysis. *J. Biogeogr.* 39: 995-1003.

Leimu R, Fischer M. 2008. A meta-analysis of local adaptation in plants. *PloS One* 3(12), e4010.

Lytle DA, Poff NLR. 2004. Adaptation to natural flow regimes. *Trends in Ecology and Evolution* 19(2): 94-100.

Mahoney JM, Rood SB. 1998. Streamflow requirements for cottonwood seedling recruitment – An integrative model. *Wetlands* 18: 634-645.

Marcer A, Méndez-Vigo B, Alonso-Blanco C, Picó FX. 2016. Tackling intraspecific genetic structure in distribution models better reflects species geographical range. *Ecology and Evolution* 6(7).

McKay L, Bondelid T, Dewald T, Johnston J, Moore, R, Rea A. 2012. "NHDPlus Version 2: User Guide."

McPherson JM, Jetz W, Rogers DJ. 2004. The effects of species' range sizes on the accuracy of distribution models: ecological phenomenon or statistical artefact? *Journal of Applied Ecology* 41: 811-823.

McPherson JM, Jetz W. 2007. Effects of species' ecology on the accuracy of distribution models. *Ecography* 30: 135-151.

Odling-Smee FJ, Laland KN, Feldman MW. 2003. Chapter 1: Introduction. *Niche Construction: The Neglected Process in Evolution*.

Odling-Smee FJ. 1988. Niche-constructing phenotypes. *The role of behavior in evolution*.

Oksanen J. 2017. Vegan: ecological diversity. In *R Package Version 2.4-4*.

Oney B, Reineking B, O'Neill G, Kreyling J. 2013. Intraspecific variation buffers projected climate change impacts on Pinus contorta. *Ecology and Evolution* 3(2).

Parmesan C. 2006. Ecological and Evolutionary Responses to Recent Climate Change. *Annual Review of Ecology, Evolution, and Systematics* 37: 637-669.

Pearman PB, D'Amen M, Graham CH, Thuiller W, Zimmermann NE. 2010. Within-taxon niche structure: niche conservatism, divergence and predicted effects of climate change. Ecography 33, 990-1003.

Peterson AT, Soberón J, Pearson RG, Anderson RP, Martínez-Meyer E, Nakamura M, Araújo MB. 2011. *Ecological Niches and Geographic Distributions.* Princeton University Press.

Peterson ML, Doak DF, Morris WF. 2019. Incorporating local adaptation into forecasts of species' distribution and abundance under climate change. *Global Change Biology* 25(3).

Petitpierre B, Broennimann O, Kueffer C, Daehler C, Guisan A. 2017. Selecting predictors to maximize the transferability of species distribution models: lessons from cross-continental plant invasions. Global Ecol. Biogeogr. 26: 275-287.

Phillips SJ, Anderson RP, Schapire RE. 2006. Maximum entropy modeling of species geographic distributions. *Ecological Modelling* 190, 231-259.

Regos A, Gagne L, Alcaraz-Segura D, Honrado JP, Domínguez J. 2019. Effects of species traits and environmental predictors on performance and transferability of ecological niche models. *Scientific Reports* 9, 4221.

Snyder KA, Williams DG. 2000. Water sources used by riparian trees varies among stream types on the San Pedro River, Arizona. *Agric. For. Meteorol*. 105: 227-240.

Stockwell DRB, Peterson AT. 2002. Effects of sample size on accuracy of species distribution models. *Ecological Modelling* 148: 1-13.

Swets JA. 1988. Measuring the accuracy of diagnostic systems. *Science* 240: 1285-1293.

Synes NW, Osborne PE. 2011. Choice of predictor variables as a source of uncertainty in continental-scale species distribution modelling under climate change. *Global Ecol. Biogeography*, 20: 904-914.

Van Nuland ME, Ware IM, Bailey JK, Schweitzer JA. 2018. Ecosystem feedbacks contribute to geographic variation in plant-soil eco-evolutionary dynamics across a fertility gradient. Functional Ecology, *33*: 95-106.

Van Nuland ME, Wooliver RC, Pfennigwerth AA, Read QD, Ware IM, Mueller LO, Fordyce JA, Schweitzer JA, Bailey JK. 2016. Plant-soil feedbacks: connecting ecosystem ecology and evolution. *Functional Ecology* 30(7): 1032–1042.

Ware IM, Fitzpatrick CR, Senthilnathan A, Bayliss SLJ, Beals KK, Mueller LO, Summers JL, Wooliver RC, Van Nuland ME, Kinnison MT, Palkovacs EP, Schweitzer JA, Bailey JK. 2019. Feedbacks link ecosystem ecology and evolution across spatial and temporal scales: Empirical evidence and future directions. *Functional Ecology* 33(1).

Warren DL, Glor RE, Turelli M. 2008. Environmental niche equivalency versus conservatism: Quantitative approaches to niche evolution. *Evolution* 62(11).

Whitham TG, Bailey JK, Schweitzer JA, Shuster SM, Bangert RK, LeRoy CJ, Lonsdorf EV, Allan GJ, DiFazio SP, Potts BM, Fischer DG, Gehring CA, Lindroth RL, Marks JC, Hart SC, Wimp GM, Wooley SC. 2006. A framework for community and ecosystem genetics: from genes to ecosystems. *Nature Reviews. Genetics*, 7(7): 510–523.

Woolbright SA, Whitham TG, Gehring CA, Allan GJ, Bailey JK. 2014. Climate relicts and their associated communities as natural ecology and evolution laboratories. *Trends in Ecology & Evolution* 29(7): 406–416.

APPENDIX 2

Table 3: Description of modeling experiments: Building, evaluation, and performance.

Model Name	Training Extent	Variable Selection	AUC_{train}	AUC_{test} +/- sd	N train(test)	Omission Rate
SR	Species Range	Range-Wide (RW)	0.948	0.918 +/- 0.022	75(31)	0.194
P1-RW	P1	RW	0.979	0974 +/- 0.021	9(3)	0
P1-P1	P1	P1 Range	0.988	0.986 +/- 0.01	9(3)	0
P2-RW	P2	RW	0.963	0.836 +/- 0.051	26(11)	0.455
P2-P2	P2	P2 Range	0.963	0.853 +/- 0.051	26(11)	0.364
P3-RW	P3	RW	0.973	0.902 +/- 0.033	40(17)	0.353
P3-P3	P3	P3 Range	0.976	0.9 +/- 0.036	40(17)	0.412

Table 4: Percent (%) contribution of environmental variables to SDMs. Blank cells indicate that variable was not included in final models while zeros indicate that the variable was included but contributed nothing to final models. The top contributing variables for each model are bolded. Variable abbreviations represent: ahm (annual heat moisture index), cmd (Hargreave's climatic moisture index), dd_0 (degree-days below 0°C), mar (mean annual solar radiation (MJ m-2 d-1)), nffd (number of frost-free days), pas (precipitation as snow (mm)), ppt_sm (summer (Jun to Aug) precipitation (mm)), ppt_wt (winter (Dec to Feb) precipitation (mm)), rh (mean annual relative humidity (%)), td (difference between MCMT and MWMT, continentality (°C)); near (distance to nearest stream), q_ma (mean annual streamflow), strmord (Strahler stream order), and v_ma (mean annual stream velocity).

Model Name	**Climatic Variables (AdaptWest Project)**										**Hydrologic Variables (NHDPlusV2)**			
	ahm	**cmd**	**dd_0**	**mar**	**nnfd**	**pas**	**ppt_sm**	**ppt_wt**	**rh**	**td**	**near**	**Q_ma**	**strm_ord**	**v_ma**
SR	1.9	14.8								12.4	14.1	35.7	19.6	1.6
P1-RW	41.6	1.4								0.8	4.2	0	52	0
P1-P1	19.8				26.5				20.9				42.8	
P2-RW	0.9	22.4								2.6	22.2	47	4.9	0
P2-P2			4.5			18.5	2.6				22.2	47.3	5	
P3-RW	4.8	13.8								13.8	10.2	46.4	10.7	0.3
P3-P3		13.2		4.6				10.6		9.6	10.1	41.5	10.3	

Table 5: Niche overlap measured using Schoener's D. Values fall between 0 and 1, with values closer to zero representing no overlap between models while a value of 1 indicates full overlap of models.

Each provenance model run with range-wide environmental variables (RW)

Model	Species	Provenance 1	Provenance 2	Provenance 3
SR	1	0.241	0.241	0.118
P1-RW	-	1	1	0.266
P2-RW	-	-	1	0.417
P3-RW	-	-	-	1

Each provenance model run with provenance-specific environmental variables (P1, P2, P3)

Model	Species	Provenance 1	Provenance 2	Provenance 3
SR	1	0.232	0.207	0.169
P1-P1	-	1	0.093	0.436
P2-P2	-	-	1	0.319
P3-P3	-	-	-	1

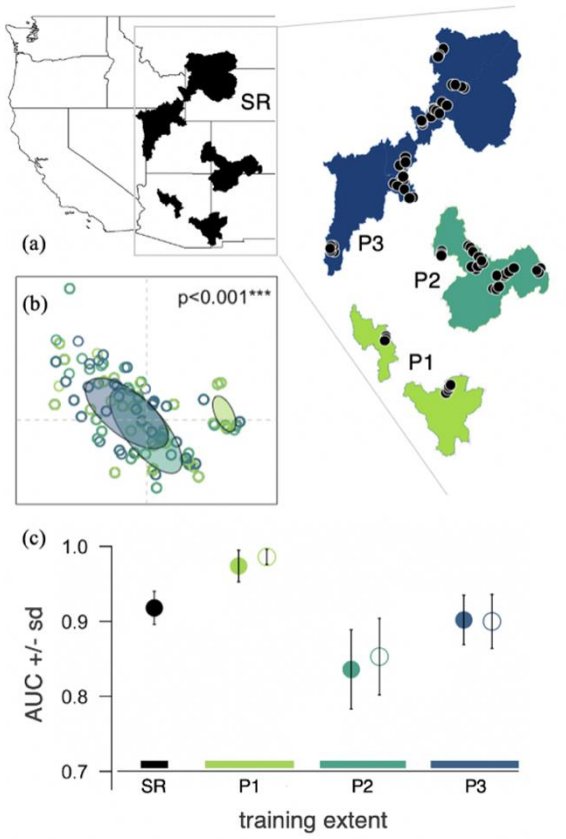

Figure 6. Geographic training extents, occurrence points, environmental variables, and model performance. Shown for range-wide experiment ("SR", black) and for genetic provenance (P) experiments 1-3 (colored outset: bottom to top) (a); and RDA (Redundancy Analysis) plot of environmental variables included in final model experiments (b); and test area under the curve of the receiver-operating characteristic values (AUC) +/- standard error for models (c). Color represents geographic training extent of model. Symbol fill (open/closed) represents the variable selection method with closed symbols = range-wide variable selection (RW) and open symbols = genetic provenance variable selection.

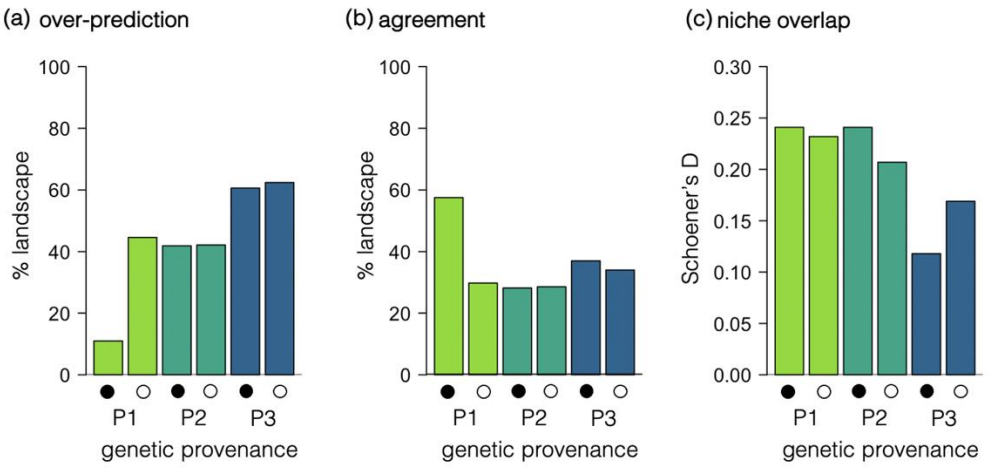

Figure 7. Comparison of species range-wide model to provenance models (P1, P2, P3) across two methods of variable selection (range-wide and within-provenance selection; closed and open symbols, respectively). Panel (a) represents the percent difference (geographic spatial disagreement) between predictions of suitable distribution made by the range-wide species model and respective provenance models. Positive values indicate that the range-wide model predicts broader suitable distribution than the provenance model. Panel (b) represents geographic spatial agreement between model predictions of suitable distribution. This value does not consider model agreement on "unsuitable" distribution. Panel (c) represents niche overlap measured using Schoener's D. Values fall between 0 and 1, with values closer to zero representing no overlap between models while a value of 1 indicates full overlap of models.

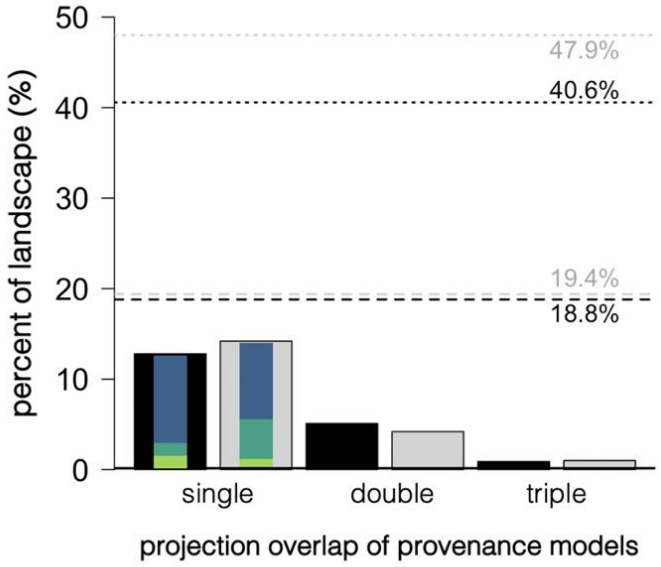

Figure 8. Provenance SDMs generate different predictions of suitable distribution across species' range. Bars in black use provenance models trained with the "range-wide" (RW) suite of variables selected for the species model. Bars in light grey represent provenance models trained with uniquely selected variables (P1-P1, P2-P2, and P3-P3 models). "Single" on the x-axis represents percentages of the landscape where only one provenance model predicted suitable distribution, "double" means any two models overlapped (agreement between two model predictions), and "triple" represents the percentage of suitable distribution that is agreed upon by all three provenance models (geographic spatial agreement). The two bars representing predictions made by a single model are split by color into the percentage of distribution predicted by each provenance model (by color, as in previous figures and Table 3). Dashed lines represent the total percentage of the landscape predicted suitable by at least one model (i.e., "single" + "double" + "triple"). Lines are colored as the bars: black range-wide models and grey unique provenance models. Dotted lines represent the total percentage of landscape predicted suitable by bioclimatic models (see Appendix 4). Note that the range-wide species model predictions are not represented in this figure, but the full geographic extent of species' range was considered for calculations.

CHAPTER III
CLIMATE-DRIVEN LOSS OF GENETIC VARIATION IN BUD BREAK ON THE LANDSCAPE

Abstract

Climate change is having profound effects on species distributions. However, less is understood about how climate change may alter the distribution of genetic variation across landscapes. Maintaining population genetic diversity is essential for the survival of species in the face of rapid climatic changes, and loss of variation will have significant consequences for both ecological and evolutionary processes. The objective of this work was to integrate genetically-based trait variation with distribution models to understand how variation is predicted to change across a species' range on the landscape with climate change. We use greenhouse trait values of spring leaf-out phenology of 400 genotypes from three geographically isolated populations (hereafter *provenances*) of *Populus angustifolia* in concert with stacked species distribution modeling to ask the following questions: (a) How will climate change predictions alter phenological variation across the species-range and within provenances; and (b) Whether changes to the distribution of phenological variation across genetic provenances will converge (become more similar) over time with future climatic conditions. We hypothesize (a) that strong climate gradients will decrease phenological variation on the landscape within all provenances, but that the trailing-edge (lowest latitude) provenance will lose the most variation; and (b) that phenological trait distributions will change within genetic provenances over time while becoming more similar among them. Our models predict a net loss of phenological variation in future climates on 20-25% of the landscape across the species' range, regardless of climate scenario, with the trailing edge provenance losing trait variation on as much as 47% of the landscape. Our models also predict that phenological trait distributions will become more similar across genetic provenances in response to future climate. This approach allows for the identification of areas expected to experience the greatest losses of genetically-based functional trait variation and areas that may be important to conserve as future genetic climate refugia.

Introduction

Climate change and other human-induced environmental perturbations are expected to continue to limit population connectivity and gene flow, thus decreasing effective population sizes[1] and ultimately reducing levels of genetic variation within species[2,3]. Maintaining genetic diversity within populations is essential for both short- and long-term survival of species facing rapid environmental change. Changes to the amount of variation within populations can have significant implications for interacting ecological and evolutionary processes. Low levels of genetic variation reduce the ability of populations to adapt to novel conditions or to colonize new areas while simultaneously increasing the risk of bottleneck effects and inbreeding depression[4–6]. In addition to evolutionary consequences, genetic variation loss will also have ecological consequences. Population genetic diversity, including variation in morphological, behavioral, or resource-use traits can have strong effects on ecosystem functions[7,8] such as biomass production and carbon cycling[9] or nitrogen mineralization[10]. Further, experimental studies indicate that the positive effects of genetic diversity may be most important in disturbed or stressful conditions[5,11–15], like those expected with a changing climate.

As species' ranges contract, expand, or shift in response to climate change[16,17] genetic variation is expected to be altered and/or reduced[18–20]. Regardless of phylum, plant population genetic diversity is related to biogeography such that core and insular populations tend to have the highest diversity[21]. Further, trailing edge (or "rear edge") populations tend to have low population diversity while harboring unique diversity (i.e., regionally diverse) due typically to isolation and local adaptation[22]. Because plant population genetic diversity differs across space so should our expectations of the ecological consequences of genetic diversity loss.

Genetic diversity can refer to many forms of intraspecific variation but understanding functional trait diversity is critical for predicting the ecological consequences of diversity[14,23]. This is problematic because functional trait distribution has received little attention at broad spatial scales[17,24]. Though there has been an increase in research examining spatial genetic variation[18], less is known about the ecological and evolutionary responses of functional traits to environmental change across species' ranges

or how traits may mediate or constrict population responses to climate change[19,23,25,26]. Some of the strongest responses to environmental change have occurred in life history traits like survival, fecundity, or phenology[27] that influence many abiotic and biotic components of ecosystems[28,29].

To address the challenge of predicting how genetically based trait variation may change on the landscape with climate change, we used three general circulation model projections of future climatic conditions, genetically based trait measurements of bud break phenology of a dominant riparian species, *Populus angustifolia*, and the technique of stacked species distribution modeling[30]. Using these tools, we identify shifts in suitable climatic conditions for a range of phenological traits and ask the following questions: (1) how climate change will alter phenological variation across the species-range and within populations; and (B) whether climate change will cause phenological trait variation to converge (become more similar) between populations. We hypothesized that strong environmental gradients associated with climate change will reduce phenological variation over the species-range, with the trailing edge (lowest latitude) population losing the most variation; We also hypothesized that trait distributions would become more similar among populations.

Materials & Methods

Study species, occurrence data, and geographic extent

Occurrence data were collected for *Populus angustifolia* James in May-June 2012. *P. angustifolia* is a dominant riparian tree species distributed from the south of Alberta, Canada along the U.S. Rocky Mountains and into the north of Mexico[31] – spanning approximately 1700km of latitude. The species exhibits a wide range of trait variation across this large geographic range and these large climatic gradients[32] and is thus ideal for examining how genetic trait variation is distributed on the landscape and may shift in response to climatic changes. Latitude and longitude coordinates were collected as decimal values from the WGS 84 World Grid system from Oregon 500 Garmin GPS units for each sampled tree. Occurrence data span the range of three genetic provenances (Arizona, Eastern, Northern/Wasatch Clusters)[33,34]. Sampling methods were designed to cover

extreme environments as well as locations near the edges of the species' geographical range. In contrast to random sampling, these methods should provide more resolved predictions of range dynamics expected with climate change[22,35–37].

Geographic extent for distribution model training should be based on assumptions about species' dispersal. In this system, genetic connectivity of populations is related to riparian network connectivity[38,39], and thus we chose to create geographic bounds for training our models with water basin information. Based on our occurrence data, we chose watersheds with the lowest level (level 6) of HUC (hydrologic unit code) from the USGS Watershed Boundary Dataset that captured all our occurrence points across the range (https://water.usgs.gov/GIS/huc.html).

Phenology data

Leaf phenological data was collected in a greenhouse at the University of Tennessee in 2016 from trees collected in 2012 at the time that occurrence data were collected. Phenology was measured as the day of first unfurling of the first leaf of each plant in the spring, and measurements were made on 400 genotypes from across the species' range. The earliest observed leaf out was recorded on Julian day 71 (March 11th) and the latest observed leaf out was recorded on Julian Day 125 (May 4th). Note that 2016 was a leap year. This results in a 54-day range across which leaf out occurred. We divided this dataset – paired phenology measurements with georeferenced field location of the parent tree – into ten smaller datasets based on deciles of the trait distribution, each part representing one-tenth of the sample. These deciles and associated coordinates were used to build separate species distribution models (see section "*Species distribution model calibration and evaluation")*. The first decile spanned a period of 14 days, while deciles 2-9 cumulatively spanned 28 days, and the tenth decile spanned a period of 12 days. See Ware et al. 2019[32] for more details regarding the establishment of greenhouse plants.

Environmental variable selection

Bioclimatic variables were obtained from the AdaptWest Project[40], and stream order (Strahler) was obtained from the National Hydrology Dataset to constrain the riparian habitat of *P. angustifolia* (NHDPlusV2)[41]. NHDPlusV2 is a companion dataset to the USGS Watershed Boundary Dataset from which we derived our watershed regions. All variables were the same spatial resolution (30 arc second; ~1 km at the Equator) and were projected into the same coordinate system (WGS1984) in ArcMap[42].

Based on a previous set of species distribution models built to describe the species' range (publication in submission), we selected a subset of the 27 available variables. This is based on common practice of using expert judgement on the ecology of the taxa[43] to reduce multi-collinearity and over-fitting of models[44]. From our previous models, we selected only those variables that had contributed at least 10% to model predictions. This selection criterion resulted in a subset of ten variables: AHM: annual heat moisture index; CMD: Hargreave's climatic moisture index; DD_0: chilling degree days / degree-days below zero °C; Eref: Hargreave's reference evaporation; MAP: mean annual precipitation; NFFD: number of frost-free days; PAS: precipitation as snow; PPT_wt: winter (dec-feb) precipitation; RH: relative humidity; and TD: difference between mean temperature of the coldest and warmest months as a measure of continentality.

Final selection of variables was made from an initial SDM run for the ten phenology deciles using the subset of variables. We summed the contributions of variables across the ten deciles and eliminated those that did not significantly contribute to models. Variables maintained for final models included: Hargreave's climatic moisture index, winter (dec-feb) precipitation, relative humidity, and continentality. Finally, stream order was included with all models and model projections to constrict the predictions to riparian zones. To reveal the relationship between environmental variables and phenology, we ran linear regressions using continuous bud break data (days, not split into deciles) with extracted values of the five environmental variables used in models.

Species distribution model calibration and evaluation

We used MaxEnt software to build ten species distribution models (Version 3.3.3k)[45]. MaxEnt is widely accepted to perform well with low sample size and with presence-only data[46,47]. Each model was trained with one-tenth of the species' occurrence data corresponding to phenological trait deciles, measured in the greenhouse. For example, the associated coordinates of origin for the first ten percent of greenhouse trees that broke bud in the spring of 2016 were modeled as "one species" for the purposes of "species" distribution modeling. This example model will be referred to as the "decile 1 model" for the rest of the manuscript (and accordingly for the 2nd, 3rd, etc. deciles). Each MaxEnt model was formatted to run with logistic output for best conceptualizing the output as estimates of the probability of suitability between values of 0 (unlikely to be present) and 1 (likely to be present). For each decile model, we ran 5-fold cross-validation and evaluated their performance with area under the receiver operating characteristic curve (AUC) metric. An AUC value of 1 indicates perfect discriminatory ability, while a value of 0.5 indicates random predictions. Each of the distribution models had good predictive accuracy with an average test AUC value of 0.85, and values ranging from 0.79 to 0.89 (Table 1; Fig. S1a)[44,48]. Analysis was repeated using all occurrence data to train final models for each trait decile, against ~10,000 background points with 340-500 iterations. To obtain binary output to test our hypotheses, we applied a 10-percentile training presence threshold rule. This threshold rule finds the suitability value at which 10% of the training presence points are predicted absent (i.e., omission error) and uses it to reclassify pixels with suitability values below that value as unsuitable (absent) and above as suitable (present). It should be noted here that each decile model ended up having slightly different sample sizes which does introduce variability in sizes of training and testing subsets (Table 1): this is due to the model omitting occurrence points if they fall within the same pixel as another point.

Using stacked distribution models to estimate effects of climate change on phenological trait variation

To estimate changes in genetically-based variation in plant phenology on the landscape, we applied the principle of stacked species' distribution modeling to binary maps of the ten trait decile models. Stacked SDMs sum ("stack") binary presence-absence maps of multiple species to estimate species richness on the landscape[49]. This "bottom-up" approach predicts first and assembles after[30]. Typically, this method has been used to estimate biodiversity patterns across ecological gradients (e.g., elevation[49,50]) or to make predictions of biodiversity change with climate change[51,52].

Stacking ten decile models allowed us to derive what is analogous to species richness –essentially "decile richness" – or the total number of trait deciles predicted at a given location. This metric describes trait variation in a location on the landscape. A maximum "decile richness" of ten indicates that phenological trait variation is genetically unconstrained at that location: Or, in other words, that all observed values of the trait could exist in the climatic conditions at that geographic location.

To test hypotheses about how future climate will affect phenological trait distributions, we projected each of the ten decile models into 12 future climate scenarios [3 general circulation models x 2 relative concentration pathways x 2 time periods], resulting in 130 distribution maps. Future climate data was from ClimateNA AdaptWest Project, with the Coupled Model Intercomparison Project Phase 5 (CMIP5) database derived from the 5th IPCC assessment report (AdaptWest Project 2015). We selected three Atmosphere and Ocean General Circulation/Climate Models (AOGCMs) to capture the "best case," "median case," and "worst case" projections in the geographic range of interest including the U.S. states of New Mexico, Arizona, Colorado, Wyoming, and Utah. For our geographic region, we selected INM-CM4, MPI-ESM-LR, and GFDL-CM3, all of which have high validation statistics[53], from which we downloaded data for representative concentration pathways (RCP) 4.5 and 8.5 for time periods 2050s and 2080s.

For each of the 12 future climate scenarios we again stacked models to calculated predicted "trait richness" on the landscape. To calculate the change in richness on the landscape we subtracted current richness values from projected richness values for each

grid cell: resulting in values from -10 to 10. Because zeros could indicate no change in richness (with or without decile composition changes) or unsuitable climatic conditions for all trait deciles, we re-calculated richness change considering which pixels were unsuitable to begin. We calculated net change as the difference between the percent of the landscape predicted to experience richness losses and gains, regardless of the degree of change (i.e., losses of 2 or 7 are both considered a loss). Stacked SDMs tend to over-estimate species richness[54] and thus, in our study, results of "richness loss" may be conservative.

To examine whether predicted changes in trait richness due to climate change would differ across genetic provenances of *P. angustifolia,* we repeated calculations of richness change within each watershed that contained occurrence points from the three genetic provenances. We tested whether predicted richness loss differed across populations, years, and emissions scenarios with linear regression models (lm function of R[55]).

Estimating phenological trait distribution similarity over time within and among genetic provenances

To estimate how distributions of phenological trait combinations may change with climate relative to their initial combinations, we constructed matrices for each genetic provenance with rows representing climate scenario and columns representing all possible combinations of deciles predicted to exist together on the landscape (i.e., there exist 1,023 possible combinations of ten numbers). This is closely analogous to an abundance "site" (climate scenario) by "species" (decile combinations) matrix, as used in community ecology. Instead of a community of species, we have communities of trait deciles. Values in the matrix represent pixel counts of suitable climatic conditions for that combination of trait deciles. There are 45 different combinations of a "decile richness" of 2, however, a 2-decile combination of decile 2 and decile 5, for example, is a "rare community" relative to a 2-decile combination of deciles 2 and 3, or deciles 4 and 5. We calculated a similarity score as an average distance between observed trait deciles in a cell. To compare changes within provenances, we compared future "sites" to the current baseline "site" composition. Increases would indicate convergence of trait communities and decreases would indicate

divergence of trait communities. We used redundancy analysis to quantify the amount of variation in trait distributions explained by genetic provenance using the function "rda" from the "vegan" package[56]. Additionally, we tested the inclusion of all factors as constraining variables in the RDA using the function "ordistep" which performs backwards and forwards model selection using permutation tests.

Results

Net loss of phenological variation in future climates

With all future climate scenarios, between 20-25 percent of the total landscape that we modeled is projected to have a net loss of trait richness (Table 7; All tables and figures can be found in Appendix 3 at the end of this chapter unless otherwise noted). This net percent loss decreases with latitude and across genetic provenance, such that the southernmost provenance is predicted to lose richness on the largest amount of land– between 36-47% – and the northernmost provenance is predicted to lose the least – between 14-29%. The central provenance is predicted to lose richness on about 24-30% (Figure 9d and Table 7; Figure 23 in Appendix 4). Differences between genetic provenances were significant but did not vary with relative concentration pathways or year (Figure 9d; $F_{provenance}=27.9$, $p_{provenance}<0.001$). However, the *total* percentage of landscape predicted to lose richness (i.e., without adjusting for richness gains) did change significantly across genetic provenance and with relative concentration pathways ($F_{provenance}=36.8$, $p_{provenance}<0.001$; $F_{rcp}=7.8$, $p_{rcp}=0.01$; $R^2=0.78$). Losing suitable climatic conditions for one decile in a location is very different from, for example, losing suitable climatic conditions for eight deciles in the same location. For this, it is important to not just quantify positive and negative losses across space, but the amount of richness – trait variation – that is changing. Following the predictions made of landscape-level net losses across populations, the southernmost provenance is predicted not only to lose the most suitable climatic conditions overall, but also to lose the highest number of trait deciles regardless of time or relative concentration pathway (Figure 10). In contrast, shifts in the number of trait deciles lost for the central and northernmost provenances are countered more by gains, suggesting phenological distributional shifts occurring in some areas, despite net loss (Figure 10).

Phenology richness patterns from stacked distribution models

Each decile model predicted suitable (current) climatic conditions on 10.7 to 33.2 percent of the landscape (Table 6). The first and tenth deciles, which represent the earliest and latest leaf bud break times, as well as the largest range of bud break days overall (as the two tails of the trait distribution) predicted the least suitable area overall (10.7 and 11.5%, respectively; Table 6; Figure 9a and 9b). The third decile predicted the most suitable area at 33.2 percent – interestingly almost the full area predicted suitable by stacked decile models: 34.3 percent (Table 6; Figure 9c). Only 2.8 percent of the land area was predicted to have suitable climatic conditions to support the full range of trait values (i.e., all ten trait deciles: Figure 9c).

Phenological trait distributions shift and converge

We examined phenological distribution change within provenances by comparing predictions made by future climate scenarios to the current ("baseline") distribution of traits. Within each provenance, the distribution of phenological variation shifts from the original state (Figure 11). With few exceptions, most AOGCMs and RCPs predicted more similar phenological trait distributions through time (i.e., points above yellow line in Figure 11). Overall, the southern provenance is predicted to see the smallest changes to phenological trait distributions, and the central and northern provenances are predicted to have greater changes in phenological distribution (Figure 11). Genetic provenance explained 51.9% of the variation in trait distributions – or community composition of trait deciles, to continue the community ecology analogy – across the species range (RDA; compared to a null model $p<0.001$). The best model included the global change model (AOGCM) in addition to genetic provenance as constrained variables, explaining 64.7% of the variation. This addition is expected given that the global change models were chosen to represent different future climatic conditions in the study area. Though distributions of trait variation are predicted to change within all three genetic provenances, the effect of relative concentration pathways on the degree of change appears variable, suggesting that significant losses and shifts will occur even in lower emissions scenarios.

We also examined the average frequencies of the earliest (decile 1) and latest (decile 10) 10% of bud breaking individuals across time relative to the amount of landscape projected to have suitable climates for at least one trait decile. In other words, landscape that was predicted to have a richness of 1 or greater. The southern provenance began with a higher frequency of early breakers relative to late breakers, and the northern provenance began with a higher frequency of later breakers relative to early breakers (Figure 12; also Figure 9a, 9b). The central provenance began with a similar frequency of both deciles (Figure 12). Across time, the loss of early and late breakers in the southern provenance is proportional to the beginning frequencies (Figure 12). The central provenance loses late breakers while the northern provenance loses late breakers and gains early breakers (Figure 12).

Model reliability and environmental variables

Distribution models for each trait decile had good predictive accuracy with an average test AUC of 0.85 (Figure 20 in Appendix 4 (A4)). Stream order contributed consistently high (between 30-54 percent) to all modeled trait deciles (Figure 20 in A4), suggesting that the inclusion of this variable is working as intended to constrain *P. angustifolia* to a riparian habitat. Climatic moisture index contributed significantly more to later decile models (Figure 20 in A4; R^2=0.68, p=0.0031) while winter precipitation and relative humidity (Figure 20 in A4) contributed significantly more to earlier phenological trait decile models (respectively, R^2=0.53, p=0.017; R^2= 0.49, p=0.024). Continentality contributed between 1.5 to 22 percent to the ten models (Figure 20 in A4). These significant relationships reflect environmental variable contribution to model predictions, and thus should not be interpreted as a description of the variable's relationship to trait values – earlier bud break was related to higher climatic moisture index (p<0.001), higher winter precipitation (p=0.003), lower relative humidity (p<0.001) and lower continentality (p<0.001; Figure 21 and 22 in A4).

Discussion

While it is thought that climatic changes that impact patterns of temperature and precipitation will exert strong selective forces affecting genetic variation across species, there are very few studies demonstrating such effects (but see Ware et al. 2019). This lack of data and approaches by which the relationship between climate change and genetic variation can be examined is significant. By integrating phenological trait variation of 400 *Populus angustifolia* genotypes and stacked species distribution models, our results predict a large loss of phenological trait variation across the species' range in response to future climatic conditions and convergence among populations in phenological trait distributions irrespective of emission scenario. These results have large implications for: 1) the ability of populations to respond and persist in the face of ongoing climate change; 2) the potential of those populations to support associated species that depend upon them as food and habitat; and 3) for the potential of climate driven ecosystem disassembly. To our knowledge we are the first to take this stacked distribution modeling approach to map the potential distribution of a genetically diverse functional trait on the landscape.

Species can go extinct, shift their distribution, adapt, or acclimate in response to a changing climate. All potential responses depend upon trait variation[58], yet most research on trait responses to climate change focus on shifts to mean trait values[59]. While shifts among population mean trait values are important indicators of evolution on the landscape, they provide very little information or context into how those populations may respond to selective pressures exerted by changing climates in the future. Previous work in this system demonstrates that broad-sense heritability in bud break phenology decreases (less genetic trait variation) across a gradient of increasing temperature[32]. Overall, our models predict a net loss of genetic variation across all *P. angustifolia* riparian forest populations in the western US if these mature adult trees do not survive. The loss of genetic variation occurs irrespective of emission scenario and could be seen as soon as 2055. Losses of genetic trait variation will be greatest in the trailing edge (low latitude) population – occurring on up to 47% of the landscape (Figure 9d). In general, though trailing edge populations tend to have low diversity, they also tend to be regionally diverse due to isolation and/or strong local adaptation[22]. Furthermore, our models predict that traits distributions will homogenize

between the three populations over time (Figure 11; Figure 12), a result that has been empirically demonstrated across elevation for four European temperate trees[28]. The convergence of all populations on a similar functional trait distribution is concerning as it suggests that the ability of individual populations to respond uniquely to climatic changes may be constrained in future climate scenarios. Importantly, the predictions made from these models occur regardless of relative concentration pathways (4.5 and 8.5), year (2050s and 2080s) and AOGCMs, suggesting that regardless of climate scenario, the changes are predicted to occur by mid-century.

It is increasingly clear that genetic variation in functional traits is critical in mediating patterns in biodiversity and ecosystem functions [7,8,60]. This is especially true for dominant species like *P. angustifolia* whose genetic diversity has been shown to have wide-ranging, landscape-scale effects on the land-atmosphere and plant-soil linkage and feedback affecting carbon and nitrogen cycles[7,32,62]. Changes to plant phenology can affect growing season length, and thus biomass production and carbon cycling[32,61,62], evapotranspiration, stream discharge[63,64], and resource availability for dependent organisms[29]. Phenology has also been shown to be important to soil microbial community structure and function that can feedback to affect plant performance under climate change[32]. If one of the consequences of climate change is a general reduction in genetic variation in functional plant traits, the associated loss of biodiversity and ecosystem functions are potential cascading effects.

The relationships between biodiversity – including genetic – and climate are critical for conserving natural ecosystems and their functions[65]. Climate relict populations have persisted under a changing climate and are largely considered "life-boats" for associated species and ecosystem functions[36]. Cottonwood riparian forests of the western US are already rare, estimated to occupy less than 5% of the landscape, and yet support most of the biodiversity of the west[66]. Our previous research indicates that trailing edge population of *P. angustifolia* are locally adapted in functional traits related to water and carbon cycling[67] that drive land-atmosphere feedbacks. Further, genotypes from the trailing-edge population are an important source of heat and water stress-tolerant individuals, making them critically important for conservation. If the loss of genetic variation in these

populations is non-random (i.e., driven by selection) as our models suggest, and genetic variation in functional traits supports variation in ecosystem functions on the landscape[26,32,67], then climate driven loss of genetic variation may be an important driver of ecosystem disassembly.

REFERENCES

1. Wright, S. Evolution in Mendelian Populations. *Genetics* **16**, 97–159 (1931).
2. DiBattista, J. D. Patterns of genetic variation in anthropogenically impacted populations. *Conserv. Genet.* **9**, 141–156 (2008).
3. Ellegren, H. & Galtier, N. Determinants of genetic diversity. *Nat. Rev. Genet.* **17**, 422–433 (2016).
4. Nei, M., Maruyama, T. & Chakraborty, R. The Bottleneck Effect and Genetic Variability in Populations. *Evolution* **29**, 1–10 (1975).
5. Frankham, R. Stress and adaptation in conservation genetics. *J. Evol. Biol.* **18**, 750–755 (2005).
6. Mimura, M. *et al.* Understanding and monitoring the consequences of human impacts on intraspecific variation. *Evol. Appl.* **10**, 121–139 (2017).
7. Whitham, T. G. *et al.* A framework for community and ecosystem genetics: from genes to ecosystems. *Nat. Rev. Genet.* **7**, 510–523 (2006).
8. Hughes, A., Inouye, B., Johnson, M., Underwood, N. & Vellend, M. Ecological consequences of genetic diversity. *Ecol. Lett.* **11**, 609–23 (2008).
9. Hughes, A. R., Stachowicz, J. J. & Williams, S. L. Morphological and physiological variation among seagrass (Zostera marina) genotypes. *Oecologia* **159**, 725–733 (2009).
10. Schweitzer, J. A. *et al.* Genetically based trait in a dominant tree affects ecosystem processes: Plant genetics impact ecosystems. *Ecol. Lett.* **7**, 127–134 (2004).
11. Hughes, A. R. & Stachowicz, J. J. Genetic diversity enhances the resistance of a seagrass ecosystem to disturbance. *Proc. Natl. Acad. Sci. U. S. A.* **101**, 8998–9002 (2004).
12. Wimp, G. M. *et al.* Conserving plant genetic diversity for dependent animal communities. *Ecol. Lett.* **7**, 776–780 (2004).
13. Reusch, T. B. H., Ehlers, A., Hämmerli, A. & Worm, B. Ecosystem recovery after climatic extremes enhanced by genotypic diversity. *Proc. Natl. Acad. Sci.* **102**, 2826–2831 (2005).
14. Cardinale, B. J. *et al.* Biodiversity loss and its impact on humanity. *Nature* **486**, 59–67 (2012).
15. Salo, T. & Gustafsson, C. The Effect of Genetic Diversity on Ecosystem Functioning in Vegetated Coastal Ecosystems. *Ecosystems* **19**, 1429–1444 (2016).
16. Chen, I.-C., Hill, J., Ohlemüller, R., Roy, D. B. & Thomas, C. Rapid Range Shifts of Species Associated with High Levels of Climate Warming. *Science* **333**, 1024–6 (2011).
17. Fei, S. *et al.* Divergence of species responses to climate change. *Sci. Adv.* **3**, e1603055 (2017).
18. Excoffier, L., Foll, M. & Petit, R. J. Genetic Consequences of Range Expansions. *Annu. Rev. Ecol. Evol. Syst.* **40**, 481–501 (2009).

19. Alsos, I. G. *et al.* Genetic consequences of climate change for northern plants. *Proc. R. Soc. B Biol. Sci.* **279**, 2042–2051 (2012).
20. Pauls, S. U., Nowak, C., Bálint, M. & Pfenninger, M. The impact of global climate change on genetic diversity within populations and species. *Mol. Ecol.* **22**, 925–946 (2013).
21. De Kort, H. *et al.* Life history, climate and biogeography interactively affect worldwide genetic diversity of plant and animal populations. *Nat. Commun.* **12**, 516 (2021).
22. Hampe, A. & Petit, R. J. Conserving biodiversity under climate change: the rear edge matters. *Ecol. Lett.* **8**, 461–467 (2005).
23. Zettlemoyer, M. A. & Peterson, M. L. Does Phenological Plasticity Help or Hinder Range Shifts Under Climate Change? *Front. Ecol. Evol.* **9**, 392 (2021).
24. Yiming, L. *et al.* Latitudinal gradients in genetic diversity and natural selection at a highly adaptive gene in terrestrial mammals. *Ecography* **44**, 206–218 (2021).
25. Stahl, U., Reu, B. & Wirth, C. Predicting species' range limits from functional traits for the tree flora of North America. *Proc. Natl. Acad. Sci.* **111**, 13739–13744 (2014).
26. Van Nuland, M. E. *et al.* Intraspecific trait variation across elevation predicts a widespread tree species' climate niche and range limits. *Ecol. Evol.* **10**, 3856–3867 (2020).
27. Peterson, M. L., Angert, A. L. & Kay, K. M. Experimental migration upward in elevation is associated with strong selection on life history traits. *Ecol. Evol.* **10**, 612–625 (2019).
28. Vitasse, Y., Signarbieux, C. & Fu, Y. H. Global warming leads to more uniform spring phenology across elevations. *Proc. Natl. Acad. Sci.* **115**, 1004–1008 (2018).
29. Piao, S. *et al.* Plant phenology and global climate change: Current progresses and challenges. *Glob. Change Biol.* **25**, 1922–1940 (2019).
30. Ferrier, S. & Guisan, A. Spatial modelling of biodiversity at the community level. *J. Appl. Ecol.* **43**, 393–404 (2006).
31. Cooke, J. E. K. & Rood, S. B. Trees of the people: the growing science of poplars in Canada and worldwideThis commentary is one of a selection of papers published in the Special Issue on Poplar Research in Canada. *Can. J. Bot.* **85**, 1103–1110 (2007).
32. Ware, I. M. *et al.* Climate-driven reduction of genetic variation in plant phenology alters soil communities and nutrient pools. *Glob. Change Biol.* **25**, 1514–1528 (2019).
33. Evans, L. M., Allan, G. J., Meneses, N., Max, T. L. & Whitham, T. G. Herbivore host-associated genetic differentiation depends on the scale of plant genetic variation examined. *Evol. Ecol.* **27**, 65–81 (2013).
34. Evans, L. M. *et al.* Geographical barriers and climate influence demographic history in narrowleaf cottonwoods. *Heredity* **114**, 387–396 (2015).
35. Hargreaves, A. L., Samis, K. E., Eckert, C. G., Schmitz, A. E. O. J. & Bronstein, E. J. L. Are Species' Range Limits Simply Niche Limits Writ Large? A Review of Transplant Experiments beyond the Range. *Am. Nat.* **183**, 157–173 (2014).

36. Woolbright, S. A., Whitham, T. G., Gehring, C. A., Allan, G. J. & Bailey, J. K. Climate relicts and their associated communities as natural ecology and evolution laboratories. *Trends Ecol. Evol.* **29**, 406–416 (2014).
37. Gotelli, N. J. & Stanton-Geddes, J. Climate change, genetic markers and species distribution modelling. *J. Biogeogr.* **42**, 1577–1585 (2015).
38. Cushman, S. A. *et al.* Landscape genetic connectivity in a riparian foundation tree is jointly driven by climatic gradients and river networks. *Ecol. Appl.* **24**, 1000–1014 (2014).
39. Bothwell, H. M. *et al.* Conserving threatened riparian ecosystems in the American West: Precipitation gradients and river networks drive genetic connectivity and diversity in a foundation riparian tree (*Populus angustifolia*). *Mol. Ecol.* **26**, 5114–5132 (2017).
40. Hamann, A., Wang, T., Spittlehouse, D. L. & Murdock, T. Q. A Comprehensive, High-Resolution Database of Historical and Projected Climate Surfaces for Western North America. *Bull. Am. Meteorol. Soc.* **94**, 1307–1309 (2013).
41. Lucinda McKay *et al.* NHDPlus Version 2: User Guide. (2012).
42. ESRI. *ArcMap*. (2018).
43. Elith, J. & Leathwick, J. R. Species Distribution Models: Ecological Explanation and Prediction Across Space and Time. *Annu. Rev. Ecol. Evol. Syst.* **40**, 677–697 (2009).
44. Franklin, J. *Mapping Species Distributions: Spatial Inference and Prediction*. (Cambridge University Press, 2009).
45. Elith, J. *et al.* A statistical explanation of MaxEnt for ecologists. *Divers. Distrib.* **17**, 43–57 (2011).
46. Elith*, J. *et al.* Novel methods improve prediction of species' distributions from occurrence data. *Ecography* **29**, 129–151 (2006).
47. Pearson, R. G., Raxworthy, C. J., Nakamura, M. & Townsend Peterson, A. Predicting species distributions from small numbers of occurrence records: a test case using cryptic geckos in Madagascar. *J. Biogeogr.* **34**, 102–117 (2007).
48. Swets, J. A. Measuring the Accuracy of Diagnostic Systems. *Science* **240**, 1285–1293 (1988).
49. Syfert, M. M., Brummitt, N. A., Coomes, D. A., Bystriakova, N. & Smith, M. J. Inferring diversity patterns along an elevation gradient from stacked SDMs: A case study on Mesoamerican ferns. *Glob. Ecol. Conserv.* **16**, e00433 (2018).
50. Mateo, R. G., Felicísimo, Á. M., Pottier, J., Guisan, A. & Muñoz, J. Do Stacked Species Distribution Models Reflect Altitudinal Diversity Patterns? *PLOS ONE* **7**, e32586 (2012).
51. Engler, R. *et al.* 21st century climate change threatens mountain flora unequally across Europe. *Glob. Change Biol.* **17**, 2330–2341 (2011).
52. Randin, C. F. *et al.* Climate change and plant distribution: local models predict high-elevation persistence. *Glob. Change Biol.* **15**, 1557–1569 (2009).

53. Knutti, R., Masson, D. & Gettelman, A. Climate model genealogy: Generation CMIP5 and how we got there. *Geophys. Res. Lett.* **40**, 1194–1199 (2013).
54. Mateo, R. G., Mokany, K. & Guisan, A. Biodiversity Models: What If Unsaturation Is the Rule? *Trends Ecol. Evol.* **32**, 556–566 (2017).
55. R Core Team. *R: A Language and Environment for Statistical Computing*. (R Foundation for Statistical Computing, 2020).
56. Oksanen, J. *et al. vegan: Community Ecology Package*. (2020).
57. John A. Endler. *Geographic Variation, Speciation, and Clines*. (Princeton University Press, 1977).
58. May, R. M. & Godfrey, J. Biological Diversity: Differences between Land and Sea [and Discussion]. *Philos. Trans. Biol. Sci.* **343**, 105–111 (1994).
59. Des Roches, S. *et al.* The ecological importance of intraspecific variation. *Nat. Ecol. Evol.* **2**, 57–64 (2018).
60. Van Nuland, M. E., Bailey, J. K. & Schweitzer, J. A. Divergent plant–soil feedbacks could alter future elevation ranges and ecosystem dynamics. *Nat. Ecol. Evol.* **1**, 0150 (2017).
61. Richardson, A. D. *et al.* Influence of spring and autumn phenological transitions on forest ecosystem productivity. *Philos. Trans. R. Soc. B Biol. Sci.* **365**, 3227–3246 (2010).
62. Andrew D. Richardson *et al.* Influence of spring phenology on seasonal and annual carbon balance in two contrasting New England forests. *Tree Physiol.* **29**, 321–321 (2009).
63. Huntington, T. G. CO2-induced suppression of transpiration cannot explain increasing runoff. *Hydrol. Process.* **22**, 311–314 (2008).
64. Kim, J. H. *et al.* Warming-Induced Earlier Greenup Leads to Reduced Stream Discharge in a Temperate Mixed Forest Catchment. *J. Geophys. Res. Biogeosciences* **123**, 1960–1975 (2018).
65. Mori, A. S. *et al.* Biodiversity–productivity relationships are key to nature-based climate solutions. *Nat. Clim. Change* **11**, 543–550 (2021).
66. Robert J. Naiman, Henri Décamps, Michael E. McClain, & editors. *Riparia: ecology, conservation, and management of streamside communities*. (Elsevier Academic Press, 2005).
67. Bayliss, S. L. J., Mueller, L. O., Ware, I. M., Schweitzer, J. A. & Bailey, J. K. Plant genetic variation drives geographic differences in atmosphere–plant–ecosystem feedbacks. *Plant-Environ. Interact.* **1**, 166–180 (2020).

APPENDIX 3

Table 6: Summary and evaluation of decile distribution models. Predicted suitable climatic conditions on the landscape are listed both as pixel number and as percent area of the total extent of the landscape (total pixels = 156,659). Each pixel has an area of ~1km^2, a resolution of 30 arc seconds. Test AUC (area under the receiving operating characteristic curve) +/- standard deviations are given from 5-fold cross-validation. Training AUC is for final models. Training omission rate is for the 10-percentile training presence threshold rule.

modeled trait decile	N_{occ}	predicted suitable		model evaluation		
		pixel #	% area	AUC_{test} ± sd	AUC_{train}	omission rate
D1	39	16,840	10.7	0.797 ± 0.090	0.950	0.077
D2	46	47,386	30.2	0.875 ± 0.056	0.933	0.043
D3	41	52,064	33.2	0.845 ± 0.071	0.913	0.098
D4	39	41,900	27.2	0.884 ± 0.049	0.920	0.077
D5	38	49,687	31.7	0.812 ± 0.067	0.896	0.079
D6	39	32,359	20.6	0.848 ± 0.050	0.911	0.077
D7	39	40,574	25.9	0.831 ± 0.050	0.900	0.077
D8	44	29,752	19.0	0.886 ± 0.042	0.940	0.091
D9	41	32,326	20.6	0.856 ± 0.052	0.902	0.098
D10	34	17,959	11.5	0.879 ± 0.049	0.943	0.088
Stacked Models	**400**	**53,727**	**34.3**			

Table 7: Net loss calculated as percent loss minus percent gain and 95 percent confidence bounds averaged for the three global circulation models across geographic range, year, and relative concentration pathway (RCP).

geographic extent	year	net loss (%) [lower CI, upper CI]	
		RCP 4.5	RCP 8.5
species range	2050s	20.4 [9.8, 31.0]	25.4 [14.8, 36.0]
	2080s	22.7 [12.1, 33.3]	23.0 [12.4, 33.6]
northern	2050s	14.6 [-1.3, 30.4]	18.8 [2.9, 34.6]
	2080s	16.5 [0.6, 32.3]	14.1 [-1.7, 30.0]
central	2050s	24.7 [22.6, 26.8]	29.4 [27.2, 31.5]
	2080s	28.3 [26.1, 30.4]	29.5 [27.4, 31.6]
southern	2050s	36.1 [25.5, 46.6]	44.5 [33.9, 55.0]
	2080s	37.8 [27.2, 48.4]	47.0 [36.4, 57.6]

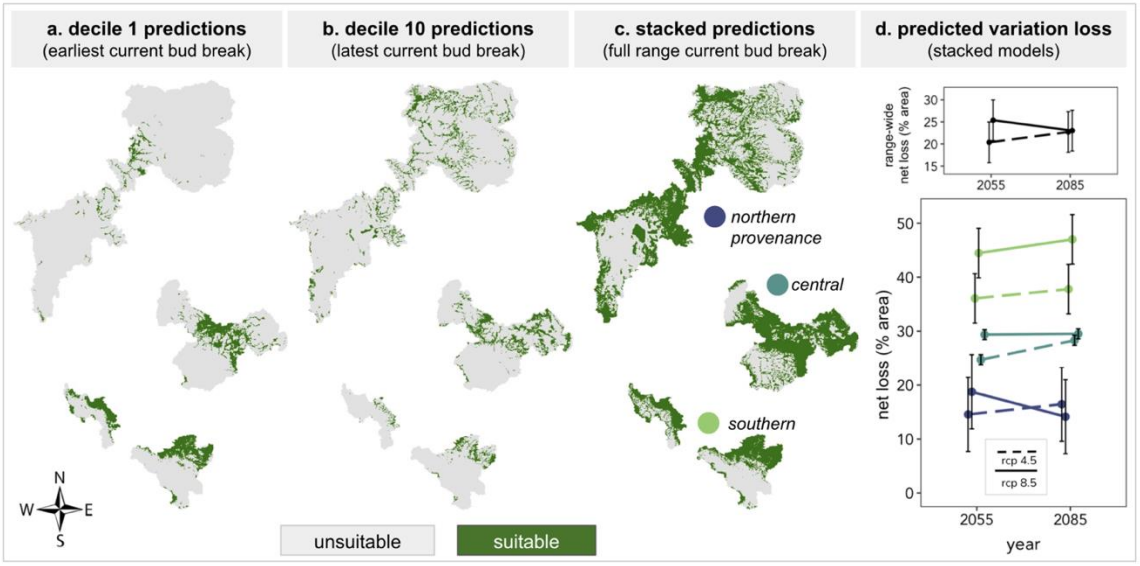

Figure 9. Maps of (a) bud break decile 1, (b) bud break decile 10, and (c) stacked deciles 1 through 10 as binary (presence-absence) predictions on current climate; and (d) Percent of the landscape predicted to lose trait variation across three genetic provenances, two future time periods (2055, 2085), and two relative concentration pathways (RCP 4.5 and RCP 8.5). In (a-c), green represents suitable climatic conditions for the modeled trait decile (or deciles) and grey represents unsuitable climatic conditions for the modeled trait decile (or deciles). In (d), "net" percent loss is calculated as the difference between percent loss and percent gain. Points represent average predictions from three Atmosphere and Ocean General Circulation/Climate models (AOGCMs) that capture "best", "worst", and "median" climate projections for this geographic region. Color represents genetic provenance of *P. angustifolia*, as labelled in (c). Yellow green represents the southern provenance, green blue the central provenance, and blue purple the northern provenance. Line type (dashed or solid) represent RCP 4.5 and 8.5 respectively. For visual clarity, this map does not show occurrence data. These data, with latitudes and longitudes, can be found in the supplemental information.

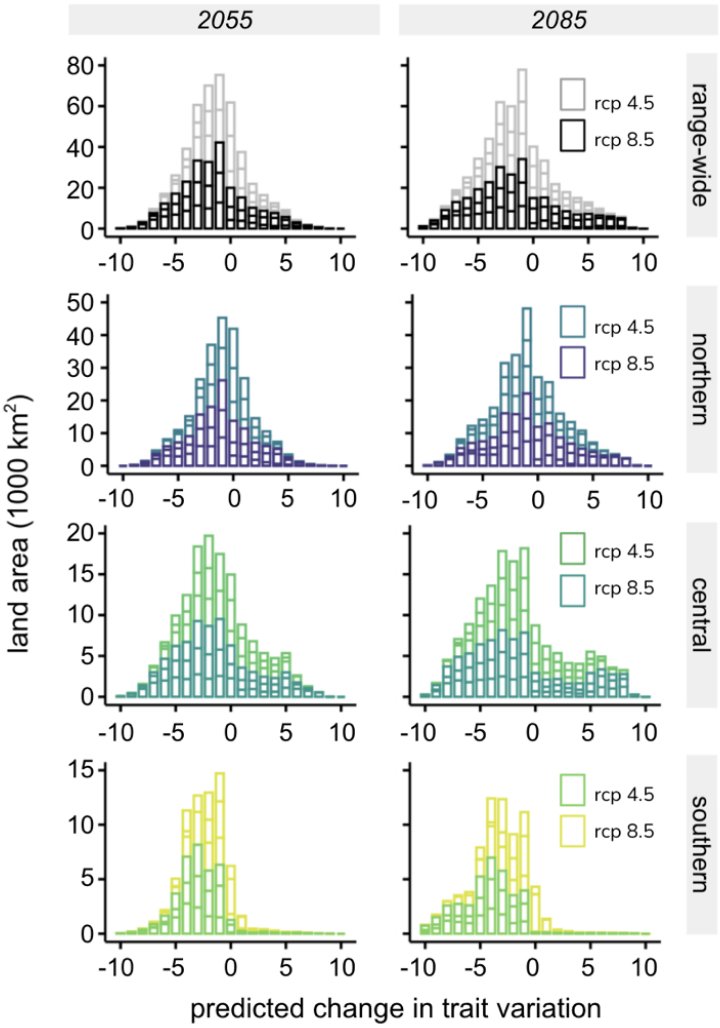

Figure 10. Predicted changes in phenological trait variation (decile richness) on the landscape (area) across the species range, three genetic provenances, two future time periods (2055 and 2085), and two relative concentration pathways (RCP 4.5 and 8.5). The lighter color lines within each bar represents RCP 4.5 predictions while the darker color within each bar represents RCP 8.5 predictions. Lines across each bar represent the predictions made from each of the three Atmosphere and Ocean General Circulation/Climate models (AOGCMs) for each time and RCP. Zeros only represent no change in trait variation if there was variation to begin with (i.e., they do not represent area of unsuitable climatic conditions).

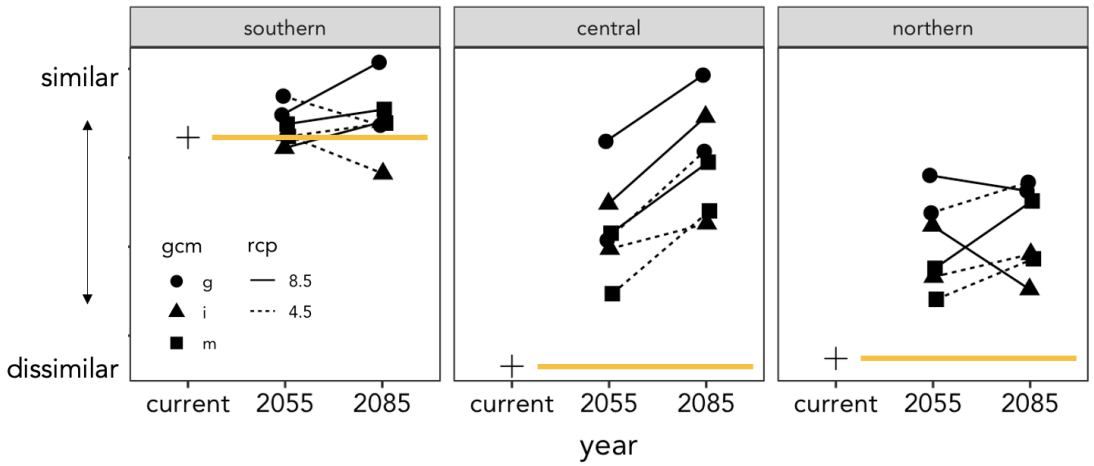

Figure 11. Changes in similarity for phenological trait distributions across time and relative concentration pathways as predicted by three Atmosphere and Ocean General Circulation/Climate models (AOGCMs). Each point represents an average similarity value for each general circulation model abbreviated as "i" (inm-cm4), "m" (mpi-esm-lr), and "g" (gfdl-cm3). Higher similarity represents a narrow range of phenological trait values. The yellow lines extend from the baseline similarity within each provenance as predicted on climate norms. Values above the yellow line indicate that trait values are becoming more similar over time.

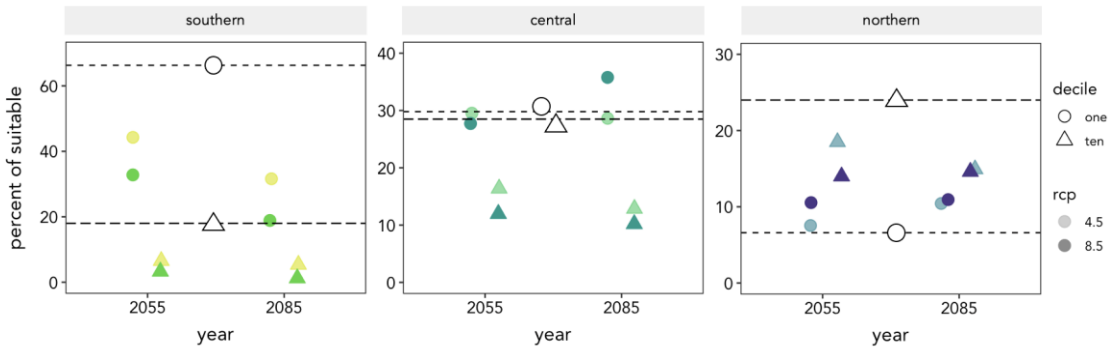

Figure 12. Average projected change in frequency of the earliest 10% (decile one) and latest 10% (decile 10) of bud breakers relative to the total landscape with at least a richness value of 1 (i.e., excluding unsuitable area) across genetic provenances. Empty symbols and dotted lines represent climate norms or starting conditions and filled symbols represent frequencies at each time averaged across AOGCMs. Circles represent decile 1 and triangles represent decile 10. Lighter shades represent RCP 4.5 and darker shades represent RCP 8.5.

CONCLUSION

The findings of this dissertation confirm that plant populations have evolved to differ in their ability to maintain favorable water balance on landscapes with different hydrologic histories. These differences should influence a population's ability to cope with changing atmospheric demands for water that are expected with a warmer climate. Results also emphasize the large degree of error that is possible if ecologists continue to make projections of future suitable habitats by considering a species' as un-varying in genetic diversity or functional trait variation across its' geographic range. Species-range distribution models that did not include genetic information provided overly-broad projections of suitable conditions compared to models that include population genetic structure. Furthermore, a net loss of trait variation in future climates is predicted across all populations of *P. angustifolia*, with the trailing-edge population predicted to lose the most. These ideas have broad implications for predicting population-level ecological and evolutionary responses to climate change as decreases to genetic variation reduce a species' ability to adapt to novel conditions and have profound effects on ecosystem processes and ecological communities.

APPENDIX 4

Table 8: Description of modeling experiments that used only bioclimatic variables: Building, evaluation, and performance.

Model Name	Training Extent	Variable Selection	AUC_{train}	AUC_{test} +/- sd	N train(test)	Omission Rate
SR-CO	Species Range	Range-Wide (RW)	0.862	0.852 +/- 0.027	75(31)	0.65
P1-RW-CO	P1	RW	0.987	0.948 +/- 0.015	9(3)	0.333
P1-P1-CO	P1	P1 Range	0.983	0.948+/- 0.014	9(3)	0.667
P2-RW-CO	P2	RW	0.874	0.68 +/- 0.065	26(11)	0.455
P2-P2-CO	P2	P2 Range	0.875	0.72 +/- 0.058	26(11)	0.182
P3-RW-CO	P3	RW	0.0.927	0.862 +/- 0.028	40(17)	0.294
P3-P3-CO	P3	P3 Range	0.942	0.892 +/- 0.021	40(17)	0.353

Table 9: Percent contribution (%) of environmental variables to SDMs. The lower panel represents models built with only bioclimatic variables. Blank cells indicate that variable was not included in final models while zeros indicate that the variable was included but contributed nothing to final models. Variable abbreviations represent: ahm (annual heat moisture index), cmd (Hargreave's climatic moisture index), dd_0 (degree-days below 0°C), mar (mean annual solar radiation (MJ m-2 d-1)), nffd (number of frost-free days), pas (precipitation as snow (mm)), ppt_sm (summer (Jun to Aug) precipitation (mm)), ppt_wt (winter (Dec to Feb) precipitation (mm)), rh (mean annual relative humidity (%)), td (difference between MCMT and MWMT, continentality (°C)).

Model Name	Climatic Variables (AdaptWest Project)									
	ahm	**cmd**	**dd_0**	**mar**	**nnfd**	**pas**	**ppt_sm**	**ppt_wt**	**rh**	**td**
SR-CO	1.9	14.8								12.4
P1-RW-CO	41.6	1.4								0.8
P1-P1-CO	19.8				26.5				20.9	
P2-RW-CO	0.9	22.4								2.6
P2-P2-CO			4.5			18.5	2.6			
P3-RW-CO	4.8	13.8								13.8
P3-P3-CO		13.2		4.6				10.6		9.6

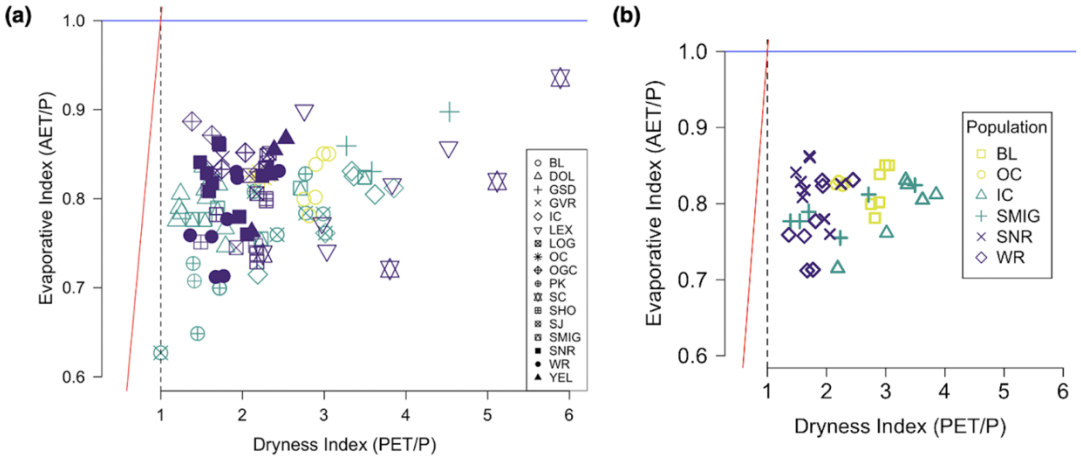

Figure 13. A comprehensive representation of all 17 populations from which biomass was calculated (a), and field sites within six populations used for stomatal measurements (b) represented on the Budyko Theoretical Model. Colors represent population membership to each provenance, as in main figures in chapter 1 (yellow= provenance 1, green= provenance 2, purple= provenance 3). Each symbol represents a unique river population, and each point represents a unique sampling location for that population. River abbreviations are ordered alphabetically as follows: BL = Blue River, Arizona; DOL= Dolores River, Colorado; GSD= Great Sand Dunes, Colorado, GVR= Gros Ventre River, Wyoming; IC= Indian Creek, Utah; LEX= Lexington River, Nevada; LOG= Logan River, Utah; OC = Oak Creek, Arizona; OGC = Ogden Canyon, Utah; PK= Park Creek, Utah; SC = Snake Creek, Nevada; SHO= Shoshone River, Wyoming; SJ= San Juan River, Colorado; SMIG = San Miguel River, Colorado; SNR= Snake River, Wyoming; WR = Weber River, Utah; YEL= Yellowstone River, Wyoming.

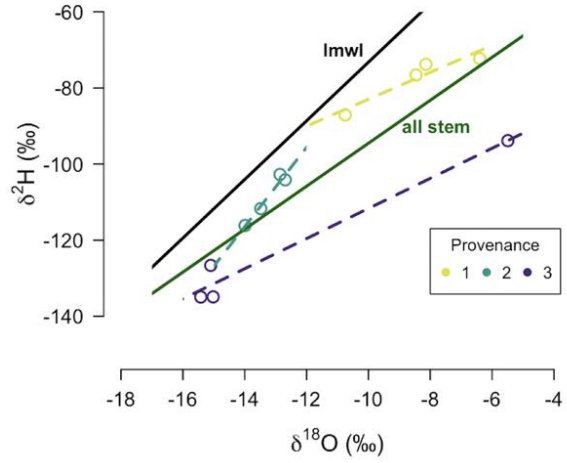

Figure 14. The slope of the regression line between oxygen and hydrogen isotope compositions of stem water differ among genetic provenances of P. angustifolia. LMWL (black line): slope =7.00, r^2= 0.98; all stems (dark green line), as represented in figure 4: n=12, slope=5.6, r^2= 0.77; Provenance 1: N=4, slope = 3.5, r^2= 0.89; Provenance 2: N=4, slope =10.4, r^2= 0.95; Provenance 3: N=4, slope =3.9, r^2= 0.96.

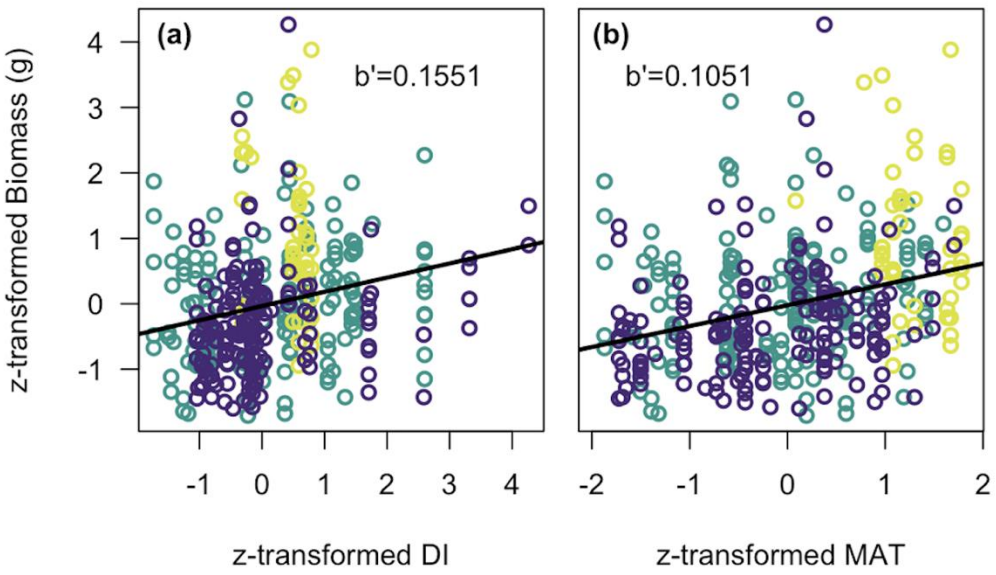

Figure 15. Standardized slopes (b') compared between greenhouse biomass measurements and (a) mean annual dryness index, and (b) mean annual temperature. All variables have been centered and scaled (z-transformed). Full models include (a) evaporative index, and (b) precipitation as factors and both models included genetic provenance as a random effect.

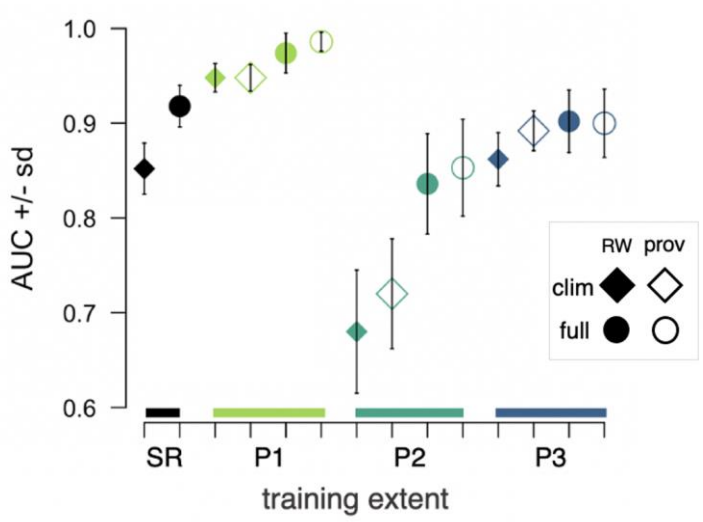

Figure 16. Test area under the curve of the receiver-operating characteristic values (AUC) +/- standard error for models. Color represents geographic training extent of model, symbol fill represents the variable selection method (closed = range-wide variable selection (RW); open = genetic provenance variable selection). Diamonds represent models built with bioclimatic variables only and circles represent values from full models.

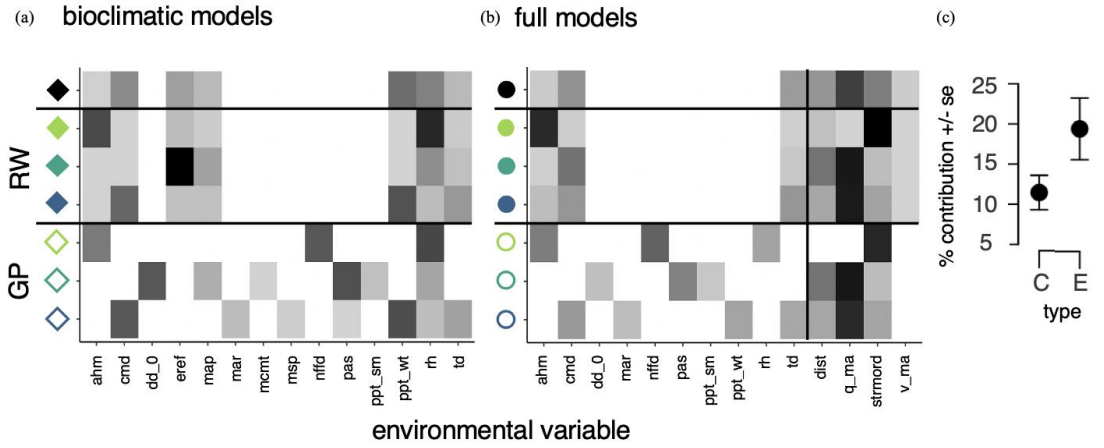

Figure 17. Test percent contribution of environmental variables to different SDMs. Panel (a) represents model experiments using only bioclimatic variables, and **panel (b)** represents model experiments using both bioclimatic + hydrological variables (y-axis); **panel (c)** shows the average percent (%) contributions of variable type (bioclimatic (C) or hydrologic (E)) +/- se based on the seven full models represented in panel b, significant at p=0.07 using an unpaired two-tailed t-test. The percent contribution (%) of environmental variables (x-axis) is represented in grey scale, where the gradient of light grey to black represents 0-50% contribution in **panel (a)** and 0-60% contribution in **panel (b)**; Exact values are given in Table 9. In **panels (a) and (b)**, blank white squares represent variables not selected for inclusion in the model experiment. Each model experiment is represented by color (training extent), symbol (variable inclusion), and symbol fill (variable selection method). Environmental variable abbreviations, in alphabetical order, represent: ahm (annual heat moisture index), cmd (Hargreave's climatic moisture index), dd_0 (degree-days below 0°C), eref (Hargreave's reference evaporation), map (mean annual precipitation (mm)), mar (mean annual solar radiation (MJ m-2 d-1)), mcmt (mean temperature of the coldest month (°C)), msp (mean summer (May to Sep) precipitation (mm)), nffd (number of frost-free days), pas (precipitation as snow (mm)), ppt_sm (summer (Jun to Aug) precipitation (mm)), ppt_wt (winter (Dec to Feb) precipitation (mm)), rh (mean annual relative humidity (%)), td (difference between MCMT and MWMT, continentality (°C)), and in panel **(b)** dist (distance to nearest stream), q_ma (mean annual streamflow), strmord (Strahler stream order), and v_ma (mean annual stream velocity).

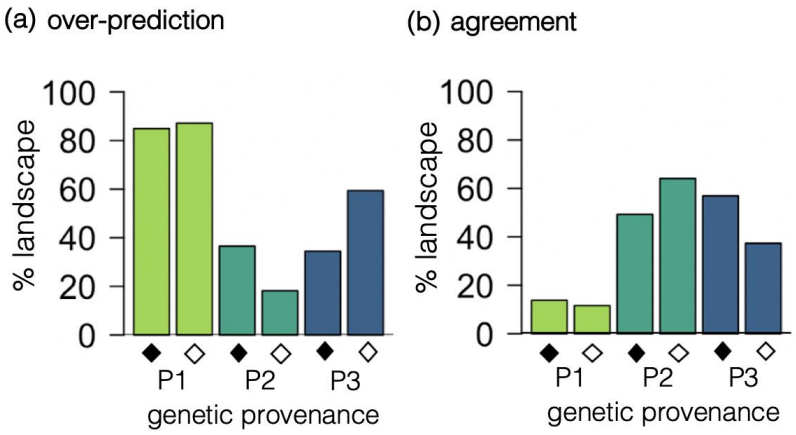

Figure 18. Models built with bioclimatic variables only: Comparison of species SDMs to provenance SDMs (P1, P2, P3) across two methods of variable selection (RW and P; closed and open symbols). Panel **(a)** represents the percent difference (spatial disagreement) between predictions of suitable distribution made by the range-wide species model and respective provenance models. Positive values indicate that the range-wide model predicts broader suitable distribution than the provenance model. Panel **(b)** represents spatial agreement between model predictions of suitable distribution. This value is not considering model agreement on "unsuitable" distribution.

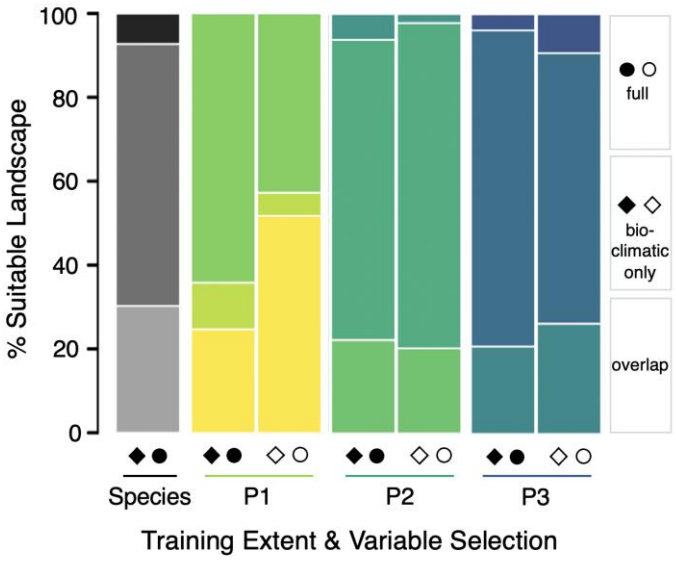

Figure 19. Comparisons of area predicted suitable by variable type. Stacked bars represent 100% of suitable distribution predicted within each model experiment's training extent (represented by color). Lighter shades of color (bottom) represent the percentage of the landscape predicted suitable by both model types, medium shades of color (middle) represent the percentage of the landscape predicted suitable by only the bioclimatic models, and the darker shades (top) represent the percentage of suitable landscape predicted only by the full models. As in earlier figures, color represents model training extent, symbols represent variable type (bioclimatic only = diamond; full = circle), and symbol fill represents variable selection (range-wide = closed, provenance = open).

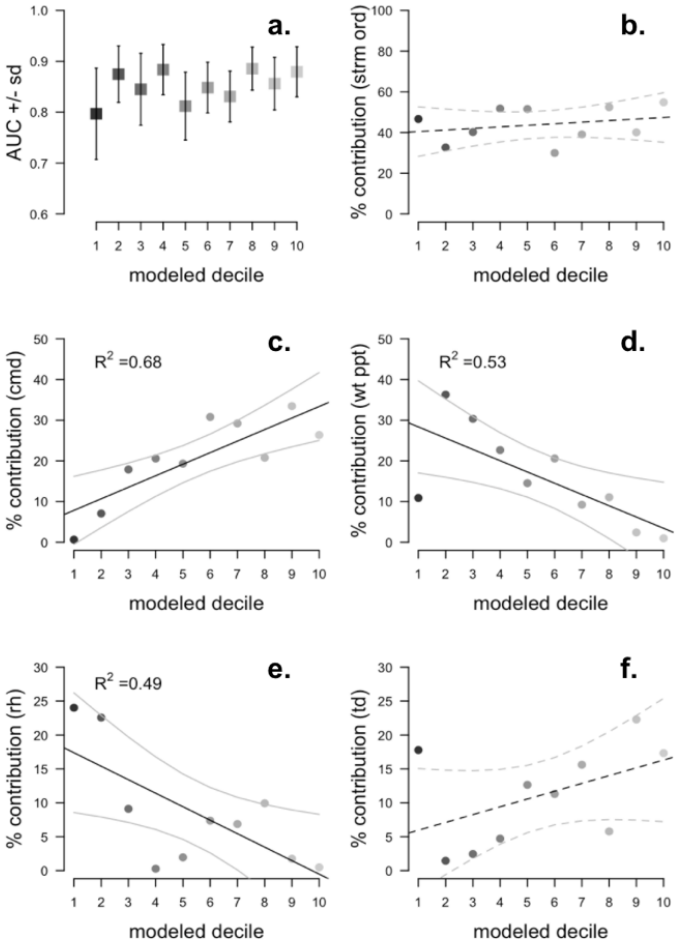

Figure 20. Model performance and environmental variable contributions to bud break decile distribution models. (a) represents the average test area under the receiver operating characteristic curve (AUC) +/- standard deviation from 5-fold cross-validation of decile models. An AUC value of 1 indicates perfect discriminatory ability, while a value of 0.5 indicates random predictions. Panels **(b-f)** represent the percent contributions of each environmental variable to the predictions made by decile models: **(b)** Strahler stream order, **(c)** Hargreave's climatic moisture index in mm, **(d)** winter precipitation in mm, **(e)** percent relative humidity, and **(f)** continentality, measured as the difference between mean temperature of the coldest and warmest months in degrees Celsius. Note the different scales of y-axes. Solid lines represent significant linear relationships at a threshold of p=0.05.

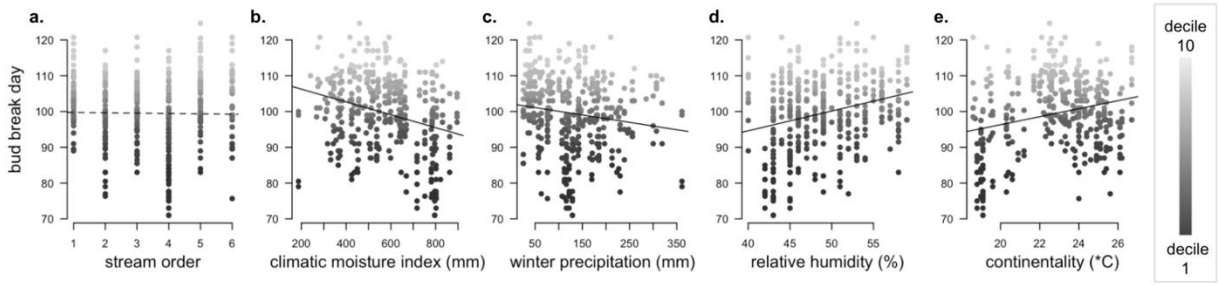

Figure 21. Relationship between bud break day and the environmental variables used in distribution models. **(a)** Strahler stream order, **(b)** Hargreave's climatic moisture index in mm, **(c)** winter precipitation in mm, **(d)** percent relative humidity, **(e)** continentality, measured as the difference between mean temperature of the coldest and warmest months in degrees Celsius. The greyscale represents the distribution of bud break day values sorted into ten deciles. Solid lines represent significant linear relationships at a threshold of p=0.05.

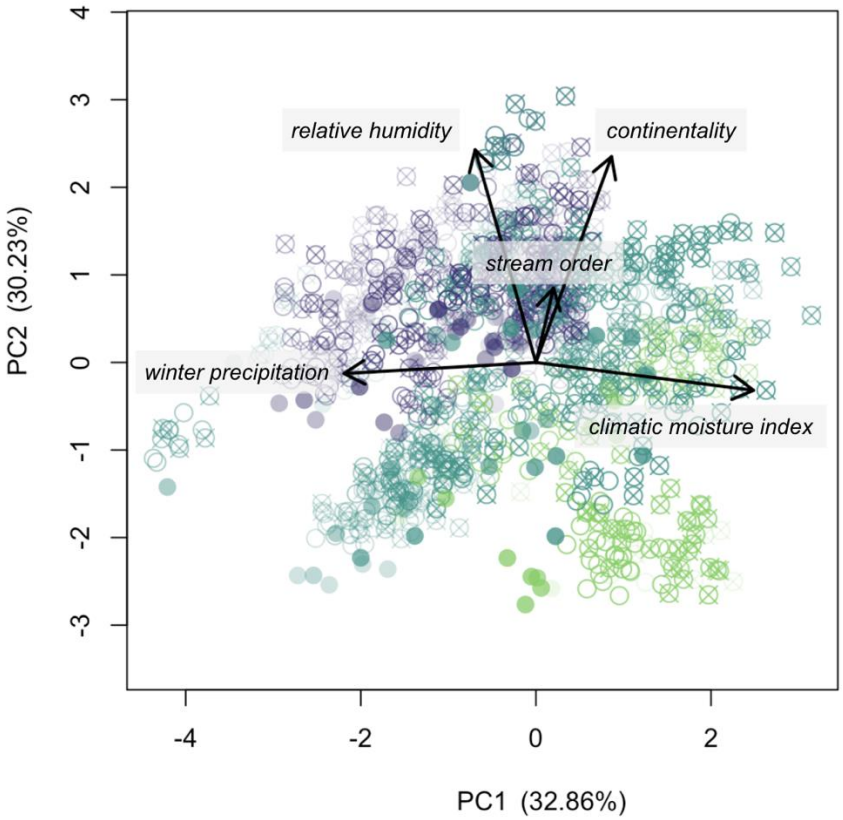

Figure 22. Principal coordinate axes 1 and 2 of the five environmental variables used in distribution models. Different symbols represent different climatic scenarios (time, RCP, AOGCM); Color represents genetic provenance (purple= northern; teal= central; green= southern).

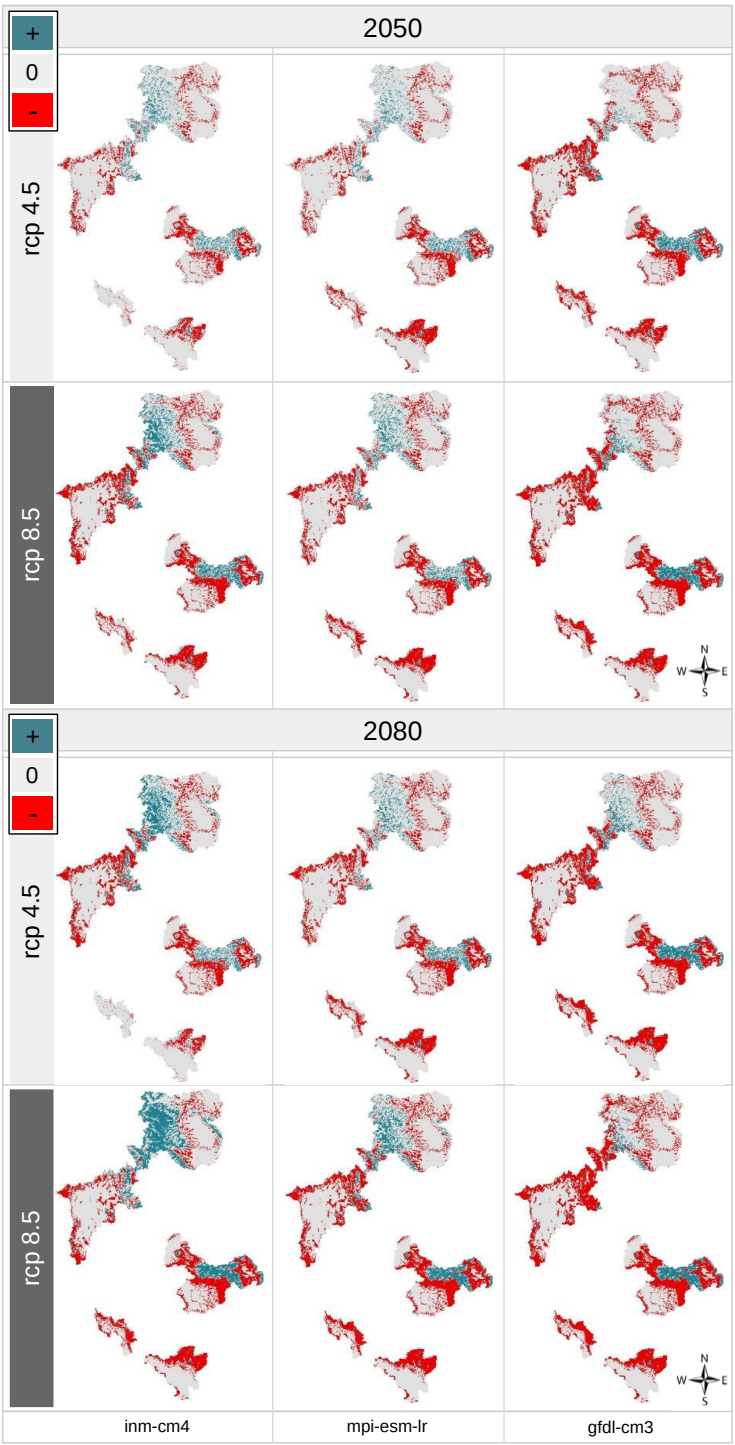

Figure 23. Maps of richness loss and gain by two future time periods (2050s and 2080s), two emissions scenarios (RCP 4.5 and RCP 8.5), and three Atmosphere and Ocean General Circulation/Climate models (AOGCMs; inm-cm4, mpi-esm-lr, and gfdl-cm3). Areas predicted to gain trait richness are represented in blue. Areas predicted to lose trait richness are represented in red. Grey areas are areas where no change in richness is predicted.

VITA

Shannon Lee Jo-Ann Bayliss graduated from the University of Virginia in 2012 with a Bachelor of Science degree in Environmental Sciences and a minor in Art History. She earned her Master of Science in Biology from California State University, Northridge in 2016 working with Dr. Casey terHorst studying the relationship between genetic diversity and ecosystem function of the algal symbionts of coral reefs. Her interest in science writing led her to pursue a degree in Communication and Information with a concentration in Journalism and Electronic Media at the University of Tennessee. Her 2021 master's thesis was influenced by her love of music and her doctoral research. It is titled: *Unearthing Tree Symbolism in Song: A Sentiment Analysis.* She will graduate from the University of Tennessee, Knoxville in 2021 with a doctorate in Ecology and Evolutionary Biology.